



HAL
open science

Modèles Mathématiques pour l'Inspection Nondestructive des Pipelines

Kaouthar Louati

► **To cite this version:**

Kaouthar Louati. Modèles Mathématiques pour l'Inspection Nondestructive des Pipelines. Mathématiques [math]. Ecole Polytechnique X, 2006. Français. NNT: . tel-00125751

HAL Id: tel-00125751

<https://pastel.hal.science/tel-00125751>

Submitted on 22 Jan 2007

HAL is a multi-disciplinary open access archive for the deposit and dissemination of scientific research documents, whether they are published or not. The documents may come from teaching and research institutions in France or abroad, or from public or private research centers.

L'archive ouverte pluridisciplinaire **HAL**, est destinée au dépôt et à la diffusion de documents scientifiques de niveau recherche, publiés ou non, émanant des établissements d'enseignement et de recherche français ou étrangers, des laboratoires publics ou privés.

Thèse présentée pour obtenir le grade de
DOCTEUR DE L'ÉCOLE POLYTECHNIQUE

spécialité : Mathématiques Appliquées

par

Kaouthar LOUATI

Modèles Mathématiques pour l'Inspection Nondestructive des Pipelines

Soutenue le 13 décembre devant le jury composé de

MM. Habib Ammari	Directeur de thèse
Mourad Choulli	Rapporteur
Josselin Garnier	Examineur
Vincent Giovangigli	Examineur
Ioan Ionescu	Rapporteur
Bertrand Maury	Rapporteur

Remerciements

A Habib

Les mots ne suffiraient pas pour exprimer ma profonde gratitude envers Habib Ammari, mon Directeur de thèse. Sans sa confiance, sa générosité, et sa patience, cette thèse n'aurait vu le jour. Je veux vivement le remercier pour la liberté qu'il m'a accordée et les responsabilités qu'il m'a confiées qui m'ont permis d'atteindre une maturité scientifique que je n'aurais pas imaginée auparavant. Ses qualités scientifiques exceptionnelles associées à ses qualités humaines aussi merveilleuses m'ont aidé à surmonter même les moments les plus délicats de cette thèse. Nos discussions sur le plan professionnel et aussi amical ont toujours été un moment fort agréable me permettant de retrouver réconfort et sérénité. Merci pour tout Habib !

A mon Jury

Un grand merci à Vincent Giovangigli pour avoir accepté de présider mon Jury. Je tiens à le remercier particulièrement pour sa sympathie, sa perpétuelle bonne humeur et pour son soutien moral constant. Je suis très sensible à l'honneur que m'ont fait Mourad Choulli, Ioan Ionescu et Bertrand Maury en acceptant de lire mon manuscrit en si peu de temps. Je les remercie vivement pour leurs bons rapports. Je remercie également Josselin Garnier pour sa participation à mon Jury.

A mes collègues

Cette thèse a bénéficié d'une collaboration avec une équipe de recherche à l'université de Séoul à qui j'exprime ma sincère reconnaissance pour l'aide et les conseils apportés à mes recherches. J'ai eu le grand plaisir de travailler aussi avec Lim Mikyoung (post-doctorante d'Habib Ammari au CMAP), ses conseils scientifiques très précieux, ses relectures très assidues, son tendre soutien et sa joie de vivre ont contribué au bon déroulement de mon travail. Son amitié m'est aussi très chère.

A toute l'équipe du CMAP

Je ne saurais oublier ici le personnel administratif de notre laboratoire le CMAP, un personnel exceptionnel qui veille sur notre confort. Je tiens à saluer les énormes efforts que fournit notre chère secrétaire Jeanne pour nous faciliter toutes les tâches lourdes. Je la remercie pour son sourire constant et sa serviabilité sans limite. Je tiens à remercier infiniment Liliane, ancienne secrétaire au CMAP, pour tous les moments d'attention et d'affection qu'elle a su m'accorder à chaque fois que j'en sentais le besoin. Tu nous manques Lili ! Je remercie également Nasséra, Sébastien et Véronique pour leur bonne humeur, leur aide non négligeable et leur présence agréable. Mes soucis informatiques disparaissaient vite par un coup d'appel magique au 4626, merci Sylvain ça aurait été très dur sans toi !

Tous mes remerciements à mes chers copains avec qui j'ai partagé le même bureau ces années de thèse sans qui l'ambiance de travail n'aurait pu être aussi chaleureuse. Merci Erwan pour toutes tes blagues incontournables et ton sourire constant. Merci Benjamin de m'avoir fait le plaisir de venir avec Audrey chez ma famille en Tunisie et merci pour tes nombreux conseils techniques et scientifiques toujours très pertinents. Merci Gabriel pour toute ta gentillesse, ta galanterie, ta modestie et pour tous les gâteaux que tu nous offrais. Merci mon cher Charles pour

toutes les longues et nombreuses discussions intéressantes qu'on a eu, pour tout ce que j'ai pu apprendre de toi, pour tous les moments qu'on a pu partagé avec nos petites familles en dehors du bureau. Je te remercie pour la confiance que tu m'as accordée en proposant à ta chérie, Christine, de me confier ses élèves en colles. Je finirai par ma très chère Asma, quel beau cadeau de t'avoir eu à mes côtés tout au long de ces années et jusqu'aux dernières heures pour finir ce long travail. C'était bien et tout simplement bien, même les moments les plus durs étaient bien grâce à ta présence. Ces beaux moments qu'on a partagés ensemble resteront à jamais gravés dans ma mémoire. Mille merci ma chère !

Je ne peux me passer d'exprimer mes sincères remerciements à tous ceux qui ont su me redonner énergie avant ma soutenance. Merci Aldgia pour les heures que tu m'avais consacré et pour tous les bons compliments que tu m'avais fait. Merci Serafan de m'avoir toujours proposé de l'aide. Merci Gloria et un merci ne suffira pas pour te dire combien ton aide m'a été indispensable pour la préparation de ma soutenance. Merci ma chère Karima, ce fut un plaisir de t'avoir rencontrée, tu as su être une copine unique, je tiens à te dire que tu vas me manquer.

A toute l'équipe de MODAL'X

Je tiens à remercier en premier, Gérard Kerkyacharian, président de la commission de spécialiste à Modal'x Paris X, pour m'avoir recrutée en tant qu'ATER à l'Université de Nanterre. Je le remercie pour son accueil chaleureux et pour toute la confiance qu'il m'a accordée. J'adresse mes sincères remerciements à tous mes collègues : Christian, Pierre, Patrick, Laurent, Salah, et Hector pour leur sympathie, leur modestie, leur gentillesse et pour l'énorme travail qu'ils fournissent pour le bon déroulement des enseignements. Sans oublier de remercier la jeune équipe de Modal'x, qui m'a permis une intégration facile et naturelle à cette grande famille. Merci Chi et Yoann, votre amitié m'est vite venue mais m'est vite devenue très chère, merci de me laisser la possibilité

de m'incruster souvent dans votre fameux bureau le E12. Je remercie Stéphane avec qui je partage le même bureau à Nanterre, ses petites attentions, ses messages sur le tableau, et les chocolats qu'il me laisse sur le bureau ne m'ont pas laissé indifférente. Enfin je remercie Luc Miller, qui malgré un emploi de temps chargé, s'est déplacé spécialement pour m'écouter le jour de ma soutenance.

A ma famille

Ma dette de reconnaissance va en premier lieu à ceux grâce à qui j'ai vu le jour, à mes parents, sans qui je n'aurais jamais été ce que je suis, sans leur appui moral et sans leurs nombreux sacrifices, ce travail n'aurait jamais pu aboutir. Vous êtes des parents exceptionnels, merci de m'avoir appris à ne jamais s'arrêter avant d'y arriver, merci de m'avoir appris à donner sans compter, merci de m'avoir appris à aimer sans limite, merci de m'avoir appris à viser loin, merci de m'avoir indiqué les bons chemins, merci de m'avoir encouragé à réaliser des rêves chers. Merci maman pour tous les messages que tu m'envoyais, ils étaient source de mon énergie, tu étais certes loin de moi mais toujours dans mes pensées. Merci papa, d'avoir toujours cru en moi, ta confiance en moi était la clé de ma réussite. Je ne peux écrire tout ce que j'ai envie de vous dire peur de ne jamais pouvoir s'arrêter, merci d'avoir été si formidables !

Je tiens à remercier, mon cher et tendre époux Tarek, pour avoir accepté tant de sacrifices pour l'aboutissement de cette thèse. Je le remercie pour le respect qu'il donne à mes choix et pour toutes les bonnes conditions qu'il a su me mettre pour motiver mon travail. Je lui dis tout simplement, merci d'avoir donné un meilleur sens à ma vie qui sans toi ne serait pas une vie !

J'associe mes sincères remerciements à une personne qui m'est très cher, à mon frère Moez. Je le remercie pour son aide sans limite, pour ses nombreux conseils, pour la chance que j'ai de l'avoir à mes côtés sur Paris. Je le remercie pour son affection, pour sa générosité, pour toute

son attention et pour son écoute.

Tous mes remerciements à ma très chère grand-mère pour sa contribution non négligeable à mon éducation et pour toutes les valeurs qu'elle a su me transmettre. J'étais très touchée par sa présence à ma soutenance.

Je tiens à remercier ma cousine Leila, qui a toujours été pour moi la petite soeur que je n'ai jamais eu et avec qui j'ai partagé tous les bons moments de mon enfance. J'étais très sensible à ces nombreux mails d'encouragement et à sa présence à ma soutenance.

J'adresse mon extrême gratitude à mes beaux parents pour avoir fait le déplacement pour venir me soutenir et pour avoir participé à mon pot de thèse. J'étais très enchantée et assez touchée par leur présence. Une petite pensée à mon cher beau-frère Walid qui ne manquait pas d'envie d'être parmi nous.

Un grand merci, à mon oncle Raouf et son épouse Insaf, pour l'amour qu'ils m'ont témoigné depuis toute petite, et qui n'ont pas manqué d'être à mes côtés à l'attribution de ce diplôme tant attendu. Tout en les remerciant pour tous les bons gâteaux qu'ils ont fait pour mon pot.

Merci à toute ma famille qui a su me soutenir de loin tout au long de ce parcours.

A mes amis

Ceux qui ne croient pas aux amis, c'est parce qu'ils n'ont jamais connu les miens ! Un très grand merci à mes chers amis : Basma, Emna, Ghada, Hanene, Linda, Senda et Sonia pour leurs aides et leur soutien continu qui m'a aidé à surmonter les moments de fatigue. Je remercie également mes chers copains Amine, Hammadi, Faouzi, Slim et Oualid, d'avoir sacrifié leurs responsabilités pour venir me féliciter.

A Eya

Je finirai par embrasser la petite lumière qui a éclairé mon pot, ma petite Eya, dont le regard innocent m'a toujours redonné sourire.

*Je dédie cette thèse,
à celui qui m'a appris à aimer cette science,
à celui qui m'a appris à faire des maths,
à mon père...*

Contents

- 1 Detection by Impedance Tomography** **23**
 - 1.1 Introduction 23
 - 1.2 Layer Potentials 25
 - 1.3 Representation Formula 28
 - 1.4 Asymptotic Expansion 32
 - 1.5 MUSIC type algorithm for reconstruction 36
 - 1.5.1 Numerical Results 42
 - 1.6 Conclusion 46

- 2 Vibration Testing** **51**
 - 2.1 Introduction 51
 - 2.2 Formal Derivations 53
 - 2.3 Reconstruction Method 55
 - 2.4 Numerical Results 58
 - 2.5 Justification of the Asymptotic Expansion 60
 - 2.6 Conclusion 71

- 3 Ultrasonic Detection** **75**
 - 3.1 Introduction 75
 - 3.2 Preliminaries and Formulation of the Inverse Problem 76
 - 3.3 Asymptotic Formula 80
 - 3.4 Reconstruction Methods 82

3.4.1	A MUSIC-Type Algorithm	83
3.4.2	Kaczmarz Procedure	85
3.4.3	Fourier Method	87
3.5	High Frequency Instabilities	89
3.6	Large-Argument Large-Order Asymptotics of the Bessel Functions	91
3.7	Green's Function	92
4	Small Perturbations of Scatterers	95
4.1	Introduction	95
4.2	Formulation of the Electric Problem	97
4.2.1	Representation Formula	98
4.2.2	Expansion of \mathcal{N}_{ϵ_f} using the field expansions method	99
4.2.3	Far Field Expansion	102
4.2.4	Algorithm for the Inverse Shape Problem	105
4.3	Formulation of the Acoustic Problem	106
4.3.1	Representation Formula	107
4.3.2	Expansion of \mathcal{N}_{ϵ_f}	108
4.3.3	Far-Field Asymptotic Formula	110
4.3.4	Algorithm for the Inverse Shape Problem	113

Présentation Générale

“Vendredi, 20 octobre 2006. Incendie sur des pipelines de la raffinerie de Bizerte : Un incendie s’est déclaré, vendredi matin, sur les pipelines d’arrivée des produits pétroliers du dépôt de la raffinerie de Bizerte. Le feu, qui a provoqué deux déflagrations, a causé des dégâts matériels sans faire de victimes. Les raisons précises de l’incendie ne sont pas encore connues. Mais des travaux étaient en cours sur les pipelines, avant l’incident. Les forces de la Protection civile, des unités de l’Armée nationale et les services de la Société Tunisienne des Industries de Raffinage (STIR) sont intervenus rapidement pour éteindre l’incendie, qui a été circonscrit en un seul foyer. Les efforts se poursuivent pour venir à bout du feu.”

Voilà une récente dépêche qui malheureusement nous rappelle qu’il reste beaucoup à faire dans l’inspection des pipelines. La grande partie du travail présenté dans cette thèse y est consacrée. Nous proposons dans les trois premiers chapitres de nouvelles méthodes directes pour l’identification et la localisation des corrosions internes dans les pipelines. La première est par impédance électrique, la deuxième par ondes guidées ou vibration, et la troisième par ultrasons. Nous jetons les bases mathématiques de ces méthodes et présentons quelques tests numériques qui montrent leur efficacité. Notre approche rentre dans la “stratégie asymptotique” développée par Ammari et Kang [4] pour la résolution des problèmes inverses d’une manière robuste et sta-

ble. Nous exploitons l'existence d'un petit paramètre (la mesure de Hausdorff de la partie corrosive) pour extraire des données la localisation de la partie corrosive et estimer son étendue. Le tout, d'abord, à travers des formules asymptotiques des mesures dépendantes du petit paramètre, rigoureusement établies, et ensuite, par le biais de nouveaux algorithmes non-itératifs d'inversion. La plupart de nos algorithmes sont de type MUSIC (multiple signal classification).

Le dernier chapitre est indépendant des trois premiers. Il est consacré à la reconstruction de la forme d'un objet perturbé connaissant le champ lointain électrique ou acoustique.

Rappelons que les pipelines sont largement utilisés pour acheminer le gaz, le pétrole et l'eau de leurs sources émettrices aux usines de traitement et chez les consommateurs. Les détériorations subies par un pipeline sont très coûteuses. Non seulement le coût de remplacement est conséquent mais également les dommages potentiels causés à l'environnement et la menace à la vie des êtres humains peuvent être importants. Afin de transporter de grandes quantités de liquide ou de gaz sous la terre ou sous la mer (à partir des champs pétroliers situés en pleine mer) ou même à la surface de la terre, les pipelines sont fabriqués en acier pour les protéger de la pression. Par conséquent, la détérioration des pipelines n'est pas seulement occasionnée par la fissuration, mais également par la corrosion de l'acier. Dans ce contexte, la détection non-destructive des ruptures par fissuration ou corrosion sous ses différentes formes présente un sujet d'activité considérable dans la communauté des problèmes inverses, le but étant d'améliorer les techniques d'identification des défauts cachés et de réduire les coûts de la production perdue et du renouvellement des infrastructures.

Comme nous l'avons déjà souligné, notre travail dans cette thèse est essentiellement consacré à l'étude de quelques méthodes qui permettent de retrouver les caractéristiques des défauts le long des pipelines.

Nous considérons trois nouvelles approches d'inversion qui sont à la fois physiquement et mathématiquement différentes. Notre première méthode d'imagerie est par tomographie d'impédance, la deuxième est par vibration et la dernière est par ondes ultrasonores.

Dans le premier chapitre, nous considérons l'équation de Laplace dans une section de la pipeline qui est satisfaite par le potentiel électrique et nous décrivons l'effet de la corrosion à l'aide de conditions de frontière de type Robin.

Différents modèles de corrosion ont été abordés dans la littérature, voir par exemple les travaux de Kaup et Santosa [31], Vogelius et Xu [46], Banks et al. [11].

Le choix du modèle considéré dans ce chapitre s'appuie sur les différentes études faites sur le sujet. D'une part, il a été observé que la partie corrosive a tendance à devenir une surface rugueuse qui peut être modélisée par une couche mince rapidement oscillante. Dans la limite où l'épaisseur de cette couche est presque nulle et la rapidité des oscillations diverge, le surgissement des conditions de frontière de Robin a été justifié par Buttazo et Kohn [13]. D'autre part, l'étude du processus de corrosions électrochimiques peut être basé sur la loi de Faraday qui montre que la perte massive considérée comme une mesure de corrosion est proportionnelle au flux du courant, voir Vogelius et Xu [46]. Si nous linéarisons les conditions aux bords proposées dans [46] par rapport au coefficient de transfert, nous obtenons des conditions de frontière de type Robin.

Le problème inverse que nous considérons dans le premier chapitre consiste en la détermination des dégâts de la corrosion sur la partie inaccessible de la structure connaissant quelques mesures électriques sur la partie accessible.

La difficulté du problème considéré vient du fait qu'il est mal posé et fortement non-linéaire. En effet, la majorité des techniques de détection

utilise des méthodes itératives comme l'algorithme des moindres carrés récursifs ou des schémas itératifs de type Newton. Toutes ces méthodes demandent des temps de calcul énormes pour obtenir une bonne approximation de la vraie solution et surtout ne convergent pas à coût sûr. Leur éventuelle convergence nécessite un bon choix de configuration initiale, proche de la configuration à trouver.

Nous commençons par établir une formule de représentation asymptotique pour les perturbations des champs électriques causées par la présence de petites parties corrosives internes. Notre approche est basée sur des techniques de potentiel de couche à travers des formules de représentation intégrales et nos calculs asymptotiques découlent des analyses fines de ces opérateurs intégraux singuliers. En se basant sur cette nouvelle formule, nous développons ensuite une méthode directe (non-itérative) pour localiser ces parties corrosives. Notre algorithme est de type MUSIC (Multiple Signal Classification), un algorithme qui s'utilise fréquemment en traitement de signal afin d'estimer des fréquences individuelles d'harmoniques multiples d'un signal. Il est basé sur la décomposition singulière de la matrice de données.

Dans le deuxième chapitre, nous proposons une autre procédure d'identification de parties corrosives et ce par l'analyse de vibration. Il est connu que l'impédance électrique se limite à détecter certains types de défauts. Elle n'est pas, par exemple, appropriée à détecter des fissures dans la direction axiale. Récemment, le contrôle par ondes guidées ultrasoniques est utilisé pour ce type de défauts surgissant dans les pipelines. Cette technique d'imagerie consiste à faire propager des ondes guidées ultrasoniques dans les parois des canalisations et à observer les réflexions provenant des défauts.

L'avantage principal de l'utilisation des ondes guidées est leurs possibilités d'ausculter les structures complexes sur des longues distances. Afin de réduire la difficulté du développement de la méthode analy-

tique, un modèle simple est adopté dans ce deuxième chapitre pour déterminer les effets de la corrosion sur les fréquences de résonance ainsi que sur les formes de modes. Notre approche peut être considérée dans un premier temps pour la conception d'un algorithme en temps réel, précis et robuste pour la détection de corrosion des ondes guidées ultrasoniques.

Nous ramenons notre problème à un problème spectral. Nous prouvons que l'étude de ce problème spectral revient à l'étude d'un système d'équations intégrales et la recherche de fréquences de résonances se transforme en la recherche des valeurs caractéristiques d'une fonction méromorphe à valeur d'opérateurs intégraux. Un développement asymptotique de cette fonction, suivi d'une application du théorème de Rouché généralisé, nous mèneront à des asymptotiques des valeurs et des vecteurs propres.

Le troisième chapitre porte sur la détermination des parties corrosives de corrosion à partir de mesures ultrasoniques sur la surface accessible. La technologie des laser-ultrasons est générique et peut être utilisée pour les métaux, les polymères et les composites. Comme par exemple la détection de la corrosion des joints à recouvrement en aluminium provenant du fuselage d'un avion.

Nous développons d'abord un algorithme de type MUSIC. Nous insistons sur l'importance de notre méthode pour la détermination du nombre des parties corrosives présentes sur la surface inaccessible. Ensuite nous présentons la procédure de Kaczmarz. Nous appliquons l'algorithme de retro-propagation utilisé en tomographie par ultrasons où une seule onde ultrasonique est générée par un point source fixe; une application de cette méthode a été développée dans le livre de Natterer et Wübbeling [39]. Nous terminons par donner une méthode de reconstruction simple basée sur les coefficients de Fourier. Chacune de ces différentes approches repose sur la formulation asymptotique de

l'onde réfléchi par les parties corrosives. Le bon déroulement de ces méthodes a nécessité une étude approfondie des différentes propriétés des fonctions de Bessel et de leurs différents comportements asymptotiques ainsi qu'une exploitation assez fine des propriétés des fonctions de Green.

Dans la dernière partie de ce manuscrit, nous considérons le problème de détermination des perturbations sur le bord d'un objet par des mesures du champ lointain acoustique ou électrique. Ce problème d'inversion de forme a été un domaine de recherche actif pendant plusieurs décennies. Nous développons pour les deux cas électriques et acoustique une relation linéarisée entre le champ lointain résultant des données sur le bord de condition de Dirichlet fixe comme paramètre et la forme de la structure perturbée comme variable. Cette relation nous ouvre la voie à la reconstruction des coefficients de Fourier de la perturbation et nous aide à formuler un développement asymptotique complet de l'opérateur Dirichlet-Neumann. Nous prouvons également, dans le cas où les oscillations angulaires sont inférieures à $1/n$, qu'il faut utiliser les n premiers vecteurs propres de l'opérateur de Dirichlet-Neumann correspondant à la forme non perturbée comme donnée de Dirichlet afin de reconstruire d'une manière stable la forme perturbée.

Les différents chapitres de ce document sont autonomes et peuvent être lus indépendamment. Les résultats obtenus font l'objet de quatre pré-publications [5, 6, 7, 36].

Introduction

Natural gas is supplied through a million miles of vast pipeline network. Pipeline companies have an impressive safety record due to the proactive role of standards and inspection of pipelines. Since the pipelines are getting old, there is a great need to identify corrosion, cracks, and other defects that can cause potential problems. Stress corrosion cracking can occur under a range of pipeline field conditions including soil type, stress, cathode potential, coating conditions and temperature. This type of defect is usually oriented along the lengthwise direction of the pipe. If not found and conditions persist, the cracks may grow and/or coalesce and eventually result in a leak or pipe rupture. There are also other types of defects that can occur in pipe structures. They are either critical to the safety of the pipeline like corrosion, welding cracks, pits etc or benign stringer-like internal inclusions. Non-destructive Inspection systems are strongly needed to be able to locate the defects early without false alarms from benign inclusions, and to characterize and size the defects for repair or replacement management.

In the field of nondestructive evaluation, new and improved techniques are constantly being sought to facilitate the detection of hidden corrosion in pipelines. Hidden corrosion and defects can cause serious problems and is responsible for millions of euros annually in cost of replacement infrastructure and lost production, and is a dangerous threat to safety and to the environment. It is of great importance to

detect and to quantify most unseen potential hazards before they become problems.

Corrosion occurs in many different forms and several different models can be encountered in the literature (see, for example, Kaup and Santosa [31], Kaup et al. [32], Vogelius and Xu [46], Inglese [25], Luong and Santosa [26], Banks et al. [11] and references therein).

In this thesis, the effect of corrosion is described by means of Robin boundary conditions. This is motivated by a number of favorable indications. A first indication is based on the observation that corrosion tends to roughen a surface: in fact, this effect can be modelled by the introduction of a thin coating characterized by rapid oscillations. In the limit where the thickness of the coating goes to zero and the rapidity of the oscillations diverges, the arising of Robin boundary conditions has been observed by Buttazo and Kohn [13]. On the other hand, the study of electrochemical corrosion processes can be based on Faraday's law which says that the mass loss which is a measure of corrosion is proportional to the normal current flux. In Vogelius and Xu [46] a potential model of this kind of process is proposed. If we linearize with respect to the transfer coefficient the nonlinear boundary conditions in [46], we get Robin boundary conditions.

The inverse problem of corrosion detection consists of the determination of the corrosion damage of an inaccessible part of the surface of a specimen when the available data are on the accessible part.

Difficulties of this inverse problem result from its inherent ill-posedness and nonlinearity. Most of the techniques for detecting the corrosion are based on iterative algorithms: least-square algorithms and Newton-type iteration schemes. In these methods, one needs tremendous computational costs and time to get a close image to the true solution, since these iterative algorithms may not converge to an approximate solution.

The purpose of this work is to design a direct (non-iterative) tech-

nique for detecting corrosion in pipelines from voltage-to-current observations. Our new algorithm is of MUSIC-type (multiple signal classification) and is based on an accurate asymptotic representation formula for the steady state current perturbations.

Following an asymptotic formalism, in much the same spirit as the work in [8] and recent text [4], we develop in this thesis new non-iterative methods to address the inverse problem of identifying an internal corrosive part of small Hausdorff measure in a pipeline by (i) electrical impedance, (ii) vibration analysis, and (iii) ultrasonic waves. Our new algorithms are based on accurate asymptotic representation formulae for the data.

In the first chapter, we establish an asymptotic representation formula for the steady state currents caused by internal corrosive parts of small Hausdorff measures. Based on this formula we design a non-iterative method of MUSIC (multiple signal classification) type for localizing the corrosive parts from voltage-to-current observations.

The vibration behavior of structures can be characterized in terms of resonance frequencies and mode shapes which describe properties of the tested object in a global way but do not in general provide information about structural details. Our aim in the second chapter is to develop a simple method to address the inverse problem of identifying an internal corrosive part of small Hausdorff measure in a pipeline by vibration analysis. The viability of our reconstruction method is documented by a variety of numerical results from synthetic, noiseless and noisy data.

In the third chapter, we develop three closely-related methods to address the inverse problem of identifying a collection of disjoint internal corrosive parts of small Hausdorff measures in pipelines from exterior ultrasonic boundary measurements. Our approaches also allow us to determine the actual number of corrosive parts present, as well as make use of one or multiple ultrasonic waves.

In the fourth chapter, we consider the problem of determining the boundary perturbations of an object from far-field electric or acoustic measurements. Assuming that the unknown object boundary is a small perturbation of a circle, we develop a linearized relation between the far-field data that result from fixed Dirichlet boundary conditions, entering as parameters, and the shape of the object, entering as variables. This relation is used to find the Fourier coefficients of the perturbation of the shape and makes use of an expansion of the Dirichlet-to-Neumann operator. It turns out that if the angular oscillations in the perturbation are less than $1/n$ then one needs to use the first n eigenvectors of the Dirichlet-to-Neumann operator corresponding to the unperturbed shape as Dirichlet boundary data.

The four chapters of this manuscript are self-contained and can be read independently. Results from this thesis will appear in [5, 6, 7, 36].

Chapter 1

A MUSIC-type Algorithm for Detecting Internal Corrosion from Electrostatic Boundary Measurements

1.1 Introduction

In this chapter, we establish an asymptotic representation formula for the steady state currents caused by internal corrosive parts of small Hausdorff measures. Based on this formula we design a non-iterative method of MUSIC (multiple signal classification) type for localizing the corrosive parts from voltage-to-current observations.

The purpose of this work is to design a direct (non-iterative) technique for detecting corrosion in pipelines from voltage-to-current observations. Our new algorithm is of MUSIC-type (multiple signal classification) and is based on an accurate asymptotic representation formula for the steady state current perturbations.

To set up our problem mathematically, we consider a simply con-

nected bounded C^2 domain U in \mathbb{R}^2 , and a simply connected C^2 domain D compactly contained in U . Let $\Omega = U \setminus \overline{D}$ represent the specimen to be inspected. We define $\Gamma_e = \partial U$ and $\Gamma_i = \partial D$ so that $\partial\Omega = \Gamma_i \cup \Gamma_e$. Suppose that the inaccessible surface Γ_i contains some corrosive parts I_s , $s = 1, \dots, m$. The parts I_s are well-separated and the reciprocal of the surface impedance (the corrosion coefficient) of each I_s , $s = 1, \dots, m$, is $\gamma_s \geq 0$, not identically zero. We assume that each $\gamma_s \in C^1(I_s)$. Let

$$\gamma(x) = \sum_{s=1}^m \gamma_s \chi_s(x), \quad x \in \Gamma_i, \quad (1.1.1)$$

where χ_s denotes the characteristic function on I_s . The domain Ω in two dimensions may be considered as a cross section of a pipe inside which there are corrosive parts. A typical shape of Ω is an annulus. We assume that the one-dimensional Hausdorff measures of I_s are small:

$$|I_s| = O(\epsilon), \quad s = 1, \dots, m, \quad (1.1.2)$$

where ϵ is a small parameter representing the common order of magnitude of I_s . Here and throughout this chapter $|\cdot|$ denotes the one-dimensional Hausdorff measure. Then for each $p \geq 1$, we have

$$\|\gamma\|_{L^p(\Gamma_i)} \leq C\epsilon^{1/p}. \quad (1.1.3)$$

The voltage potential u_ϵ generated by a voltage f applied on Γ_e satisfies

$$\begin{cases} \Delta u_\epsilon = 0 & \text{in } \Omega, \\ -\frac{\partial u_\epsilon}{\partial \nu} + \gamma u_\epsilon = 0 & \text{on } \Gamma_i, \\ u_\epsilon = f & \text{on } \Gamma_e, \end{cases} \quad (1.1.4)$$

where ν is the outward unit normal to Ω on Γ_e and inward on Γ_i . Since f may have a variable sign, u_ϵ may vanish somewhere on Γ_i and thus, the formula $\gamma = (1/u_\epsilon) \partial u_\epsilon / \partial \nu$ may be undetermined or highly unstable.

The Cauchy data continuation technique as described in the paper by Yang, Choulli, and Cheng [47], which is well justified for the heat equation since the assumption of a non-negative prescribed boundary data is realistic, fails for the electrostatic model for detecting corrosion.

The aim of this chapter is to detect the well-separated corrosive parts I_s , in particular, their locations $z_s \in I_s$, $s = 1, \dots, m$, from measurements of the boundary perturbations $u_\epsilon - u_0$ on Γ_e , where u_0 is the solution in absence of the corrosion, *i. e.*, the solution to the problem

$$\begin{cases} \Delta u_0 = 0 & \text{in } \Omega, \\ -\frac{\partial u_0}{\partial \nu} = 0 & \text{on } \Gamma_i, \\ u_0 = f & \text{on } \Gamma_e. \end{cases} \quad (1.1.5)$$

The chapter is organized as follows. We review in the next section some basic facts on the layer potentials. In Section 1.3 we establish a representation formula for the unique solution to (1.1.4). This formula generalizes the formula proved by Kang and Seo in [27, 28]. Our aim in Section 1.4 is to rigorously derive an asymptotic expansion of $u_\epsilon - u_0$ on Γ_e . Section 1.5 is devoted to the imaging of the corrosive parts I_s . We present a non-iterative method of MUSIC type that allows us to reconstruct their locations $z_s \in I_s$ from measurements of current boundary perturbations.

1.2 Layer Potentials

Let us first review some well-known properties of the layer potentials for the Laplacian and prove some useful identities. The theory of layer potentials has been developed in relation to boundary value problems.

Let $\Phi(x)$ be the fundamental solution of the Laplacian Δ ,

$$\Phi(x) = \frac{1}{2\pi} \ln |x|, \quad x \neq 0.$$

Let D be a bounded Lipschitz domain D in \mathbb{R}^2 , and let $\Gamma := \partial D$. Let $H^1(D)$ denote the set of functions $f \in L^2(D)$ such that $\nabla f \in L^2(D)$. Further, we define $H^2(D)$ as the space of functions $u \in H^1(D)$ such that $\partial^2 u \in L^2(D)$ and the space $H^{3/2}(D)$ as the interpolation space $[H^1(D), H^2(D)]_{1/2}$. Let $H^{1/2}(\partial D)$ be the set of traces of functions in $H^1(D)$ and $H^{-1/2}(\partial D) = (H^{1/2}(\partial D))^*$. Finally, let $H^1(\partial D)$ denote the set of functions $f \in L^2(\partial D)$ such that $\partial f / \partial T \in L^2(\partial D)$, where $\partial / \partial T$ is the tangential derivative.

We will denote the single and double layer potentials of a function $\varphi \in L^2(\Gamma)$ as $\mathcal{S}_\Gamma[\varphi]$ and $\mathcal{D}_\Gamma[\varphi]$, respectively, where

$$\mathcal{S}_\Gamma[\varphi](x) := \int_\Gamma \Phi(x-y)\varphi(y) ds(y), \quad x \in \mathbb{R}^2, \quad (1.2.1)$$

$$\mathcal{D}_\Gamma[\varphi](x) := \int_\Gamma \frac{\partial}{\partial \nu_y} \Phi(x-y)\varphi(y) ds(y), \quad x \in \mathbb{R}^2 \setminus \Gamma. \quad (1.2.2)$$

For a function u defined on $\mathbb{R}^2 \setminus \Gamma$, we denote

$$\frac{\partial u}{\partial \nu} \Big|_{\pm}(x) := \lim_{t \rightarrow 0^+} \langle \nabla u(x \pm t\nu_x), \nu_x \rangle, \quad x \in \Gamma,$$

if the limit exists. Here ν is the outward unit normal to $\Gamma = \partial D$ at x , and $\langle \cdot, \cdot \rangle$ denotes the scalar product in \mathbb{R}^2 . $u|_{\pm}$ is defined likewise.

Throughout this chapter we assume that the domains under consideration have \mathcal{C}^2 boundaries. It is just for the simplicity and all the results of this chapter are valid even if the domains are $\mathcal{C}^{1,\alpha}$ for some positive α .

It is well-known, see [21] for example, that for a \mathcal{C}^2 -domain that for $\varphi \in L^2(\Gamma)$

$$\frac{\partial(\mathcal{S}_\Gamma[\varphi])}{\partial \nu} \Big|_{\pm}(x) = \left(\pm \frac{1}{2}I + \mathcal{K}_\Gamma^* \right) [\varphi](x), \quad x \in \Gamma, \quad (1.2.3)$$

$$\mathcal{D}_\Gamma[\varphi] \Big|_{\pm}(x) = \left(\mp \frac{1}{2}I + \mathcal{K}_\Gamma \right) [\varphi](x), \quad x \in \Gamma, \quad (1.2.4)$$

where \mathcal{K}_Γ is defined by

$$\mathcal{K}_\Gamma[\varphi](x) = \frac{1}{2\pi} \int_\Gamma \frac{\langle y-x, \nu_y \rangle}{|x-y|^2} \varphi(y) ds(y)$$

and \mathcal{K}_Γ^* is the L^2 -adjoint of \mathcal{K}_Γ , i. e.,

$$\mathcal{K}_\Gamma^*[\varphi](x) = \frac{1}{2\pi} \int_\Gamma \frac{\langle x-y, \nu_x \rangle}{|x-y|^2} \varphi(y) ds(y).$$

Since Γ is a \mathcal{C}^2 curve, there is a constant C such that

$$\frac{|\langle x-y, \nu_x \rangle|}{|x-y|^2} \leq C, \quad x, y \in \Gamma \quad (1.2.5)$$

Therefore \mathcal{K}_Γ^* is a compact operator on $L^p(\Gamma)$ for any $p \geq 1$. Let $L_0^p(\Gamma) := \{\varphi \in L^p(\Gamma) : \int_\Gamma \varphi ds = 0\}$. A proof of the following lemma can be found in [21].

Lemma 1.2.1 *If $p \geq 1$, then the operator $\frac{1}{2}I + \mathcal{K}_\Gamma$ is invertible on $L^p(\Gamma)$ as well as on $\mathcal{C}^k(\Gamma)$ for $k = 1, 2$.*

If Γ is a circle of radius r , then for $x, y \in \Gamma$,

$$\frac{\langle \nu_x, x-y \rangle}{|x-y|^2} = \frac{1}{2r},$$

and hence

$$\mathcal{K}_\Gamma^*[\varphi](x) = \frac{1}{4\pi r} \int_\Gamma \varphi(y) ds(y). \quad (1.2.6)$$

It then follows from (1.2.3) and (1.2.6) that

$$\mathcal{S}_\Gamma[1](x) = \begin{cases} r \log r & \text{if } |x| \leq r, \\ r \log |x| & \text{if } |x| \geq r. \end{cases} \quad (1.2.7)$$

Finally, we recall the following mapping properties of the single layer potentials for later use. If $p > 1$, there is a constant C_p such that

$$\|\mathcal{S}_\Gamma[\varphi]\|_{L^\infty(\Gamma)} \leq C_p \|\varphi\|_{L^p(\Gamma)} \quad (1.2.8)$$

for all $\varphi \in L^p(\Gamma)$. In fact, (1.2.8) can be proved using the Hölder inequality. The following property is well-known:

$$\|\mathcal{S}_\Gamma[\varphi]\|_{H^1(D)} \leq C \|\varphi\|_{L^2(\Gamma)} \quad (1.2.9)$$

for any $\varphi \in L^2(\Gamma)$.

1.3 Representation Formula

Recall that $\Omega = U \setminus \overline{D}$ and where U and D are bounded domains with \mathcal{C}^2 boundaries. Let $\Gamma_e = \partial U$ and $\Gamma_i = \partial D$. For $f \in H^1(\Gamma_e)$, let u_0 be the solution in absence of the corrosion, *i.e.*, the solution to the problem (1.1.5). We seek to represent the solution u_0 to (1.1.5) in the following form:

$$u_0 = \mathcal{D}_{\Gamma_e}[\varphi_0] + \mathcal{S}_{\Gamma_i}[\psi_0] \quad \text{in } \Omega$$

for some functions $\varphi_0 \in H^1(\Gamma_e)$ and $\psi_0 \in L^2(\Gamma_i)$. Then by the boundary conditions in (1.1.5) and jump relations (1.2.4) and (1.2.3), the pair (φ_0, ψ_0) should satisfy

$$\begin{pmatrix} \frac{1}{2}I + \mathcal{K}_{\Gamma_e} & \mathcal{S}_{\Gamma_i} \\ -\frac{\partial}{\partial \nu_i} \mathcal{D}_{\Gamma_e} & -\frac{1}{2}I - \mathcal{K}_{\Gamma_i}^* \end{pmatrix} \begin{pmatrix} \varphi_0 \\ \psi_0 \end{pmatrix} = \begin{pmatrix} f \\ 0 \end{pmatrix} \in H^1(\Gamma_e) \times L^2(\Gamma_i), \quad (1.3.1)$$

where ν_e and ν_i indicate the normal derivatives on Γ_e and Γ_i in the direction outward to U and D , respectively.

Lemma 1.3.1 *For $p > 1$, let $X_p := L^p(\Gamma_e) \times L^p(\Gamma_i)$ and*

$$A_0 := \begin{pmatrix} \frac{1}{2}I + \mathcal{K}_{\Gamma_e} & \mathcal{S}_{\Gamma_i} \\ -\frac{\partial}{\partial \nu_i} \mathcal{D}_{\Gamma_e} & -\frac{1}{2}I - \mathcal{K}_{\Gamma_i}^* \end{pmatrix}.$$

Then A_0 is invertible on X_p as well as on $H^1(\Gamma_e) \times L^2(\Gamma_i)$.

Proof. Since there is a distance between Γ_e and Γ_i , the operator A_0 is a compact perturbation of

$$\begin{pmatrix} \frac{1}{2}I + \mathcal{K}_{\Gamma_e} & 0 \\ 0 & -\frac{1}{2}I - \mathcal{K}_{\Gamma_i}^* \end{pmatrix},$$

which is known to be invertible on X_p (Lemma 1.2.1). Therefore, it suffices, by applying the Fredholm alternative, to show that the operator A_0 is injective.

Suppose that $(\varphi, \psi) \in X_p$ satisfies

$$A_0 \begin{pmatrix} \varphi \\ \psi \end{pmatrix} = 0.$$

Since $(\frac{1}{2}I + \mathcal{K}_{\Gamma_e})[\varphi] = -\mathcal{S}_{\Gamma_i}[\psi]$ on Γ_e and $\mathcal{S}_{\Gamma_i}[\psi]$ is \mathcal{C}^2 in Γ_e , we have in particular $\varphi \in H^1(\Gamma_e)$. Likewise we can show that $\psi \in L^2(\Gamma_i)$. Therefore, the function u defined by $u = \mathcal{D}_{\Gamma_e}[\varphi] + \mathcal{S}_{\Gamma_i}[\psi]$ in Ω is the solution in $H^{3/2}(\Omega)$ to (1.1.5) with $f = 0$. Since such a solution to (1.1.5) is unique, we have

$$\mathcal{D}_{\Gamma_e}[\varphi] + \mathcal{S}_{\Gamma_i}[\psi] = 0 \quad \text{in } \Omega,$$

and hence

$$\mathcal{D}_{\Gamma_e}[\varphi] + \mathcal{S}_{\Gamma_i}[\psi] = 0 \quad \text{in } U.$$

It then follows from (1.2.3) that

$$\begin{aligned} \psi &= \frac{\partial}{\partial \nu} \mathcal{S}_{\Gamma_i}[\psi] \Big|_+ - \frac{\partial}{\partial \nu} \mathcal{S}_{\Gamma_i}[\psi] \Big|_- \\ &= \frac{\partial}{\partial \nu} (\mathcal{D}_{\Gamma_e}[\varphi] + \mathcal{S}_{\Gamma_i}[\psi]) \Big|_+ - \frac{\partial}{\partial \nu} (\mathcal{D}_{\Gamma_e}[\varphi] + \mathcal{S}_{\Gamma_i}[\psi]) \Big|_- = 0 \quad \text{on } \Gamma_i. \end{aligned}$$

Now we have $\mathcal{D}_{\Gamma_e}[\varphi] = 0$ in U . Since $\frac{1}{2}I + \mathcal{K}_{\Gamma_e}$ is invertible on $L^2(\Gamma_e)$, it follows from (1.2.4) that $\varphi = 0$.

Note that A_0 maps $H^1(\Gamma_e) \times L^2(\Gamma_i)$ into itself. Moreover if $A_0 \begin{pmatrix} \varphi \\ \psi \end{pmatrix} \in H^1(\Gamma_e) \times L^2(\Gamma_i)$, then $(\frac{1}{2}I + \mathcal{K}_{\Gamma_e})[\varphi] + \mathcal{S}_{\Gamma_i}[\psi] \in H^1(\Gamma_e)$. Since $\mathcal{S}_{\Gamma_i}[\psi] \in H^1(\Gamma_e)$, it follows that $\psi \in H^1(\Gamma_e)$. Hence A_0 is invertible on $H^1(\Gamma_e) \times L^2(\Gamma_i)$. This completes the proof. \square

As an immediate consequence of Lemma 1.3.1, we obtain the following theorem.

Theorem 1.3.2 *The solution u_0 to (1.1.5) can be represented as*

$$u_0 = \mathcal{D}_{\Gamma_e}[\varphi_0] + \mathcal{S}_{\Gamma_i}[\psi_0] \quad \text{in } \Omega,$$

where (φ_0, ψ_0) is the unique solution to (1.3.1).

We now derive a similar representation for u_ϵ , the solution to (1.1.4). The method of derivation is basically the same as before. In this case the relevant integral operator is

$$A_\gamma := \begin{pmatrix} \frac{1}{2}I + \mathcal{K}_{\Gamma_e} & \mathcal{S}_{\Gamma_i} \\ -\frac{\partial}{\partial \nu_i} \mathcal{D}_{\Gamma_e} + \gamma \mathcal{D}_{\Gamma_e} & -\frac{1}{2}I - \mathcal{K}_{\Gamma_i}^* + \gamma \mathcal{S}_{\Gamma_i} \end{pmatrix}.$$

Observe that

$$A_\gamma = A_0 + M_\gamma B, \tag{1.3.2}$$

where M_γ is the multiplier by γ and

$$B = \begin{pmatrix} 0 & 0 \\ \mathcal{D}_{\Gamma_e} & \mathcal{S}_{\Gamma_i} \end{pmatrix}.$$

Then we have

$$\begin{aligned} \left\| M_\gamma B \begin{pmatrix} \varphi \\ \psi \end{pmatrix} \right\|_{X_p} &\leq \|\gamma\|_{L^p(\Gamma_i)} \|\mathcal{D}_{\Gamma_e}[\varphi] + \mathcal{S}_{\Gamma_i}[\psi]\|_{L^\infty(\Gamma_i)} \\ &\leq C\epsilon^{1/p} \left\| \begin{pmatrix} \varphi \\ \psi \end{pmatrix} \right\|_{X_p}, \end{aligned}$$

for some C independent of ϵ provided that $p > 1$. In other words, we have a bound for the operator norm $\|M_\gamma B A_0^{-1}\|_p$ of $M_\gamma B A_0^{-1}$ on X_p :

$$\|M_\gamma B A_0^{-1}\|_p \leq C\epsilon^{1/p}. \tag{1.3.3}$$

Thus, if ϵ is sufficiently small, then A_γ is invertible on X_p and we have the following theorem.

Theorem 1.3.3 *The solution u_ϵ to (1.1.4) can be represented as*

$$u_\epsilon = \mathcal{D}_{\Gamma_\epsilon}[\varphi_\epsilon] + \mathcal{S}_{\Gamma_i}[\psi_\epsilon] \quad \text{in } \Omega,$$

where $(\varphi_\epsilon, \psi_\epsilon)$ is the unique solution in X_2 to

$$A_\gamma \begin{pmatrix} \varphi_\epsilon \\ \psi_\epsilon \end{pmatrix} = \begin{pmatrix} f \\ 0 \end{pmatrix}.$$

We now derive a complete expansion for u_ϵ in terms of u_0 . We first note that because of (1.3.2)

$$A_\gamma = (I + M_\gamma B A_0^{-1}) A_0, \quad (1.3.4)$$

and hence

$$A_\gamma^{-1} = A_0^{-1} (I + M_\gamma B A_0^{-1})^{-1}. \quad (1.3.5)$$

Note that

$$M_\gamma B \begin{pmatrix} \varphi \\ \psi \end{pmatrix} = \begin{pmatrix} 0 \\ \gamma (\mathcal{D}_{\Gamma_\epsilon}[\varphi] + \mathcal{S}_{\Gamma_i}[\psi]) \end{pmatrix}. \quad (1.3.6)$$

By expanding (1.3.5) in terms of the Neumann series, we have

$$A_\gamma^{-1} = A_0^{-1} + \sum_{n=1}^{+\infty} (-1)^n A_0^{-1} (M_\gamma B A_0^{-1})^n.$$

Let

$$\begin{pmatrix} \varphi_n \\ \psi_n \end{pmatrix} := A_0^{-1} (M_\gamma B A_0^{-1})^n \begin{pmatrix} f \\ 0 \end{pmatrix}, \quad n = 0, 1, 2, \dots \quad (1.3.7)$$

Then we have

$$\begin{pmatrix} \varphi_\epsilon \\ \psi_\epsilon \end{pmatrix} = \sum_{n=0}^{+\infty} (-1)^n \begin{pmatrix} \varphi_n \\ \psi_n \end{pmatrix}.$$

Moreover, one can see from (1.3.7) that the following recursive relation holds:

$$\begin{pmatrix} \varphi_{n+1} \\ \psi_{n+1} \end{pmatrix} = A_0^{-1} M_\gamma B \begin{pmatrix} \varphi_n \\ \psi_n \end{pmatrix}, \quad n = 0, 1, 2, \dots \quad (1.3.8)$$

Let

$$u_n := \mathcal{D}_{\Gamma_e}[\varphi_n] + \mathcal{S}_{\Gamma_i}[\psi_n] \quad \text{in } \Omega, \quad n = 0, 1, 2, \dots, \quad (1.3.9)$$

so that

$$u_\epsilon = \sum_{n=0}^{+\infty} (-1)^n u_n \quad \text{in } \Omega.$$

Then u_0 is the solution to (1.1.5). By (1.3.6) and (1.3.8), we have

$$\begin{pmatrix} \varphi_n \\ \psi_n \end{pmatrix} = A_0^{-1} \begin{pmatrix} 0 \\ \gamma(\mathcal{D}_{\Gamma_e}[\varphi_{n-1}] + \mathcal{S}_{\Gamma_i}[\psi_{n-1}]) \end{pmatrix} = A_0^{-1} \begin{pmatrix} 0 \\ \gamma u_{n-1}|_{\Gamma_i} \end{pmatrix},$$

and hence u_n , $n \geq 1$, is the solution to

$$\begin{cases} \Delta u_n = 0 & \text{in } \Omega, \\ -\frac{\partial u_n}{\partial \nu} = \gamma u_{n-1} & \text{on } \Gamma_i, \\ u_n = 0 & \text{on } \Gamma_e. \end{cases} \quad (1.3.10)$$

So far we obtain the following result:

Theorem 1.3.4 *Let u_ϵ be the solution to (1.1.4) for a given $f \in H^1(\Gamma_e)$. Then*

$$u_\epsilon = \sum_{n=0}^{+\infty} (-1)^n u_n \quad \text{in } \Omega, \quad (1.3.11)$$

where u_0 is the solution to (1.1.5) and u_n is the solution to (1.3.10). The series converges in $H^{3/2}(\Omega)$.

1.4 Asymptotic Expansion

We now derive an asymptotic expansion of $\frac{\partial}{\partial \nu}(u_\epsilon - u_0)$ on Γ_e as $\epsilon \rightarrow 0$, on which our detection algorithm will be based. Let us begin with

investigating a regularity property of the boundary value problem

$$\begin{cases} \Delta u = 0 & \text{in } \Omega, \\ -\frac{\partial u}{\partial \nu} = \gamma g & \text{on } \Gamma_i, \\ u = 0 & \text{on } \Gamma_e. \end{cases} \quad (1.4.1)$$

We have shown that the solution u to (1.4.1) can be represented as

$$u := \mathcal{D}_{\Gamma_e}[\varphi] + \mathcal{S}_{\Gamma_i}[\psi] \quad \text{in } \Omega,$$

where (φ, ψ) is the solution to

$$A_0 \begin{pmatrix} \varphi \\ \psi \end{pmatrix} = \begin{pmatrix} 0 \\ \gamma g \end{pmatrix},$$

namely,

$$\begin{cases} \left(\frac{1}{2}I + \mathcal{K}_{\Gamma_e}\right) [\varphi] + \mathcal{S}_{\Gamma_i}[\psi] = 0 & \text{on } \Gamma_e, \\ -\frac{\partial}{\partial \nu} \mathcal{D}_{\Gamma_e}[\varphi] - \left(\frac{1}{2}I + \mathcal{K}_{\Gamma_i}^*\right) [\psi] = \gamma g & \text{on } \Gamma_i. \end{cases} \quad (1.4.2)$$

Since A_0 is invertible on X_p , we have in particular that

$$\|\psi\|_{L^p(\Gamma_i)} \leq \|\gamma g\|_{L^p(\Gamma_i)} \leq C\epsilon^{1/p} \|g\|_{L^\infty(\Gamma_i)}. \quad (1.4.3)$$

Let $2\delta = \text{dist}(\Gamma_i, \Gamma_e)$ and $\Omega_\delta := \{x \in \Omega \mid \text{dist}(x, \Gamma_e) \leq \delta\}$. Then, we have

$$\|\mathcal{S}_{\Gamma_i}[\psi]\|_{C^2(\Omega_\delta)} \leq C \|\psi\|_{L^p(\Gamma_i)} \leq C\epsilon^{1/p} \|g\|_{L^\infty(\Gamma_i)}.$$

It then follows from the first equation in (1.4.2) and Lemma 1.2.1 that

$$\begin{aligned} \|\varphi\|_{C^2(\Gamma_e)} &= \left\| \left(\frac{1}{2}I + \mathcal{K}_{\Gamma_e}\right)^{-1} [(\mathcal{S}_{\Gamma_i}\psi)|_{\Gamma_i}] \right\|_{C^2(\Gamma_e)} \\ &\leq C \|\mathcal{S}_{\Gamma_i}[\psi]\|_{C^2(\Gamma_e)} \\ &\leq C_p \epsilon^{1/p} \|g\|_{L^\infty(\Gamma_i)}. \end{aligned} \quad (1.4.4)$$

Therefore, we have

$$\left\| \frac{\partial u}{\partial \nu} \right\|_{C^1(\Gamma_e)} \leq \| \mathcal{D}_{\Gamma_e}[\varphi] + \mathcal{S}_{\Gamma_i}[\psi] \|_{C^2(\Omega_\delta)} \leq C_p \epsilon^{1/p} \|g\|_{L^\infty(\Gamma_i)}.$$

We have proved the following lemma.

Lemma 1.4.1 *Let u be the solution to (1.4.1). Then, for each $p > 1$ there is a constant C_p independent of g such that*

$$\left\| \frac{\partial u}{\partial \nu} \right\|_{C^1(\Gamma_e)} \leq C_p \epsilon^{1/p} \|g\|_{L^\infty(\Gamma_i)}. \quad (1.4.5)$$

We now have from (1.3.10), (1.3.11), and (1.4.5) that

$$\sum_{n=2}^{+\infty} \left\| \frac{\partial u_n}{\partial \nu} \right\|_{C^1(\Gamma_e)} \leq C_p \sum_{n=2}^{+\infty} \epsilon^{1/p} \|u_{n-1}\|_{L^\infty(\Gamma_i)}.$$

We also get from (1.3.9) that

$$\|u_{n-1}\|_{L^\infty(\Gamma_i)} = \| \mathcal{D}_{\Gamma_e}[\varphi_{n-1}] + \mathcal{S}_{\Gamma_i}[\psi_{n-1}] \|_{L^\infty(\Gamma_i)} \leq C_p \left\| \begin{pmatrix} \varphi_{n-1} \\ \psi_{n-1} \end{pmatrix} \right\|_{X_p}.$$

It then follows from (1.3.3) and (1.3.7) that

$$\|u_{n-1}\|_{L^\infty(\Gamma_i)} \leq C_p \epsilon^{\frac{n-1}{p}} \|f\|_{L^p(\Gamma_e)},$$

and hence for $k = 1, 2, \dots$,

$$\sum_{n=k}^{+\infty} \left\| \frac{\partial u_n}{\partial \nu} \right\|_{C^1(\Gamma_e)} \leq C_p \sum_{n=k}^{+\infty} \epsilon^{n/p} \|f\|_{L^p(\Gamma_e)} \leq C_p (\epsilon^{k/p} / (1 - \epsilon^{1/p})) \|f\|_{L^p(\Gamma_e)}.$$

Thus we obtain the following theorem.

Proposition 1.4.2 *For all $p > 1$, there is a constant C_p such that*

$$\left\| \frac{\partial u_\epsilon}{\partial \nu} - \frac{\partial u_0}{\partial \nu} \right\|_{C^1(\Gamma_e)} \leq C_p \epsilon^{1/p} \|f\|_{L^p(\Gamma_e)}. \quad (1.4.6)$$

We now derive an approximation of the leading order term of $\frac{\partial u_\epsilon}{\partial \nu} - \frac{\partial u_0}{\partial \nu}$. We have

$$\frac{\partial u_\epsilon}{\partial \nu}(x) = \frac{\partial u_0}{\partial \nu}(x) - \frac{\partial u_1}{\partial \nu}(x) + O(\epsilon^{2/p})$$

uniformly in $x \in \Gamma_e$. Let us now derive a further approximation of $\frac{\partial u_1}{\partial \nu}$. For that purpose, let $G(x, y)$ be the Green's function for the problem (1.4.1), i.e., for each $x \in \Omega$, $G(x, y)$ is the solution to

$$\begin{cases} \Delta_y G(x, y) = -\delta_x & \text{in } \Omega, \\ \frac{\partial}{\partial \nu_y} G(x, y) = 0, & y \in \Gamma_i, \\ G(x, y) = 0, & y \in \Gamma_e. \end{cases} \quad (1.4.7)$$

Then the solution u to (1.4.1) is given by

$$u(x) = \int_{\Gamma_i} G(x, y) \gamma(y) g(y) ds(y), \quad x \in \Omega.$$

For each $x \in \Gamma_e$ we have

$$\frac{\partial u_1}{\partial \nu}(x) = \int_{\Gamma_i} \frac{\partial}{\partial \nu_x} G(x, y) \gamma(y) u_0(y) ds(y).$$

Since $\frac{\partial}{\partial \nu_x} G(x, y)$ is a C^2 function in $y \in \Gamma_i$ as long as $x \in \Gamma_e$, we have

$$\frac{\partial}{\partial \nu_x} G(x, y) \gamma(y) u_0(y) = \sum_{s=1}^m \left[\frac{\partial}{\partial \nu_x} G(x, z_s) u_0(z_s) + O(\epsilon) \right] \gamma(y) \chi_s(y),$$

where χ_s is the characteristic function of I_s . Thus we obtain

$$\frac{\partial u_1}{\partial \nu}(x) = \sum_{s=1}^m \frac{\partial}{\partial \nu_x} G(x, z_s) u_0(z_s) \int_{I_s} \gamma ds + O(\epsilon^2).$$

Put

$$\langle \gamma \rangle_s := \int_{I_s} \gamma ds.$$

Then we have obtained the following approximation formula.

Theorem 1.4.3 *The following formula holds uniformly for $x \in \Gamma_e$:*

$$\frac{\partial u_\epsilon}{\partial \nu}(x) = \frac{\partial u_0}{\partial \nu}(x) - \sum_{s=1}^m \langle \gamma \rangle_s u_0(z_s) \frac{\partial}{\partial \nu_x} G(x, z_s) + O(\epsilon^{1+\alpha}) \quad (1.4.8)$$

for some $\alpha > 0$.

1.5 MUSIC type algorithm for reconstruction

We now apply the asymptotic expansion (1.4.8) to design a MUSIC (MUltiple Signal Classification) algorithm for locating small internal corrosive parts from boundary measurements. MUSIC is generally used in signal processing problems as a method for estimating the individual frequencies of multiple-harmonic signals [43]. The MUSIC algorithm makes use of the eigenvalue structure of the multistatic response matrix for the Helmholtz equation and of the spectral structure of the boundary map for the Laplace operator, corresponding to a zero wavenumber. The eigenvectors corresponding to significant eigenvalues span some kind of signal subspace in the sense that they contain nearly all the information about the corrosive parts which can be extracted from the boundary map. The others span some kind of noise subspace. The aim of the MUSIC type of algorithm is to use the eigensystem analysis of a discrete version of the boundary map to determine the location and estimate the size of the small corrosive parts from the signal space.

It is worth mentioning that this algorithm is related to the linear sampling method of Colton and Kirsch [19]. We refer to Cheney [16] and Kirsch [34] for detailed discussions of the connection between the MUSIC algorithm and the linear sampling method.

Define the (voltage-to-current) map Λ_γ from $H^{1/2}(\Gamma_e)$ into $H^{-1/2}(\Gamma_e)$ by

$$\Lambda_\gamma(f) = \frac{\partial u_\epsilon}{\partial \nu} \Big|_{\Gamma_e}, \quad (1.5.1)$$

where u_ϵ is the solution to (1.1.4). Let Λ_0 be the Dirichlet-to-Neumann map for the case when no corrosion is present. We seek to use $\Lambda_\gamma - \Lambda_0$ to determine the corrosive parts.

The estimate (1.4.6) yields that

$$\|(\Lambda_\gamma - \Lambda_0)(f)\|_{C^1(\Gamma_e)} \leq C_p \epsilon^{1/p} \|f\|_{L^2(\Gamma_e)}, \quad (1.5.2)$$

for all p with $1 < p \leq 2$. The above estimate shows that the operator $\Lambda_\gamma - \Lambda_0$ originally defined on $H^{1/2}(\Gamma_e)$ can be extended to an operator on $L^2(\Gamma_e)$ and it is a compact operator. Thus we have the following lemma.

Lemma 1.5.1 $\Lambda_\gamma - \Lambda_0$ is self-adjoint, positive, and compact on $L^2(\Gamma_e)$.

The identity (1.4.8) shows that

$$(\Lambda_\gamma - \Lambda_0)(f)(x) = - \sum_{s=1}^m \langle \gamma \rangle_s u_0(z_s) \frac{\partial}{\partial \nu_x} G(x, z_s) + O(\epsilon^{1+\alpha}), \quad x \in \Gamma_e. \quad (1.5.3)$$

where $1+\alpha = 2/p$ and the remainder term $O(\epsilon^{1+\alpha})$ is bounded by $C_p \epsilon^{1/2} \|f\|_{L^2(\Gamma_e)}$.

Define the operator T on $H^{1/2}(\Gamma_e)$ by

$$(Tf)(x) = - \sum_{s=1}^m \langle \gamma \rangle_s u_0(z_s) \frac{\partial}{\partial \nu_x} G(x, z_s), \quad x \in \Gamma_e, \quad (1.5.4)$$

so that

$$\Lambda_\gamma - \Lambda_0 = T + O(\epsilon^{1+\alpha}). \quad (1.5.5)$$

Since u_0 depends linearly on f , T is linear. We first establish the following.

Lemma 1.5.2 The operator T can be extended to a compact, self-adjoint, positive semi-definite operator on $L^2(\Gamma_e)$.

Proof. We first observe that T is a finite-dimensional operator and hence, it is compact. In order to prove that T is self-adjoint it suffices to show that it is symmetric. Let g and h be in $H^{1/2}(\Gamma_e)$ and denote u_0

and v_0 the solutions to (1.1.5) corresponding respectively to g and h . Then v_0 is given by

$$v_0(y) = - \int_{\Gamma_e} \frac{\partial}{\partial \nu_x} G(x, y) h(x) ds(x), \quad y \in \Omega, \quad (1.5.6)$$

and hence we have

$$\int_{\Gamma_e} T(g)h = \sum_{s=1}^m \langle \gamma \rangle_s u_0(z_s) v_0(z_s).$$

Consequently, we infer that T is self-adjoint, positive semi-definite. \square

Introduce now the linear operator $\mathcal{G} : L^2(\Gamma_e) \rightarrow \mathbb{R}^m$ defined by

$$\mathcal{G}f = (u_0(z_1), \dots, u_0(z_m)), \quad (1.5.7)$$

where u_0 is the solution to (1.1.4). Endowing \mathbb{R}^m with the standard Euclidean inner product, we then obtain

$$\langle \mathcal{G}f, a \rangle = \sum_{s=1}^m a_s u_0(z_s) = - \int_{\Gamma_e} \left(\sum_{s=1}^m a_s \frac{\partial}{\partial \nu_x} G(x, z_s) \right) f(x) ds(x),$$

for arbitrary $a = (a_1, \dots, a_m) \in \mathbb{R}^m$. Therefore, the adjoint $\mathcal{G}^* : \mathbb{R}^m \rightarrow L^2(\Gamma_e)$ is given by

$$\mathcal{G}^* a = - \sum_{s=1}^m a_s \frac{\partial}{\partial \nu_x} G(x, z_s). \quad (1.5.8)$$

Following Brühl et al. [12], the following characterization of the range of the operator T can be obtained.

Lemma 1.5.3 (i) \mathcal{G}^* is injective;

(ii) \mathcal{G} is surjective;

(iii) $T = \mathcal{G}^* \mathcal{M} \mathcal{G}$, where

$$\mathcal{M}a = \left(\gamma_1 a_1, \dots, \gamma_m a_m \right), \quad a = (a_1, \dots, a_m) \in \mathbb{R}^m;$$

(iv) $\text{Range}(T) = \text{span}\left\{\frac{\partial}{\partial \nu_x} G(x, z_s); s = 1, \dots, m\right\}$.

Proof. Suppose that $\mathcal{G}^* a = 0$. Then $\sum_{s=1}^m a_s v(z_s) = 0$ for any harmonic function v in Ω such that $\frac{\partial v}{\partial \nu} = 0$ on Γ_i . Since there exist a harmonic function v in $\mathbb{R}^2 \setminus \overline{D}$ such that $\frac{\partial v}{\partial n} = 0$ and $v = \varphi$ on Γ_i for any φ smooth on Γ_i , it follows that $a_s = 0$ for $s = 1, \dots, m$, and thus assertion (i) holds. Assertion (ii) follows from (i) and the well-known relation between the ranges and the null spaces of adjoint finite-dimensional operators: $\text{Range}(\mathcal{G}) = \text{Ker}(\mathcal{G}^*)^\perp$. Using (1.5.4), (1.5.7), and (1.5.8), it is easy to see that (iii) holds. Now according to (iii), we have $\text{Range}(T) = \text{Range}(\mathcal{G}^* \mathcal{M} \mathcal{G}) = \text{Range}(\mathcal{G}^*)$, since \mathcal{M} and \mathcal{G} are surjective. This yields (iv), and the proof is complete. \square

Now we present the main tool for the identification of the locations z_s of the small corrosive parts.

Theorem 1.5.4 *A point $z \in \Gamma_i$ belongs to the set $\{z_s : s = 1, \dots, m\}$ if and only if $\frac{\partial}{\partial \nu_x} G(\cdot, z)|_{\Gamma_e} \in \text{Range}(T)$.*

Proof. Assume that $\frac{\partial}{\partial \nu_x} G(\cdot, z)|_{\Gamma_e} \in \text{Range}(T)$. As a consequence of (iv) of Lemma 1.5.3, g_z may be represented as

$$\frac{\partial}{\partial \nu_x} G(x, z) = \sum_{s=1}^m a_s \frac{\partial}{\partial \nu_x} G(x, z_s), \quad \text{for } x \in \Gamma_e. \quad (1.5.9)$$

Since $G(x, z) = 0$ for any $x \in \Gamma_e$ and $z \in \Omega$, we have

$$G(x, z) = \sum_{s=1}^m a_s G(x, z_s), \quad \text{for } x \in \Omega. \quad (1.5.10)$$

This is only possible if $z \in \{z_s : s = 1, \dots, m\}$, and so we have established the necessity of this condition. The sufficiency follows immediately from (iv) in Lemma 1.5.3. \square

We are now ready to present the MUSIC type algorithm for detection of internal corrosion. The finite-dimensional self-adjoint operator T has the spectral decomposition

$$T = \sum_{p=1}^m \kappa_p v_p \otimes v_p, \quad \|v_p\|_{L^2(\Gamma_e)} = 1, \quad (1.5.11)$$

where κ_p are (non-zero) eigenvalues of T and v_p is the corresponding eigenfunction. Here we assume that $\kappa_1 \geq \kappa_2 \geq \dots \geq \kappa_m > 0$. Let $P_p : L_0^2(\Gamma_e) \rightarrow \text{span} \{v_1, \dots, v_p\}$, $p = 1, \dots, m$, be the orthogonal projector $P_p = \sum_{q=1}^p v_q \otimes v_q$. It then follows from Theorem 1.5.4 that

$$z \in \{z_s : s = 1, \dots, m\} \quad \text{iff} \quad (I - P_m) \left(\frac{\partial}{\partial v_x} G(\cdot, z) \Big|_{\Gamma_e} \right) = 0, \quad (1.5.12)$$

or equivalently,

$$z \in \{z_s : s = 1, \dots, m\} \quad \text{iff} \quad \cot \theta(z) = +\infty, \quad (1.5.13)$$

where the angle $\theta(z) \in [0, \pi/2)$ is defined by

$$\cot \theta(z) = \frac{\left\| P_m \left(\frac{\partial}{\partial v_x} G(\cdot, z) \Big|_{\Gamma_e} \right) \right\|_{L^2(\Gamma_e)}}{\left\| (I - P_m) \left(\frac{\partial}{\partial v_x} G(\cdot, z) \Big|_{\Gamma_e} \right) \right\|_{L^2(\Gamma_e)}}. \quad (1.5.14)$$

On the other hand, since $\Lambda_\gamma - \Lambda_0$ is a self-adjoint, positive, and compact operator on $L^2(\Gamma_e)$, it admits, the spectral decomposition

$$\Lambda_\gamma - \Lambda_0 = \sum_{p=1}^{+\infty} \kappa_p^\epsilon v_p^\epsilon \otimes v_p^\epsilon, \quad \|v_p^\epsilon\|_{L^2(\Gamma_e)} = 1, \quad (1.5.15)$$

with $\kappa_1^\epsilon \geq \kappa_2^\epsilon \geq \dots \geq \kappa_m^\epsilon \geq \dots \geq 0$. Let $P_p^\epsilon : L^2(\Gamma_e) \rightarrow \text{span} \{v_1^\epsilon, \dots, v_p^\epsilon\}$, $p = 1, 2, \dots$, be the orthogonal projector $P_p^\epsilon = \sum_{q=1}^p v_q^\epsilon \otimes v_q^\epsilon$. Because of (1.5.5) where the $O(\epsilon^{1+\alpha})$ term is bounded by $C\epsilon^{1+\alpha}\|f\|_{L^2(\Gamma_e)}$, standard arguments from perturbation theory for linear operators give (after appropriate enumeration of $\kappa_p^\epsilon, p = 1, \dots, m$)

$$\kappa_p^\epsilon = \kappa_p + O(\epsilon^{1+\alpha}) \quad \text{for } p = 1, 2, \dots, \quad (1.5.16)$$

where we have set $\kappa_p = 0$ for $p > m$, and

$$P_p^\epsilon = P_m + O(\epsilon^\alpha) \quad \text{for } p \geq m. \quad (1.5.17)$$

Now in view of (1.5.16) the number m of inclusions may be estimated by looking for a gap in the set of eigenvalues of $\Lambda_\gamma - \Lambda_0$. In order to recover the locations $z_s, s = 1, \dots, m$, one can estimate, using (1.5.17), the $\cot \theta_p(z)$ by

$$\cot \theta_p(z) = \frac{\left\| P_m^\epsilon \left(\frac{\partial}{\partial \nu_x} G(\cdot, z) \Big|_{\Gamma_e} \right) \right\|_{L^2(\Gamma_e)}}{\left\| (I - P_m^\epsilon) \left(\frac{\partial}{\partial \nu_x} G(\cdot, z) \Big|_{\Gamma_e} \right) \right\|_{L^2(\Gamma_e)}}. \quad (1.5.18)$$

If one plots $\cot \theta_m(z)$ as a function of z , we may see large values $\cot \theta_m(z)$ for z which are close to the locations z_s .

Once the locations z_s are found, we can estimate corrosion impedance $\langle \gamma \rangle_s$. Our procedure for doing this is the following. Define $u_s, s = 1, \dots, m$, to be the solution to

$$\begin{cases} \Delta u_s = 0 & \text{in } \Omega, \\ \frac{\partial u_s}{\partial \nu} = 0 & \text{on } \Gamma_i, \\ u_s(x) = \frac{\partial}{\partial \nu_x} G(x, z_s) & x \in \Gamma_e. \end{cases} \quad (1.5.19)$$

It then follows from (1.5.3) and (1.5.15) that

$$\begin{aligned} - \sum_{s=1}^m \langle \gamma \rangle_s u_{s'}(z_s) \frac{\partial}{\partial \nu_x} G(\cdot, z_s) &\approx (\Lambda_\gamma - \Lambda_0) \left(\frac{\partial}{\partial \nu_x} G(\cdot, z_{s'}) \right) \\ &\approx \sum_{p=1}^m \kappa_p^\epsilon \left\langle v_p, \frac{\partial}{\partial \nu_x} G(\cdot, z_{s'}) \right\rangle v_p. \end{aligned}$$

By integrating both sides of the above formula against $v_{s'}$, we obtain

$$- \sum_{s=1}^m u_{s'}(z_s) \left\langle v_{s'}, \frac{\partial}{\partial \nu_x} G(\cdot, z_s) \right\rangle \langle \gamma \rangle_s \approx \kappa_{s'}^\epsilon \left\langle v_{s'}, \frac{\partial}{\partial \nu_x} G(\cdot, z_{s'}) \right\rangle, \quad (1.5.20)$$

for $s' = 1, \dots, m$. Therefore the values of $\langle \gamma \rangle_s$, $s = 1, \dots, m$, can be calculated by solving a linear system. For the simplest case $m = 1$ the formula reads

$$\langle \gamma \rangle_1 \approx -\frac{\kappa_1^\epsilon}{u_1(z_1)}.$$

1.5.1 Numerical Results

This section presents some results of numerical experiments of finding the internal corrosive parts, $I_s \subset \mathbb{R}^2$, $s = 1, 2, \dots, m$, and illustrate the viability of the MUSIC-type algorithms we have designed. In the following, U and D in \mathbb{R}^2 are assumed to be the disks centered at $(0, 0)$ with radii r_e and r_i , respectively. And let $\Omega = U \setminus \overline{D}$ as before.

We take the Dirichlet-to-Neumann map $\Lambda_\gamma - \Lambda_0$ on Γ_e as our measurements for the reconstruction. To obtain this simulation data, we solve direct problems (1.1.4) and (1.1.5) for $f(x) = \frac{\partial G}{\partial \nu_x}(x, y)$ for $x \in \Gamma_e$ and $y \in \Gamma_i$. This is done by solving integral equations (1.3.1) and (1.3.4).

Let us briefly explain how we compute $\frac{\partial G}{\partial \nu_x}(x, y)$. Let \tilde{G} be the Green's function for U , that is, for each $x \in U$, $\tilde{G}(x, y)$ is the solution to

$$\begin{cases} \Delta_y \tilde{G} = 0 & \text{in } U, \\ \frac{\partial}{\partial \nu_y} \tilde{G}(x, y) = 0 & \text{on } \Gamma_e. \end{cases} \quad (1.5.21)$$

Since U is a disk, one can compute $\tilde{G}(x, y)$ explicitly. We then compute $\frac{\partial G}{\partial \nu_x}(x, y)$ by solving (1.5.22) in the following lemma.

Lemma 1.5.5 *For any $x \in \Gamma_e$ and $y \in \Gamma_i$, let $G_y(x) := G(x, y)$ and $\tilde{G}_y(x) = \tilde{G}(x, y)$. Then the following holds:*

$$\left(I + 2\mathcal{K}_{\Gamma_e}^* - 4 \frac{\partial \mathcal{S}_{\Gamma_i}}{\partial \nu_e} \frac{\partial \mathcal{S}_{\Gamma_e}}{\partial \nu_i} \right) \left[\frac{\partial G_y}{\partial \nu_e} \right] (x) = 2 \frac{\partial \tilde{G}_y}{\partial \nu_e}(x), \quad x \in \Gamma_e, \quad (1.5.22)$$

where ν_e and ν_i denote normal vectors on Γ_i and Γ_e , respectively.

Proof. Similarly to (1.3.1), it is easy to prove that

$$(G_z - \tilde{G}_z)(x) = -\mathcal{S}_{\Gamma_e}[G_z - \tilde{G}_z](x) + \mathcal{S}_{\Gamma_i}[\psi](x), \quad x \in \Omega,$$

where the density ψ is given by

$$\psi = -2\frac{\partial \tilde{G}_z}{\partial \nu} + 2\frac{\partial \mathcal{S}_{\Gamma_e}}{\partial \nu_i} \left[\frac{\partial (G_z - \tilde{G}_z)}{\partial \nu_e} \right], \quad \text{on } \Gamma_i.$$

Since $\tilde{G}_y(x) + \mathcal{S}_{\Gamma_e}[\frac{\partial \tilde{G}_y}{\partial \nu}](x) = -\Phi(x, y)$ for $x \in U$ which was proved in [3], (1.5.22) follows. \square

For computation, we discretize Γ_e and Γ_i given by

$$\Gamma_e = \{r_e(\cos \theta_n, \sin \theta_n) | \theta_n = 2\pi(n-1)/N, n = 0, 1, \dots, N-1\}$$

and

$$\Gamma_i = \{r_i(\cos \theta_n, \sin \theta_n) | \theta_n = 2\pi(n-1)/N, n = 0, 1, \dots, N-1\},$$

with $N = 256$. Put $x_n := r_e(\cos \theta_n, \sin \theta_n)$ and $y_n := r_i(\cos \theta_n, \sin \theta_n)$ for $n = 0, 2, \dots, 255$. We then compute 256×256 matrices $(\Lambda_\gamma - \Lambda_0)(\frac{\partial G}{\partial \nu})$ and $T(\frac{\partial G}{\partial \nu})$ where $(\Lambda_\gamma - \Lambda_0)(\frac{\partial G}{\partial \nu})$ denotes $((\Lambda_\gamma - \Lambda_0)(\frac{\partial G}{\partial \nu_x}(\cdot, y_m))(x_n))_{m,n=1}^{256}$ and $T(\frac{\partial G}{\partial \nu})$ is defined likewise. We then compute the singular value decomposition (SVD) of these two matrices.

Figure 1.1 is the SVD of $\Lambda_\gamma - \Lambda_0$ and T when there are two internal corrosion. It shows that the SVD of T exhibits the clear drop of the singular values after two significant ones, from which we can conclude that there are two corrosive parts. On the other hand the SVD of $\Lambda_\gamma - \Lambda_0$ does not have this clear drop of the singular values. It has many additional significant singular values. This is due to the $O(\epsilon^2)$ discrepancy between $\Lambda_\gamma - \Lambda_0$ and T . It means that we can not determine the number of corrosive parts using the singular values of $\Lambda_\gamma - \Lambda_0$. However, this difficulty can be easily remedied.

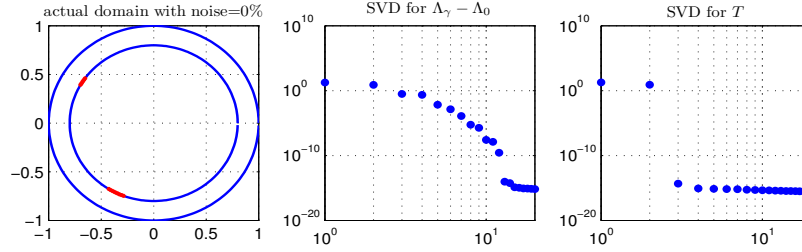


Figure 1.1: Pipe with two internal corrosive parts and SVD of $\Lambda_\gamma - \Lambda_0$ and T .

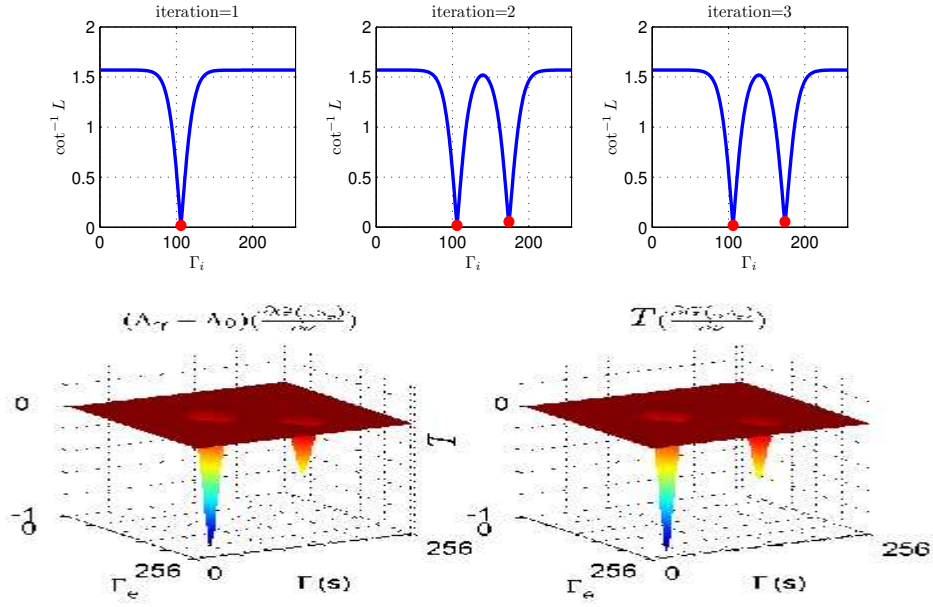
Let $\lambda_1 \geq \lambda_2 \geq \dots$ be the singular values of $\Lambda_\gamma - \Lambda_0$. Using the first m singular values, we compute the minimal values of $\cot^{-1} L$ where

$$L := \frac{\|P_m(\frac{\partial G(\cdot, z_s)}{\partial \nu})\|_{L^2(\Gamma_e)}}{\|(I - P_m)(\frac{\partial G(\cdot, z_s)}{\partial \nu})\|_{L^2(\Gamma_e)}}. \quad (1.5.23)$$

We do this process iteratively starting the largest singular value. The iteration stops if the minimal value of $\cot^{-1} L$ stabilizes.

Example 1. In this example, the outer radius $r_e = 1$ and the inner one $r_i = 0.8$ and there are two corrosive parts. Figure 1.1 shows the locations of the corrosion and the SVD of $\Lambda_\gamma - \Lambda_0$ and T . Figure 1.2 clearly shows that where there are two corrosive parts, the minimum of $\cot^{-1} L$ stabilizes after two iteration, from which we can conclude that there are two corrosive parts. The minimal points of $\cot^{-1} L$ is the locations of the corrosive parts. By solving (1.5.20), we compute the impedance of the corrosion: $\langle \gamma \rangle_1^c = 0.3846, \langle \gamma \rangle_2^c = 0.1660$. The actual impedance are $\langle \gamma \rangle_1 = 0.3927, \langle \gamma \rangle_2 = 0.1767$.

Example 2. In this example we consider the case where there are five corrosive parts. The actual data of the configuration is summarized in the top table of Table 1.1. The numbering of the corrosive parts is given



The results for iteration

iteration(k)	m	a_k	$ a_k - a_{k+1} $	z_s^c	$ z_s - z_s^c $
1	1	0.0175		(-0.6759, 0.4280)	
2	2	0.0174	2.0746e-008	(-0.6759, 0.4280)	0
		0.0547	6.0178e-012	(-0.3597, -0.7146)	0
3	2	0.0174	9.7484e-012	(-0.6759, 0.4280)	0
		0.0547	2.6916e-008	(-0.3597, -0.7146)	0

Figure 1.2: The top figure shows $\cot^{-1} L$ on each iteration. The second line of figures show $(\Lambda_\gamma - \Lambda_0)(\frac{\partial G}{\partial \nu})$, $T(\frac{\partial G}{\partial \nu})$, and $(\Lambda_\gamma - \Lambda_0 - T)(\frac{\partial G}{\partial \nu})$. In the table, m is the number of computed corrosive parts, $a_k := \min(\cot^{-1} L)$ on each iteration step k , z_s and z_s^c denote the actual locations and computed locations of the corrosive parts.

counter-clock-wise starting from the zero angles. Note that the first three corrosive parts have low corrosion coefficients while the other two have relatively high ones. The computational results with 1% noise are

summarized in Table 1.1 and Figure 1.3. It is interesting to note that the corrosion 2 and 3, which are close to each other and have low corrosion coefficients, are detected as a single one. On the other hand, the corrosion 4 and 5, which have high corrosion coefficients, are clearly detected at early stage of the iteration.

Example 3. Figure 1.4 shows the computational results with various degree of noise. The information of the location and the corrosion coefficients is summarized in Table 1.2. Observe that the first two corrosion have low corrosion coefficients. They are detected as a single one under 5% noise. The other two corrosive parts, which have high corrosion coefficients, are detected very well even under high ratio noise.

1.6 Conclusion

We have designed a non-iterative algorithm of MUSIC-type for detecting small internal corrosion from boundary measurements. Our method is based on an asymptotic representation formula for the steady state currents caused by internal corrosive parts of small Hausdorff measures. It is worth noticing the fact that it is impossible to extract the size of the corrosive parts. We can only reconstruct $\langle \gamma \rangle_s$ for $s = 1, \dots, m$. It is likely that from a certain level of signal-to-noise ratio, higher-order asymptotic expansions of the boundary perturbations yield such important information.

m	γ_s	z_s	$\langle \gamma \rangle_s$
5	0.1	(0.0686, 0.6966)	0.0120
	0.5	(-0.1197, 0.6897)	0.0430
	0.3	(-0.4307, 0.5518)	0.0206
	1.0	(0.2519, - 0.6531)	0.1203
	1.2	(0.5723, - 0.4031)	0.1031

detected data				
m^c	z_s^c	$\langle \gamma \rangle_s^c$	$ z_s - z_s^c $	$ \langle \gamma \rangle_s - \langle \gamma \rangle_s^c $
4	(-0.1027, 0.6924)	0.0514	0.0172	0.0084
	(-0.4170, 0.5622)	0.0212	0.0172	0.0006
	(0.2519, - 0.6531)	0.1181	0	0.0021
	(0.5723, - 0.4031)	0.1026	0	0.0005

result for iteration					
iteration(k)	m^c	a_k	$ a_k - a_{k+1} $	z_s^c	$ z_s - z_s^c $
1	1	0.3888		(0.3889, - 0.5820)	
2	2	0.2190		(-0.1366, + 0.6865)	
		0.3888		(0.3889, - 0.5820)	
3	3	0.2177		(-0.1366, + 0.6865)	
		0.0165		(0.2519, - 0.6531)	
		0.0143		(0.5723, - 0.4031)	
4	4	0.0742	0.0270	(-0.0686, + 0.6966)	0.0515
		0.1037	0.0502	(-0.4031, + 0.5723)	0.0344
		0.0164	7.9909e-011	(0.2519, - 0.6531)	0
		0.0141	2.0082e-005	(0.5723, - 0.4031)	0
5	4	0.0472	3.9986e-005	(-0.1027, + 0.6924)	0.0172
		0.0535	1.3118e-005	(-0.4170, + 0.5622)	0.0172
		0.0164	1.6488e-005	(0.2519, - 0.6531)	0
		0.0141	6.6178e-005	(0.5723, - 0.4031)	0
6	4	0.0471	9.8377e-006	(-0.1027, + 0.6924)	0.0172
		0.0535	3.7071e-006	(-0.4170, + 0.5622)	0.0172
		0.0164	6.9044e-006	(0.2519, - 0.6531)	0
		0.0140	4.6509e-007	(0.5723, - 0.4031)	0

Table 1.1: Summary of computational results for five corrosive parts. Two corrosive parts with low corrosion coefficient are detected as a single one.

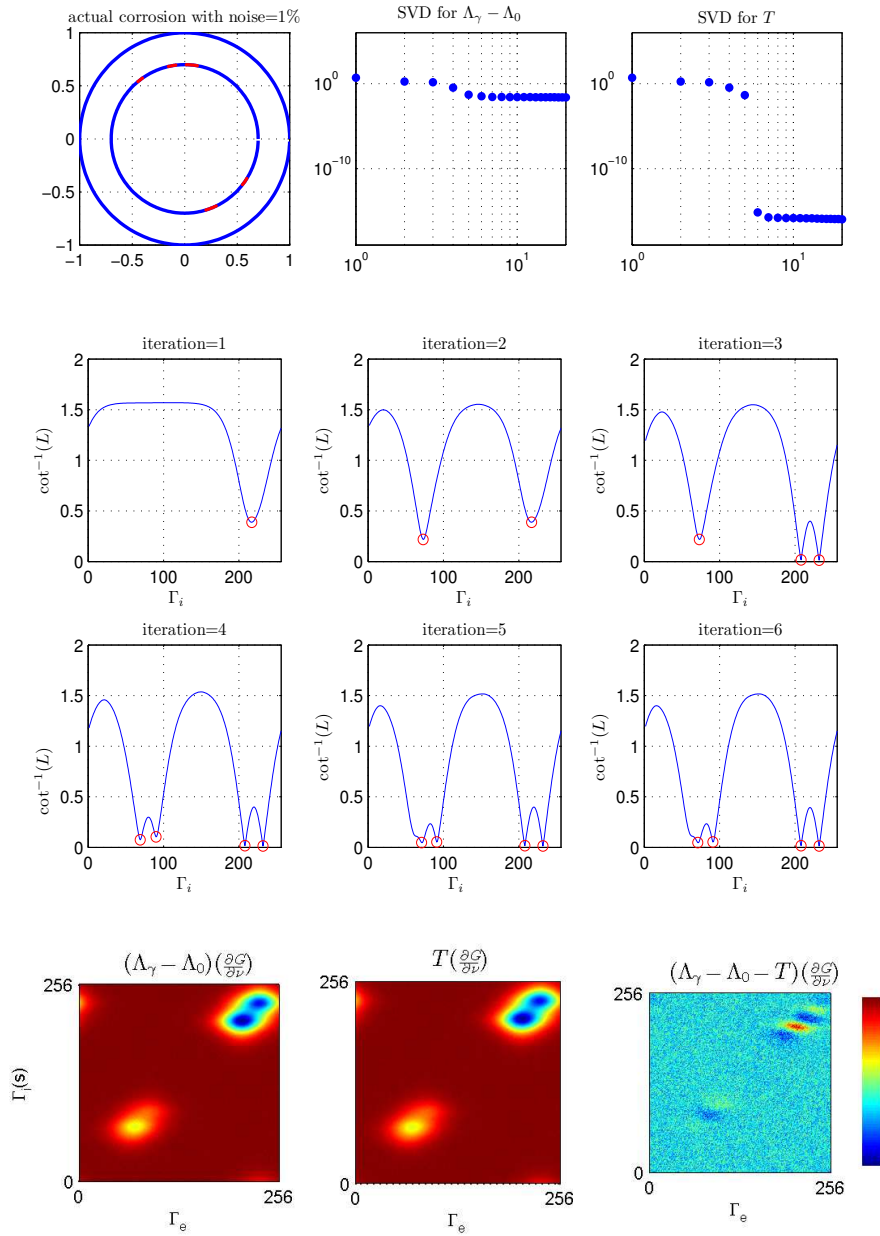


Figure 1.3: The computational results with noise 1%

m	γ_s	z_s	$\langle \gamma \rangle_s$
4	0.1	(0.5657, + 0.5657)	0.0137
	0.05	(0.3597, + 0.7146)	0.0049
	3.0	(0.6307, - 0.4922)	0.2945
	3.0	(0.6307, - 0.4922)	0.2945

Table 1.2: Pipe with four corrosive parts.

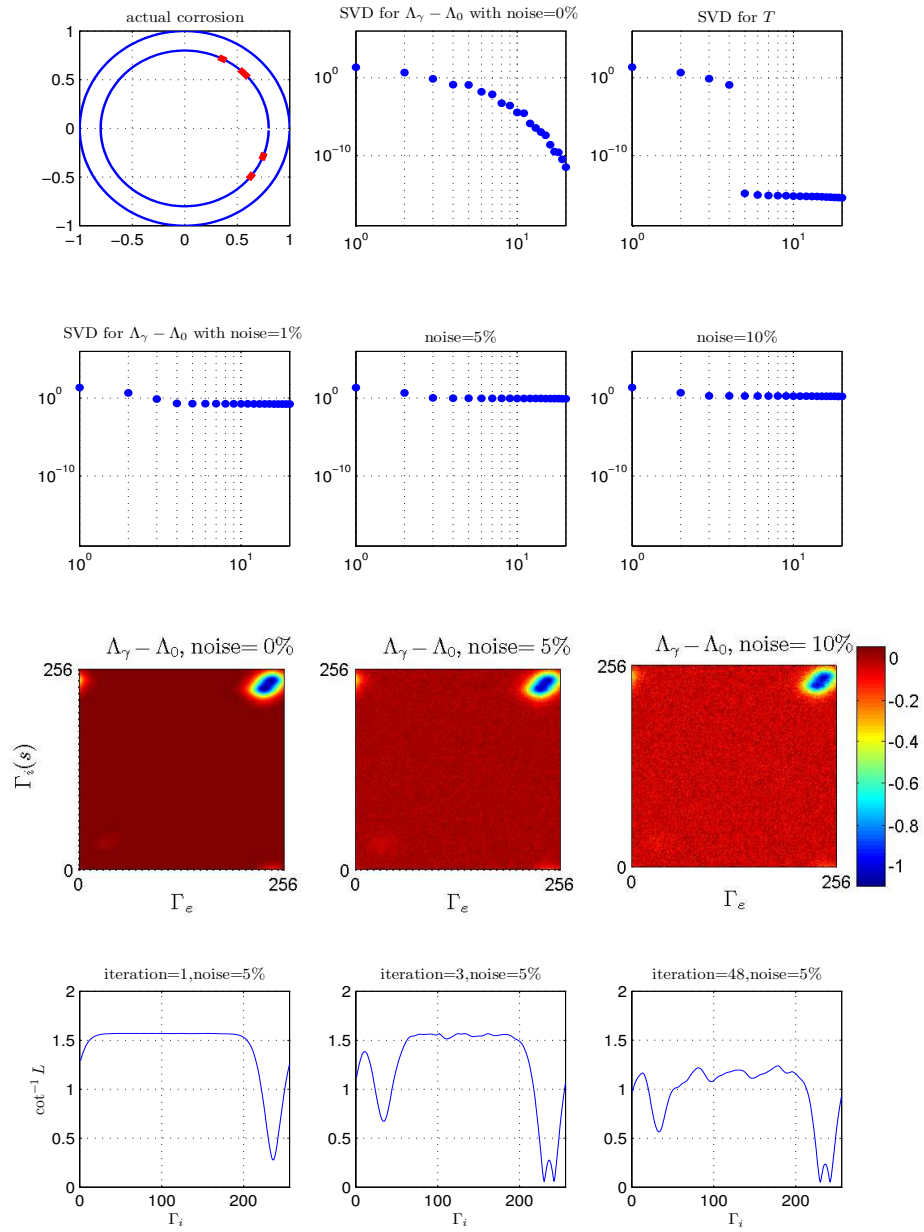


Figure 1.4: The computational results with noise 0, 1, 5, 10%

Chapter 2

Vibration Testing for Detecting Internal Corrosion

2.1 Introduction

Many technologies have been developed for pipe inspections, but they are limited to detecting certain types of defects. Most of them are not suitable for detecting flaws or cracks in the axial direction. Recently, ultrasonic guided waves are being studied for the feasibility of detecting many kinds of defects that occur in pipes. One major benefit of guided waves is their rapid global inspection capabilities which enables them to inspect a structure line-by-line instead of point-by-point. However, defect classification and sizing by guided waves are still a major problem under investigation due to the complexity of the wave propagation characteristics.

In order to reduce complicated derivation in the analytic method, a simple two-dimensional model is adopted in this work to inversely determine the corrosive parts from the resonance frequencies and mode shapes.

In this work, we follow an asymptotic formalism, in much the same

spirit as the work in [8] and recent text [4]. See also [22, 15, 35]. We derive asymptotic formulae for the effects of corrosion on resonance frequencies and mode shapes. Powerful techniques from the theory of meromorphic operator-valued functions and asymptotic analysis of integral kernels are combined for their rigorous proof. Based on these formulae we design a simple method for localizing the corrosion and estimating its extent.

Related works may be found in [38] and the references therein. Difficulties of this inverse problem result from its inherent ill-posedness and nonlinearity. Many authors have proposed various reconstruction algorithms, most of which are based on laborious least-square algorithms and Newton-type iteration schemes. In these methods, one must make a good initial guess. Without a good initial guess, one needs tremendous computational costs and time to get a close image to the true solution, since Newton-type iteration schemes may not converge to an approximate solution unless the initial guess is close to the true solution. Evidently, the success of Newton type procedures heavily depends on making a good initial guess. Unfortunately, the development of both the mathematical theory and the numerical algorithm for making a good initial guess seems to be in the early stages.

Our purpose in this work is to develop a simple method for determining the location of the corrosion and estimating its Hausdorff measure. From this information we may get an appropriate initial guess for the inverse problem .

Numerical examples are given in this chapter in order to illustrate the main features of our approach for both asymptotically exact and noisy data. A systematic discussion however is not attempted, being left to further studies in specific situations of practical applicability.

Our approach may be considered as a first step towards design of real-time, accurate and robust algorithms for corrosion detection from

ultrasonic guided waves.

2.2 Formal Derivations

To set up our inverse eigenvalue problem mathematically, we consider a simply connected bounded C^2 domain U in \mathbb{R}^2 , and a simply connected C^2 domain D compactly contained in U . Let $\Omega = U \setminus \overline{D}$ represent the specimen to be inspected. We define $\Gamma_e = \partial U$ and $\Gamma_i = \partial D$ so that $\partial\Omega = \Gamma_i \cup \Gamma_e$. Suppose that the inaccessible surface Γ_i contains a corrosive part I . The surface impedance (the corrosion coefficient) of I is a positive constant γ . The domain Ω may be considered as a cross section of a pipe inside which there is a corrosive part. We assume that the one-dimensional Hausdorff measure $|I|$ of I is small and denote it by ϵ .

We now introduce the following functional spaces. Let $H^1(\Omega)$ denote the set of functions $w \in L^2(\Omega)$ such that $\nabla w \in L^2(\Omega)$. Let $H^{1/2}(\Gamma_e)$ be the set of traces of functions in $H^1(U)$. Further, we define $H^2(\Omega)$ as the space of functions $u \in H^1(\Omega)$ such that $\partial^2 u \in L^2(\Omega)$ and the space $H^{3/2}(\Omega)$ as the interpolation space $[H^1(\Omega), H^2(\Omega)]_{1/2}$.

The eigenvalue problem in the presence of corrosion consists of finding $\omega_\epsilon > 0$ such that there exists a nontrivial solution v_ϵ to

$$\begin{cases} (\Delta + \omega_\epsilon^2)v_\epsilon = 0 & \text{in } \Omega, \\ -\frac{\partial v_\epsilon}{\partial \nu} + \gamma\chi(I)v_\epsilon = 0 & \text{on } \Gamma_i, \\ v_\epsilon = 0 & \text{on } \Gamma_e, \\ \int_\Omega v_\epsilon^2 = 1, \end{cases} \quad (2.2.1)$$

where ν is the outward unit normal to D and $\chi(I)$ denotes the characteristic function on I . Throughout this paper the normal vector ν defined on either Γ_i or Γ_e is assumed to be directed outward to the relevant domain D or U . So, it is directed inward to Ω on Γ_i .

It is well known that all eigenvalues of (2.2.1) are real, of finite multiplicity, have no finite accumulation points, and there are corresponding eigenfunctions which make up an orthonormal basis of $L^2(\Omega)$. See for example [30]. Let $\omega_0 > 0$ be for simplicity a simple eigenvalue for the Helmholtz equation in the absence of any corrosion. Let v_0 denote the corresponding eigenfunction, that is, the solution to

$$\begin{cases} (\Delta + \omega_0^2)v_0 = 0 & \text{in } \Omega, \\ -\frac{\partial v_0}{\partial \nu} = 0 & \text{on } \Gamma_i, \\ v_0 = 0 & \text{on } \Gamma_e, \end{cases} \quad (2.2.2)$$

such that $\int_{\Omega} v_0^2 = 1$.

The aim of this work is to detect the corrosive part I , in particular, its location $z \in I$ and its extend ϵ , from variations of the modal parameters

$$\left(\omega_{\epsilon} - \omega_0, \frac{\partial}{\partial \nu}(v_{\epsilon} - v_0)|_{\Gamma_e} \right). \quad (2.2.3)$$

We seek a solution of (2.2.1) for ϵ small, for which $\omega_{\epsilon} \rightarrow \omega_0$ as ϵ goes to zero. The expansion of ω_{ϵ} must begin with ω_0 , and the expansion of v_{ϵ} must begin with v_0 ; so we write:

$$\begin{aligned} \omega_{\epsilon} &= \omega_0 + \epsilon\omega_1 + \epsilon^2\omega_2 + \dots, \\ v_{\epsilon} &= v_0 + \epsilon v_1 + \epsilon^2 v_2 + \dots \quad \text{in } \Omega, \end{aligned} \quad (2.2.4)$$

where v_1, v_2, \dots and $\omega_1, \omega_2, \dots$ are to be found.

Now we substitute (2.2.4) into the Helmholtz equation (2.2.1) and equate terms of each power in ϵ . This yields:

$$\begin{cases} (\Delta + \omega_0^2)v_1 = -2\omega_0\omega_1 v_0 & \text{in } \Omega, \\ \frac{\partial v_1}{\partial \nu} = \frac{1}{\epsilon}\chi(I)\gamma v_0 & \text{on } \Gamma_i, \\ v_1 = 0 & \text{on } \Gamma_e. \end{cases} \quad (2.2.5)$$

Observe that since $|I| = \epsilon$, $\frac{1}{\epsilon}\chi(I)$ is of order 1. Since $\int_{\Omega} v_{\epsilon}^2 = \int_{\Omega} v_0^2$, we also have an orthogonality condition:

$$\int_{\Omega} v_1 v_0 dx = 0. \quad (2.2.6)$$

Multiplying (2.2.5) by v_0 and integrating by parts yields that

$$\begin{aligned} 2\omega_0\omega_1 &= - \int_{\Omega} (\Delta + \omega_0^2)v_1 \cdot v_0 dx \\ &= - \int_{\Gamma_e} \left(\frac{\partial v_1}{\partial \nu} v_0 - v_1 \frac{\partial v_0}{\partial \nu} \right) + \int_{\Gamma_i} \left(\frac{\partial v_1}{\partial \nu} v_0 - v_1 \frac{\partial v_0}{\partial \nu} \right) \\ &= \frac{\gamma}{\epsilon} \int_I v_0^2. \end{aligned}$$

So far we formally drove the following theorem, a rigorous proof of which will be given at the end of this paper.

Theorem 2.2.1 *The following asymptotic expansion holds:*

$$\omega_{\epsilon} = \omega_0 + \frac{\gamma}{2\omega_0} \int_I v_0^2 + O(\epsilon^2) \quad (2.2.7)$$

as $\epsilon \rightarrow 0$. Furthermore,

$$v_{\epsilon} = v_0 + O(\epsilon) \quad (2.2.8)$$

where $O(\epsilon)$ is in $H^{3/2}(\Omega)$ norm.

2.3 Reconstruction Method

For $h \in H^{1/2}(\Gamma_e)$ such that $\int_{\Gamma_e} h \frac{\partial v_0}{\partial \nu} = 0$, let $w_h \in H^1(\Omega)$ be the solution to

$$\begin{cases} (\Delta + \omega_0^2)w_h = 0 & \text{in } \Omega, \\ \frac{\partial w_h}{\partial \nu} = 0 & \text{on } \Gamma_i, \\ w_h = h & \text{on } \Gamma_e. \end{cases} \quad (2.3.1)$$

Applying Green's formula, we obtain

$$\gamma \int_I w_h v_\epsilon = \int_{\Gamma_i} w_h \frac{\partial v_\epsilon}{\partial \nu} = \int_{\Gamma_e} h \frac{\partial v_\epsilon}{\partial \nu} + (\omega_\epsilon^2 - \omega_0^2) \int_\Omega v_\epsilon w_h. \quad (2.3.2)$$

Dividing (2.3.2) by $\omega_\epsilon^2 - \omega_0^2$ and using (2.2.7) we induce

$$\frac{\int_I w_h v_\epsilon}{\int_I v_0^2} = \frac{1}{\omega_\epsilon^2 - \omega_0^2} \int_{\Gamma_e} h \frac{\partial v_\epsilon}{\partial \nu} + \int_\Omega v_\epsilon w_h + O(\epsilon). \quad (2.3.3)$$

By (2.2.8), we have

$$\begin{aligned} \int_I w_h v_\epsilon &= \int_I w_h v_0 + O(\epsilon^2), \\ \int_\Omega v_\epsilon w_h &= \int_\Omega v_0 w_h + O(\epsilon). \end{aligned}$$

Therefore,

$$\frac{w_h}{v_0}(z) \approx \frac{1}{2\omega_0(\omega_\epsilon - \omega_0)} \int_{\Gamma_e} \frac{\partial v_\epsilon}{\partial \nu} h + \int_\Omega v_0 w_h. \quad (2.3.4)$$

This is the key observation on which our reconstruction procedure is based. Since we are in possession of $\omega_\epsilon - \omega_0$ and $\frac{\partial v_\epsilon}{\partial \nu}|_{\Gamma_e}$, the reconstruction algorithm is as follows. Let $h = h_1, h_2, \dots, h_n$, where $\{h_i\}_{i=1}^n$ is a set of n independent functions satisfying $\int_{\Gamma_e} h_i \frac{\partial v_0}{\partial \nu} = 0$ for $i = 1, \dots, n$. For any $y \in \Gamma_i$ such that $v_0(y) \neq 0$ compute $(w_{h_i}/v_0)(y)$. The point z can be found as the unique point where

$$\frac{w_{h_i}}{v_0}(z) = \frac{1}{2\omega_0(\omega_\epsilon - \omega_0)} \int_{\Gamma_e} \frac{\partial v_\epsilon}{\partial \nu} h_i + \int_\Omega v_0 w_{h_i}, \quad \forall i = 1, \dots, n.$$

The justification of our method is quite simple and natural. Let $\langle \cdot, \cdot \rangle_{\frac{1}{2}, -\frac{1}{2}}$ denote the duality pair between $H^{1/2}(\Gamma_i)$ and $H^{-1/2}(\Gamma_i)$. Observe first that the following density result holds.

Lemma 2.3.1 *If $\langle v_0, \phi \rangle = 0$, then $\langle w_h, \phi \rangle = 0$ for all $h \in H^{1/2}(\Gamma_e)$ such that $\int_{\Gamma_e} h \frac{\partial v_0}{\partial \nu} = 0$ implies that $\phi = 0$.*

Proof. For $\phi \in H^{-1/2}(\Gamma_i)$ such that $\langle v_0, \phi \rangle = 0$, let u_ϕ be the solution to

$$\begin{cases} (\Delta + \omega_0^2)u_\phi = 0 & \text{in } \Omega, \\ \frac{\partial u_\phi}{\partial \nu} = \phi & \text{on } \Gamma_i, \\ u_\phi = 0 & \text{on } \Gamma_e. \end{cases}$$

An integration by parts shows that $\int_{\Gamma_e} h \frac{\partial u_\phi}{\partial \nu} = 0$ and therefore, by the unique continuation, $u_\phi = cv_0$ in Ω , for some constant c . Thus, $\phi = 0$, as desired. \square

Suppose now that

$$\frac{w_h}{v_0}(y) = \frac{1}{2\omega_0(\omega_\epsilon - \omega_0)} \int_{\Gamma_e} \frac{\partial v_\epsilon}{\partial \nu} h + \int_{\Omega} v_0 w_h,$$

for all $h \in H^{1/2}(\Gamma_e)$ such that $\int_{\Gamma_e} h \frac{\partial v_0}{\partial \nu} = 0$. By integrating by parts and using Theorem 2.2.1, we see that

$$\int_{\Gamma_i} \frac{\partial v_\epsilon}{\partial \nu} w_h \approx -\epsilon \gamma v_0(y) w_h(y) \quad \text{on } \Gamma_i, \quad \forall h \in H^{1/2}(\Gamma_e) \text{ such that } \int_{\Gamma_e} h \frac{\partial v_0}{\partial \nu} = 0.$$

and therefore, by the density result in Lemma 2.3.1,

$$\frac{\partial v_\epsilon}{\partial \nu} \approx -\epsilon \gamma v_0(y) \chi(I_y) \quad \text{on } \Gamma_i,$$

where $|I_y| = \epsilon$ and $y \in I_y$, from which (2.2.5) yields $y \approx z$. This shows that for n large enough z is uniquely determined by our algorithm.

Once z is determined, the Hausdorff measure of the corrosive part can be estimated by

$$\epsilon \approx \frac{2\omega_0(\omega_0 - \omega_\epsilon)}{\gamma v_0^2(z)}.$$

Note that we can not estimate ϵ separately from γ . We need to have an a priori knowledge of one of these two parameters in order to determine the other.

2.4 Numerical Results

This section presents results of some numerical experiments using the reconstruction method of the previous section. In the following, U and D are assumed to be the disks centered at the origin $(0, 0)$, and of radii r_e and r_i , respectively. We set $\Omega = U \setminus \overline{D}$, as before.

First we find the eigenvalue and eigenvector for (2.2.1) and (2.2.2). For convenience, using polar coordinates, we rewrite the equations in the following form:

$$\begin{cases} \left(\frac{\partial^2}{\partial r^2} + \frac{1}{r} \frac{\partial}{\partial r} + \frac{1}{r^2} \frac{\partial^2}{\partial \theta^2} + \omega_\epsilon^2 \right) v_\epsilon = 0 & \text{in } \Omega := [0, 2\pi] \times [r_i, r_e], \\ -\frac{\partial v_\epsilon}{\partial r} + \gamma \chi(I) v_\epsilon = 0 & \text{on } \Gamma_i := [0, 2\pi] \times \{r_i\}, \\ v_\epsilon = 0 & \text{on } \Gamma_e := [0, 2\pi] \times \{r_e\}, \\ \int_\Omega v_\epsilon^2 = 1, \end{cases}$$

and

$$\begin{cases} \left(\frac{\partial^2}{\partial r^2} + \frac{1}{r} \frac{\partial}{\partial r} + \frac{1}{r^2} \frac{\partial^2}{\partial \theta^2} + \omega_0^2 \right) v_0 = 0 & \text{in } \Omega, \\ -\frac{\partial v_0}{\partial r} = 0 & \text{on } \Gamma_i, \\ v_0 = 0 & \text{on } \Gamma_e, \\ \int_\Omega v_0^2 = 1. \end{cases}$$

We solve these equations using the finite difference method. To do this, we discretize the equations at the node points on Ω given by

$$(\theta_n, r_m) = \left(2\pi \frac{n-1}{N}, r_i + (r_e - r_i) \frac{m}{M+1} \right),$$

for $n = 1, 2, \dots, N$, and $m = 1, 2, \dots, M$, with $N = 128, M = 16$. Using the first eigenvalue and eigenvector computed, we solve (2.3.1) using the following h ,

$$h(\theta) = a_0 + a_1 \sin \theta + a_2 \sin 2\theta + \dots + a_k \sin k\theta, \quad \theta \in \Gamma_e,$$

for $k = 10$.

Examples 1, 2, 3 show the results of numerical experiments with various γ and some noise added to the data. They clearly demonstrate the viability of our reconstruction approach.

Example 1. We implement the reconstruction method for two-dimensional disks using Matlab and finite difference method. U and D are the disks centered $(0, 0)$ of radii 0.2 and 0.1 and the corrosion coefficient is set to be 2. Table 2.2 and Figure 2.1 summarize the computational results. The first figure shows the actual domain where the red part is the corrosion. The second figure is the graph of the functional J whose minimal point is the detected center of corrosion. The figures in the right-hand side are the eigenvectors with and without corrosion, v_ϵ and v_0 . The errors computed in L^∞ are $|z_s - z_s^c| = 0$ and $|\gamma\epsilon - (\gamma\epsilon)^c| = 0.0035$ where z_s^c and $(\gamma\epsilon)^c$ are the detected location of the corrosion and the corrosion coefficient.

Example 2. In this example, U and D are the disks centered $(0, 0)$ of radii 1.0 and 0.8, respectively. We test the algorithm with various corrosion coefficients $\gamma = 0.01, 2, 5$, while the size of the corrosion is fixed at $\epsilon \approx 0.04$. We also add 1%, 5%, 10% noise when we compute the eigenvectors. It turns out that higher the corrosion coefficient is, better is the performance, which is quite natural. The results also show that our algorithm works fairly well even in the presence of noise provided that the corrosion coefficient is large enough. See Figure 2.4.

Example 3. This example provides the results of numerical tests with larger size of the corrosion part, $\epsilon \approx 0.15$. The results show that the algorithm works equally as well, or even better, in detecting the location of the corrosion. However, its performance in detecting $\gamma\epsilon$ is poorer than in the case of shorter corrosion. See Figure 2.4.

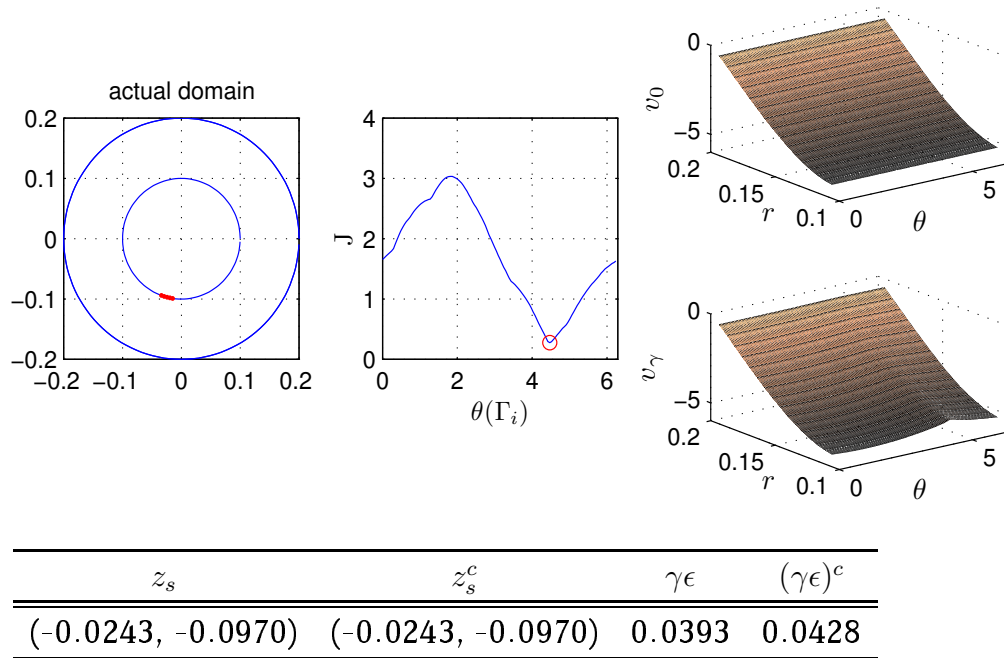


Figure 2.1: Reconstruction result without noise. z_s and $\gamma\epsilon$ are actual location and coefficients of the corrosion and z_s^c and $(\gamma\epsilon)^c$ are detected ones.

2.5 Justification of the Asymptotic Expansion

In this section we review the main results of Gohberg and Sigal in [23] and give a rigorous proof of Theorem 2.2.1 which was driven formally.

Let \mathcal{G} and \mathcal{H} be two Banach spaces and let $\mathcal{L}(\mathcal{G}, \mathcal{H})$ be the set of all bounded operators from \mathcal{G} to \mathcal{H} . Let U be an open set in \mathbb{C} . Suppose that $A(\omega)$ is an operator-valued function from U to $\mathcal{L}(\mathcal{G}, \mathcal{H})$. ω_0 is a *characteristic value* of $A(\omega)$ if

- $A(\omega)$ is holomorphic in some neighborhood of ω_0 , except possibly for ω_0 ;
- There exists a function $\phi(\omega)$ from a neighborhood of ω_0 to \mathcal{G} , holo-

morphic and nonzero at ω_0 such that $A(\omega)\phi(\omega)$ is holomorphic at ω_0 and $A(\omega_0)\phi(\omega_0) = 0$.

The function $\phi(\omega)$ in the above definition is called a *root function* of $A(\omega)$ associated to ω_0 and $\phi(\omega_0)$ is called an *eigenvector*. The closure of the space of eigenvectors corresponding to ω_0 is denoted by $\text{Ker } A(\omega_0)$.

Let ϕ_0 be an eigenvector corresponding to ω_0 . Let $V(\omega_0)$ be a complex neighborhood of ω_0 . The *rank* of ϕ_0 is the largest integer m such that there exist $\phi : V(\omega_0) \rightarrow \mathcal{G}$ and $\psi : V(\omega_0) \rightarrow \mathcal{H}$ holomorphic satisfying

$$\begin{aligned} A(\omega)\phi(\omega) &= (\omega - \omega_0)^m \psi(\omega), \\ \phi(\omega_0) &= \phi_0, \quad \psi(\omega_0) \neq 0. \end{aligned}$$

Suppose that $n = \dim \text{Ker } A(\omega_0) < +\infty$ and the ranks of all vectors in $\text{Ker } A(\omega_0)$ are finite. A system of eigenvectors ϕ_0^j , $j = 1, \dots, n$, is called a *canonical system of eigenvectors* of $A(\omega)$ associated to ω_0 if the rank of ϕ_0^j is the maximum of the ranks of all eigenvectors in some direct complement in $\text{Ker } A(\omega_0)$ of the linear span of the vectors $\phi_0^1, \dots, \phi_0^{j-1}$. Then we define the *null multiplicity* of the characteristic value ω_0 of $A(\omega)$ to be the sum of ranks of ϕ_0^j , $j = 1, \dots, n$, which is denoted by $N(A(\omega_0))$.

Suppose that $A^{-1}(\omega)$ exists and is holomorphic in some neighborhood of ω_0 , except possibly at this point itself. Then the number

$$M(A(\omega_0)) = N(A(\omega_0)) - N(A^{-1}(\omega_0))$$

is called the *multiplicity* of the characteristic value ω_0 of $A(\omega)$.

If $A(\omega)$ is holomorphic at ω_0 and $A(\omega_0)$ is invertible, the point ω_0 is called a *regular point* of $A(\omega)$. A point ω_0 is called a *normal point* of $A(\omega)$ if there exists some neighborhood $V(\omega_0)$ of ω_0 in which all the points except ω_0 are regular points of $A(\omega)$ and $A(\omega)$ admits the Laurent expansion

$$A(\omega) = \sum_{j \geq -s} (\omega - \omega_0)^j A_j.$$

where the operators A_j , $j = -s, \dots, -1$, are finite dimensional and the operator A_0 is a Fredholm operator. An operator-valued function $A(\omega)$ is called *normal* with respect to $\partial V(\omega_0)$ if $A(\omega)$ is holomorphic and invertible in $\overline{V(\omega_0)}$, except for a finite number of points of $V(\omega_0)$ which are normal points of $A(\omega)$.

Suppose that $A(\omega)$ is normal with respect to $\partial V(\omega_0)$ and ω_i , $i = 1, \dots, \sigma$, are all its characteristic values and poles lying in $V(\omega_0)$, we put

$$\mathcal{M}(A(\omega); \partial V(\omega_0)) = \sum_{i=1}^{\sigma} M(A(\omega_i)).$$

The generalization of Rouché's theorem is stated below.

Theorem 2.5.1 *Let $A(\omega)$ be an operator-valued function which is normal with respect to $\partial V(\omega_0)$. If an operator-valued function $S(\omega)$ which is holomorphic in $V(\omega_0)$ and continuous at $\partial V(\omega_0)$ satisfies the condition*

$$\|A^{-1}(\omega)S(\omega)\|_{\mathcal{L}(\mathcal{G}, \mathcal{G})} < 1, \quad \omega \in \partial V(\omega_0),$$

then $A(\omega) + S(\omega)$ is also normal with respect to $\partial V(\omega_0)$ and

$$\mathcal{M}(A(\omega); \partial V(\omega_0)) = \mathcal{M}(A(\omega) + S(\omega); \partial V(\omega_0)).$$

The generalization of the residue theorem is given by

Theorem 2.5.2 *Suppose that $A(\omega)$ is an operator-valued function which is normal with respect to $\partial V(\omega_0)$. Let $f(\omega)$ be a scalar function which is holomorphic in $V(\omega_0)$ and continuous in $\overline{V(\omega_0)}$. Then we have*

$$\frac{1}{2\pi i} \operatorname{tr} \int_{\partial V(\omega_0)} f(\omega) A^{-1}(\omega) \frac{d}{d\omega} A(\omega) d\omega = \sum_{j=1}^{\sigma} M(A(\omega_j)) f(\omega_j), \quad (2.5.1)$$

where ω_j , $j = 1, \dots, \sigma$, are all the points in $V(\omega_0)$ which are either poles or characteristic values of $A(\omega)$.

Here tr denotes the trace of operator which is the sum of all its nonzero eigenvalues. We mention the following property of the trace:

$$\text{tr} \int_{\partial V(\omega_0)} A(\omega)B(\omega)d\omega = \text{tr} \int_{\partial V(\omega_0)} B(\omega)A(\omega)d\omega, \quad (2.5.2)$$

where $A(\omega)$ and $B(\omega)$ are operator-valued functions which are finitely meromorphic in $V(\omega_0)$, which contains no poles of $A(\omega)$ and $B(\omega)$ other than ω_0 .

A fundamental solution $\Phi_\omega(x)$ to the Helmholtz operator $\Delta + \omega^2$ in \mathbb{R}^2 is given by

$$\Phi_\omega(x) = -\frac{i}{4}H_0^{(1)}(\omega|x|),$$

for $x \neq 0$, where $H_0^{(1)}$ is the Hankel function of the first kind of order 0. Let Γ be either Γ_i or Γ_e , and define $\mathcal{S}_\Gamma^\omega$ and $\mathcal{D}_\Gamma^\omega$ be the single and double layer potentials defined by Φ_ω , that is,

$$\begin{aligned} \mathcal{S}_\Gamma^\omega[\varphi](x) &= \int_\Gamma \Phi_\omega(x-y)\varphi(y) d\sigma(y), \quad x \in \mathbb{R}^2, \\ \mathcal{D}_\Gamma^\omega[\varphi](x) &= \int_\Gamma \frac{\partial \Phi_\omega(x-y)}{\partial \nu_y} \varphi(y) d\sigma(y), \quad x \in \mathbb{R}^2 \setminus \Gamma, \end{aligned}$$

for $\varphi \in L^2(\Gamma)$.

The following formulae give the jump relations obeyed by the double layer potential and by the normal derivative of the single layer potential:

$$(\mathcal{D}_\Gamma^\omega[\varphi]) \Big|_{\pm}(x) = \left(\mp \frac{1}{2}I + \mathcal{K}_\Gamma^\omega \right) [\varphi](x) \quad \text{a.e. } x \in \Gamma, \quad (2.5.3)$$

$$\frac{\partial(\mathcal{S}_\Gamma^\omega[\varphi])}{\partial \nu} \Big|_{\pm}(x) = \left(\pm \frac{1}{2}I + (\mathcal{K}_\Gamma^\omega)^* \right) [\varphi](x) \quad \text{a.e. } x \in \Gamma, \quad (2.5.4)$$

for $\varphi \in L^2(\Gamma)$, where $\mathcal{K}_\Gamma^\omega$ is the operator defined by

$$\mathcal{K}_\Gamma^\omega[\varphi](x) = \text{p.v.} \int_\Gamma \frac{\partial \Phi_\omega(x-y)}{\partial \nu_y} \varphi(y) d\sigma(y),$$

and $(\mathcal{K}_\Gamma^\omega)^*$ is the L^2 -adjoint of $\mathcal{K}_\Gamma^\omega$, that is,

$$(\mathcal{K}_\Gamma^\omega)^*[\varphi](x) = \mathbf{p.v.} \int_\Gamma \frac{\partial \Phi_\omega(x-y)}{\partial \nu_x} \varphi(y) d\sigma(y).$$

Here $\mathbf{p.v.}$ stands for the Cauchy principal value. The singular integral operators $\mathcal{K}_\Gamma^\omega$ and $(\mathcal{K}_\Gamma^\omega)^*$ are known to be bounded on $L^2(\Gamma)$. Here and throughout this paper the subscripts \pm as in (2.5.3) denote the limits from outside and inside of Γ .

In order to investigate the eigenvalues of the problem (2.2.2), we consider the operator $\mathbf{A}_0^\omega : L^2(\Gamma_e) \times H^1(\Gamma_i) \rightarrow H^1(\Gamma_e) \times H^1(\Gamma_i)$ defined by

$$\mathbf{A}_0^\omega := \begin{pmatrix} \mathcal{S}_{\Gamma_e}^\omega & \mathcal{D}_{\Gamma_i}^\omega \\ \mathcal{S}_{\Gamma_e}^\omega & \frac{1}{2}I + \mathcal{K}_{\Gamma_i}^\omega \end{pmatrix}.$$

Here $H^1(\Gamma_e)$ denotes the set of functions $f \in L^2(\Gamma_e)$ such that $\partial f / \partial T \in L^2(\Gamma_e)$, where $\partial / \partial T$ is the tangential derivative. $H^1(\Gamma_i)$ is defined likewise.

Observe that $\omega \mapsto \mathbf{A}_0^\omega$ is an operator valued holomorphic function. The relation between the eigenvalues of (2.2.2) and the characteristic values of \mathbf{A}_0^ω is given by the following theorem.

Theorem 2.5.3 *Suppose that $-\omega^2$ is not a Dirichlet eigenvalue of Δ on D . Then, $-\omega^2$ is an eigenvalue of (2.2.2) if and only if ω is a characteristic value of \mathbf{A}_0^ω .*

Proof. Suppose that ω^2 is an eigenvalue of (2.2.2) so that there is a nontrivial solution v to (2.2.2). Then by Green's representation formula we have

$$v(x) = -\mathcal{S}_{\Gamma_e}^\omega \left[\frac{\partial v}{\partial \nu} \Big|_{\Gamma_e} \right] (x) - \mathcal{D}_{\Gamma_i}^\omega [v|_{\Gamma_i}] (x), \quad x \in \Omega.$$

Put $\varphi := \frac{\partial v}{\partial \nu} \Big|_{\Gamma_e}$ and $\psi := v|_{\Gamma_i}$. Then $(\varphi, \psi) \in L^2(\Gamma_e) \times H^1(\Gamma_i)$ is not zero and satisfies

$$\mathcal{S}_{\Gamma_e}^\omega[\varphi] + \mathcal{D}_{\Gamma_i}^\omega[\psi] = 0 \quad \text{on } \Gamma_e. \quad (2.5.5)$$

On the other hand, by (2.5.3), we have

$$(\mathcal{S}_{\Gamma_e}^\omega[\varphi] + \mathcal{D}_{\Gamma_i}^\omega[\psi])|_+ - (\mathcal{S}_{\Gamma_e}^\omega[\varphi] + \mathcal{D}_{\Gamma_i}^\omega[\psi])|_- = -\psi = -v|_{\Gamma_i} \quad \text{on } \Gamma_i,$$

and hence $(\mathcal{S}_{\Gamma_e}^\omega[\varphi] + \mathcal{D}_{\Gamma_i}^\omega[\psi])|_- = 0$ on Γ_i , or equivalently,

$$\mathcal{S}_{\Gamma_e}^\omega[\varphi] + \left(\frac{1}{2}I + \mathcal{K}_{\Gamma_i}^\omega\right)[\psi] = 0 \quad \text{on } \Gamma_i. \quad (2.5.6)$$

Combining (2.5.5) and (2.5.6) shows that ω is a characteristic value of A_0^ω .

Conversely, suppose that w is a characteristic value of A_0^ω so that there is a non-zero $(\varphi, \psi) \in L^2(\Gamma_e) \times H^1(\Gamma_i)$ satisfying

$$\mathbf{A}_0^\omega \begin{pmatrix} \varphi \\ \psi \end{pmatrix} = 0, \quad (2.5.7)$$

or equivalently (2.5.5) and (2.5.6). Define

$$v(x) := -\mathcal{S}_{\Gamma_e}^\omega[\varphi](x) - \mathcal{D}_{\Gamma_i}^\omega[\psi](x), \quad x \in \Omega. \quad (2.5.8)$$

Then $v = 0$ on Γ_e by (2.5.5). On the other hand, (2.5.6) shows that $\psi \in \mathcal{C}^{1,\alpha}(\Gamma_i)$ for some $\alpha > 0$. In fact, by (2.5.6), we have

$$\psi = 2\mathcal{S}_{\Gamma_e}^\omega[\varphi] - 2\mathcal{K}_{\Gamma_i}^\omega[\psi]. \quad (2.5.9)$$

Since Γ_i is \mathcal{C}^2 , $\mathcal{K}_{\Gamma_i}^\omega$ maps $L^2(\Gamma_i)$ into $L^\infty(\Gamma_i)$, $L^\infty(\Gamma_i)$ into $\mathcal{C}^\alpha(\Gamma)$ for all $\alpha < 1$, and $\mathcal{C}^\alpha(\Gamma)$ into $\mathcal{C}^{1,\alpha}(\Gamma)$. Thus by bootstrapping using (2.5.9), we have $\psi \in \mathcal{C}^{1,\alpha}(\Gamma_i)$. Now $\frac{\partial}{\partial \nu} \mathcal{D}_{\Gamma_i}^\omega[\psi]$ is well-defined and it does not have a jump along Γ_i , i. e.,

$$\frac{\partial}{\partial \nu} \mathcal{D}_{\Gamma_i}^\omega[\psi]|_+ = \frac{\partial}{\partial \nu} \mathcal{D}_{\Gamma_i}^\omega[\psi]|_- \quad \text{on } \Gamma_i.$$

Since ω^2 is not a Dirichlet eigenvalue of $-\Delta$ on D , (2.5.6) implies that $\mathcal{S}_{\Gamma_e}^\omega[\varphi] + \mathcal{D}_{\Gamma_i}^\omega[\psi] = 0$ in D , and hence

$$\frac{\partial}{\partial \nu} (\mathcal{S}_{\Gamma_e}^\omega[\varphi] + \mathcal{D}_{\Gamma_i}^\omega[\psi])|_- = 0 \quad \text{on } \Gamma_i.$$

We thus obtain

$$\begin{aligned}\frac{\partial v}{\partial \nu} \Big|_{\Gamma_i} &= \frac{\partial}{\partial \nu} (\mathcal{S}_{\Gamma_e}^\omega[\varphi] + \mathcal{D}_{\Gamma_i}^\omega[\psi]) \Big|_+ \\ &= \frac{\partial}{\partial \nu} (\mathcal{S}_{\Gamma_e}^\omega[\varphi] + \mathcal{D}_{\Gamma_i}^\omega[\psi]) \Big|_- = 0.\end{aligned}$$

In other words, v is an eigenfunction of the problem (2.2.2). This completes the proof. \square

In a similar way, one can prove the following theorem for the problem (2.2.1).

Theorem 2.5.4 *Define the operator $\mathbf{A}_\epsilon^\omega : L^2(\Gamma_e) \times H^1(\Gamma_i) \rightarrow H^1(\Gamma_e) \times H^1(\Gamma_i)$ by*

$$\mathbf{A}_\epsilon^\omega := \begin{pmatrix} \mathcal{S}_{\Gamma_e}^\omega & \mathcal{D}_{\Gamma_i}^\omega - \mathcal{S}_{\Gamma_i}^\omega M_\epsilon \\ \mathcal{S}_{\Gamma_e}^\omega & \frac{1}{2}I + \mathcal{K}_{\Gamma_i}^\omega - \mathcal{S}_{\Gamma_i}^\omega M_\epsilon \end{pmatrix},$$

where M_ϵ means the multiplication by $\gamma\chi(I)$. Assume that $-\omega^2$ is not a Dirichlet eigenvalue of Δ on D . Then $-\omega^2$ is an eigenvalue of (2.2.1) and only if ω is a characteristic value of $\mathbf{A}_\epsilon^\omega$.

Observe that we can write

$$\mathbf{A}_\epsilon^\omega = \mathbf{A}_0^\omega + \epsilon \mathbf{B}_\epsilon^\omega, \quad (2.5.10)$$

where

$$\mathbf{B}_\epsilon^\omega := \begin{pmatrix} 0 & -\frac{1}{\epsilon} \mathcal{S}_{\Gamma_i}^\omega M_\epsilon \\ 0 & -\frac{1}{\epsilon} \mathcal{S}_{\Gamma_i}^\omega M_\epsilon \end{pmatrix}. \quad (2.5.11)$$

Since M_ϵ is of order ϵ , the operator $\mathbf{B}_\epsilon^\omega$ is of order 1.

Lemma 2.5.5 \mathbf{A}_0^ω is a Fredholm operator of index 0 and every eigenvector of \mathbf{A}_0^ω has rank one provided that $-\omega_0^2$ is not a Dirichlet eigenvalue of Δ on D .

Proof. Since, written in the following manner, \mathbf{A}_0^ω is clearly a compact perturbation of Fredholm operator of index 0

$$\mathbf{A}_0^\omega = \begin{pmatrix} \mathcal{S}_{\Gamma_e}^\omega & 0 \\ 0 & \frac{1}{2}I + \mathcal{K}_{\Gamma_i}^\omega \end{pmatrix} + \begin{pmatrix} 0 & \mathcal{D}_{\Gamma_i}^\omega \\ \mathcal{S}_{\Gamma_e}^\omega & 0 \end{pmatrix},$$

hence it is Fredholm of index 0.

Suppose that $\begin{pmatrix} \varphi \\ \psi \end{pmatrix}$ is an eigenvector of \mathbf{A}_0^ω with rank m associated with the characteristic value ω_0 , i. e., there exist φ^ω and ψ^ω , holomorphic as functions of ω , such that $\varphi^{\omega_0} = \varphi$, $\psi^{\omega_0} = \psi$, and

$$\mathbf{A}_0^\omega \begin{pmatrix} \varphi^\omega \\ \psi^\omega \end{pmatrix} = (\omega - \omega_0)^m \begin{pmatrix} \tilde{\varphi}^\omega \\ \tilde{\psi}^\omega \end{pmatrix}, \quad (2.5.12)$$

for some $(\tilde{\varphi}^\omega, \tilde{\psi}^\omega) \in H^1(\Gamma_e) \times H^1(\Gamma_i)$. Let $u^\omega := \mathcal{S}_{\Gamma_e}^\omega[\varphi^\omega] + \mathcal{D}_{\Gamma_i}^\omega[\psi^\omega]$. Then because of (2.5.12), u^ω satisfies

$$\begin{cases} (\Delta + \omega^2)u^\omega = 0 & \text{in } \mathbb{R}^2 \setminus (\Gamma_e \cup \Gamma_i), \\ u^\omega = (\omega - \omega_0)^m \tilde{\varphi}^\omega & \text{on } \Gamma_e, \\ u^\omega|_- = (\omega - \omega_0)^m \tilde{\psi}^\omega & \text{on } \Gamma_i. \end{cases}$$

Since $-\omega_0^2$ is not a Dirichlet eigenvalue of Δ on D , $\mathcal{S}_{\Gamma_i}^\omega : L^2(\Gamma_i) \rightarrow H^1(\Gamma_i)$ is invertible for ω in a neighborhood of ω_0 , and hence we have

$$u^\omega(x) = (\omega - \omega_0)^m \mathcal{S}_{\Gamma_i}^\omega \left[(\mathcal{S}_{\Gamma_i}^\omega)^{-1} \tilde{\psi}^\omega \right] (x), \quad x \in D,$$

and

$$\frac{\partial u^\omega}{\partial \nu} \Big|_+ = \frac{\partial u^\omega}{\partial \nu} \Big|_- = (\omega - \omega_0)^m \left(-\frac{1}{2}I + (\mathcal{K}_{\Gamma_i}^\omega)^* \right) \left[(\mathcal{S}_{\Gamma_i}^\omega)^{-1} \tilde{\psi}^\omega \right] \quad \text{on } \Gamma_i.$$

By Green's formula, we immediately get

$$\begin{aligned}
& (\omega^2 - \omega_0^2) \int_{\Omega} u^{\omega} u^{\omega_0} \\
&= \int_{\Gamma_e} \frac{\partial u^{\omega_0}}{\partial \nu} u^{\omega} + \int_{\Gamma_i} \frac{\partial u^{\omega}}{\partial \nu} u^{\omega_0} \\
&= (\omega - \omega_0)^m \left(\int_{\Gamma_e} \frac{\partial u^{\omega_0}}{\partial \nu} \tilde{\varphi}^{\omega} + \int_{\Gamma_i} u^{\omega_0} \left(-\frac{1}{2}I + (\mathcal{K}_{\Gamma_i}^{\omega})^* \right) [(\mathcal{S}_{\Gamma_i}^{\omega})^{-1} \tilde{\psi}^{\omega}] \right).
\end{aligned}$$

If $m > 1$, by dividing both sides by $\omega^2 - \omega_0^2$ and taking the limit as $\omega \rightarrow \omega_0$, we obtain $\int_{\Omega} (u^{\omega_0})^2 = 0$ which is a contradiction. Thus we have $m = 1$. This completes the proof. \square

By the above lemma and the generalized Rouché's theorem (Theorem 2.5.1), we know that A_{ϵ}^{ω} is normal with respect to a small neighborhood V of ω_0 and that the multiplicity of A_{ϵ}^{ω} in V is equal to the dimension of the eigenspace of (2.2.2) associated with ω_0 . Now we are ready to prove Theorem 2.2.1.

The following lemma was proved in [8]. We include a proof for the readers' sake.

Lemma 2.5.6 *Let V be a small neighborhood of ω_0 in a complex plane such that A_{ϵ}^{ω} has the simple characteristic value ω_{ϵ} in V . Then*

$$\omega_{\epsilon} - \omega_0 = \frac{1}{2\pi i} \sum_{j=1}^{\infty} \frac{(-1)^j \epsilon^j}{j} \operatorname{tr} \int_{\partial V} ((A_0^{\omega})^{-1} B_{\epsilon}^{\omega})^j d\omega. \quad (2.5.13)$$

Proof. It follows from Theorem 2.5.2 and Lemma 2.5.5 that

$$\omega_{\epsilon} - \omega_0 = \frac{1}{2\pi i} \operatorname{tr} \int_{\partial V} (\omega - \omega_0) (A_{\epsilon}^{\omega})^{-1} \frac{d}{d\omega} A_{\epsilon}^{\omega} d\omega. \quad (2.5.14)$$

By (2.5.10), one can see that

$$(A_{\epsilon}^{\omega})^{-1} = \sum_{j=0}^{\infty} (-1)^j \epsilon^j ((A_0^{\omega})^{-1} B_{\epsilon}^{\omega})^j (A_0^{\omega})^{-1}, \quad (2.5.15)$$

where the series converges in the operator norm on $L^2(\Gamma_e) \times H^1(\Gamma_i) \rightarrow H^1(\Gamma_e) \times H^1(\Gamma_i)$ if ϵ is sufficiently small. If we substitute (2.5.15) into (2.5.14), we have

$$\omega_\epsilon - \omega_0 = \frac{1}{2\pi i} \sum_{j=0}^{\infty} (-1)^j \epsilon^j \operatorname{tr} \int_{\partial V} (\omega - \omega_0) ((\mathbf{A}_0^\omega)^{-1} \mathbf{B}_\epsilon^\omega)^j (\mathbf{A}_0^\omega)^{-1} \frac{d}{d\omega} \mathbf{A}_\epsilon^\omega d\omega. \quad (2.5.16)$$

Since

$$\frac{d}{d\omega} (\mathbf{A}_0^\omega)^{-1} = -(\mathbf{A}_0^\omega)^{-1} \frac{d}{d\omega} \mathbf{A}_0^\omega \cdot (\mathbf{A}_0^\omega)^{-1},$$

we have

$$\begin{aligned} \epsilon \frac{d}{d\omega} ((\mathbf{A}_0^\omega)^{-1} \mathbf{B}_\epsilon^\omega)^j &= j ((\mathbf{A}_0^\omega)^{-1} \mathbf{B}_\epsilon^\omega)^{j-1} (\mathbf{A}_0^\omega)^{-1} \frac{d}{d\omega} \mathbf{A}_\epsilon^\omega \\ &- \epsilon j ((\mathbf{A}_0^\omega)^{-1} \mathbf{B}_\epsilon^\omega)^j (\mathbf{A}_0^\omega)^{-1} \frac{d}{d\omega} \mathbf{A}_0^\omega - j ((\mathbf{A}_0^\omega)^{-1} \mathbf{B}_\epsilon^\omega)^{j-1} (\mathbf{A}_0^\omega)^{-1} \frac{d}{d\omega} \mathbf{A}_0^\omega. \end{aligned} \quad (2.5.17)$$

We now substitute (2.5.17) into (2.5.16). Then the sum of the last two terms in (2.5.17) cancel each other and hence we have

$$\omega_\epsilon - \omega_0 = -\frac{1}{2\pi i} \sum_{j=1}^{\infty} \frac{(-1)^j \epsilon^j}{j} \operatorname{tr} \int_{\partial V} (\omega - \omega_0) \frac{d}{d\omega} ((\mathbf{A}_0^\omega)^{-1} \mathbf{B}_\epsilon^\omega)^j d\omega.$$

Now (2.5.13) immediately follows and the proof is complete. \square

Proof of Theorem 2.2.1. Let

$$(\mathbf{A}_0^\omega)^{-1} = \begin{pmatrix} A_1^\omega & A_2^\omega \\ A_3^\omega & A_4^\omega \end{pmatrix}.$$

Then we have

$$-\frac{\epsilon}{2\pi i} \operatorname{tr} \int_{\partial V} (\mathbf{A}_0^\omega)^{-1} \mathbf{B}_\epsilon^\omega d\omega = \frac{1}{2\pi i} \operatorname{tr} \int_{\partial V} (A_3^\omega \mathcal{S}_{\Gamma_i}^\omega M_\epsilon + A_4^\omega \mathcal{S}_{\Gamma_i}^\omega M_\epsilon) d\omega.$$

Let $0 < \mu_1 \leq \mu_2 \leq \dots$ be the eigenvalues of (2.2.2) and u_1, u_2, \dots be the corresponding normalized orthogonal eigenfunctions. For $\phi \in L^2(\Gamma_i)$, let

$$u := -\mathcal{S}_{\Gamma_e}^\omega (A_1^\omega \mathcal{S}_{\Gamma_i}^\omega + A_2^\omega \mathcal{S}_{\Gamma_i}^\omega) [\phi] - \mathcal{D}_{\Gamma_i}^\omega (A_3^\omega \mathcal{S}_{\Gamma_i}^\omega + A_4^\omega \mathcal{S}_{\Gamma_i}^\omega) [\phi] + \mathcal{S}_{\Gamma_i}^\omega [\phi].$$

Then, by the definition of A_i^ω 's, u satisfies

$$\begin{cases} (\Delta + \omega^2)u = 0 & \text{in } \Omega, \\ \frac{\partial u}{\partial \nu} = \phi & \text{on } \Gamma_i, \\ u = (A_3^\omega \mathcal{S}_{\Gamma_i}^\omega + A_4^\omega \mathcal{S}_{\Gamma_i}^\omega) [\phi] & \text{on } \Gamma_i, \\ u = 0 & \text{on } \Gamma_e. \end{cases}$$

Applying Green's formula, we have

$$(\omega^2 - \mu_i) \int_{\Omega} u u_i = \int_{\Gamma_i} \phi u_i,$$

and hence

$$u = \sum_{n=1}^{\infty} \frac{\langle u_i, \phi \rangle_{\Gamma_i}}{\omega^2 - \mu_i} u_i \quad \text{in } \Omega,$$

where $\langle \cdot, \cdot \rangle_{\Gamma_i}$ denotes the inner product in $L^2(\Gamma_i)$. By taking the trace on Γ_i , we obtain

$$(A_3^\omega \mathcal{S}_{\Gamma_i}^\omega + A_4^\omega \mathcal{S}_{\Gamma_i}^\omega) [\phi] = \sum_{n=1}^{\infty} \frac{\langle u_i, \phi \rangle_{\Gamma_i}}{\omega^2 - \mu_i} u_i|_{\Gamma_i}.$$

Then we have

$$\begin{aligned} \frac{1}{2\pi i} \operatorname{tr} \int_{\partial V} (A_3^\omega \mathcal{S}_{\Gamma_i}^\omega M_\epsilon + A_4^\omega \mathcal{S}_{\Gamma_i}^\omega M_\epsilon) d\omega &= \frac{1}{2\pi i} \int_{\partial V} \sum_{n=1}^{\infty} \frac{\langle u_i, \gamma \chi(I) u_i \rangle_{\Gamma_i}}{\omega^2 - \mu_i} d\omega \\ &= \frac{\gamma}{2\omega_0} \int_I v_0^2, \end{aligned}$$

since ω_0^2 is the only eigenvalue inside V . Therefore

$$\omega_\epsilon - \omega_0 = \frac{\gamma}{2\omega_0} \int_I v_0^2 + O(\epsilon^2).$$

This proves (2.2.7).

We now prove the (2.2.8). Choose $\begin{pmatrix} \varphi_\epsilon \\ \psi_\epsilon \end{pmatrix} \in \text{Ker} A_\epsilon^{\omega_\epsilon}$. Let $\Psi_\epsilon = \begin{pmatrix} \varphi_\epsilon \\ \psi_\epsilon \end{pmatrix}$ for convenience and assume that $\|\Psi_\epsilon\|_{L^2(\Gamma_e) \times H^1(\Gamma_i)} = 1$. Let us define P_ϵ by

$$P_\epsilon = \frac{1}{2\pi i} \int_{\partial V} (\mathbf{A}_\epsilon^\omega)^{-1} \frac{d}{d\omega} \mathbf{A}_\epsilon^\omega d\omega. \quad (2.5.18)$$

Then it is proved in [23] that P_ϵ is a projection (not necessarily orthogonal) from $L^2(\Gamma_e) \times H^1(\Gamma_i)$ onto $\text{Ker} A_\epsilon^{\omega_\epsilon}$. It follows from (2.5.15) that

$$P_\epsilon = P_0 + O(\epsilon) \quad (2.5.19)$$

where $O(\epsilon)$ is in the operator norm. Having both sides of (2.5.19) act on Ψ_ϵ , we obtain

$$\Psi_\epsilon = P_0 \Psi_\epsilon + O(\epsilon), \quad (2.5.20)$$

where $O(\epsilon)$ is in $L^2(\Gamma_e) \times H^1(\Gamma_i)$ -norm. Let $P_0 \Psi_\epsilon = (\varphi_\epsilon^0, \psi_\epsilon^0)$ and

$$v_\epsilon = \mathcal{S}_{\Gamma_e}^{\omega_\epsilon}[\varphi_\epsilon] + \mathcal{D}_{\Gamma_i}^{\omega_\epsilon}[\psi_\epsilon] - \mathcal{S}_{\Gamma_i}^{\omega_\epsilon} M_\epsilon[\psi_\epsilon], \quad v_0 = \mathcal{S}_{\Gamma_e}^{\omega_0}[\varphi_\epsilon^0] + \mathcal{D}_{\Gamma_i}^{\omega_0}[\psi_\epsilon^0] \quad \text{in } \Omega. \quad (2.5.21)$$

Since $\mathcal{S}_{\Gamma_e}^{\omega_\epsilon}$ and $\mathcal{D}_{\Gamma_i}^{\omega_\epsilon}$ map $L^2(\Gamma_e)$ and $H^1(\Gamma_i)$ into $H^{3/2}(\Omega)$, respectively, we have from (2.5.20) that

$$v_\epsilon = v_0 + O(\epsilon) \quad \text{in } H^{3/2}(\Omega). \quad (2.5.22)$$

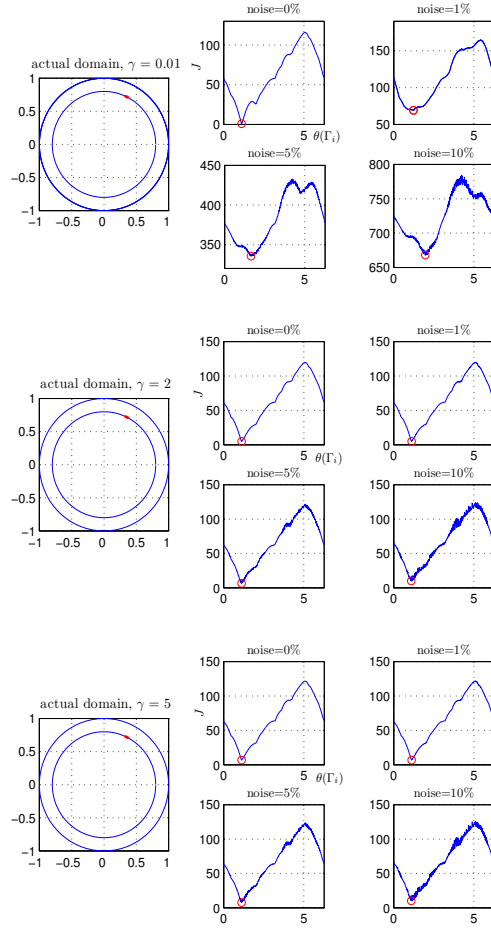
Now we normalize v_ϵ, v_0 by dividing by its $L^2(\Omega)$ norms and denote them by v_ϵ, v_0 again. Then v_ϵ, v_0 are solutions of (2.2.1), (2.2.2) respectively. Since $\|v_\epsilon\|_{L^2(\Omega)} = \|v_0\|_{L^2(\Omega)} + O(\epsilon)$, they still satisfy (2.5.22). The proof of Theorem 2.2.1 is now complete. \square

2.6 Conclusion

We have designed a simple and accurate method for detecting small internal corrosion by vibration analysis. Our method is based on asymptotic formulae for the resonance frequencies and mode shapes perturbations caused by internal corrosive parts of small Hausdorff measure.

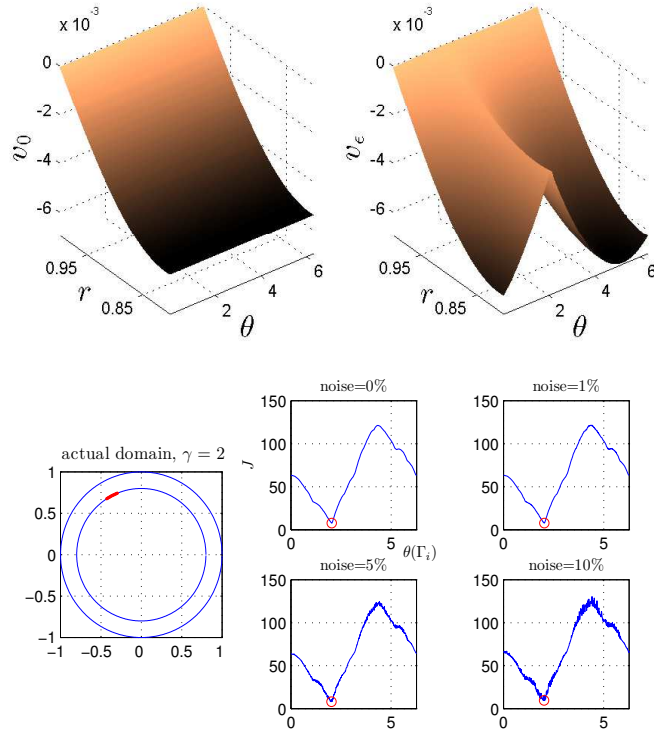
To rigorously prove our asymptotic formulae we have reduced the problem to the study of the characteristic values of integral operators in the complex plane and made use of powerful techniques from the theory of meromorphic operator-valued functions.

It is worth noticing the fact that it is impossible to extract the size of the corrosive parts and the impedance coefficient using the first order approximation. We can only reconstruct the product of these two quantities. It is likely that from a certain level of signal-to-noise ratio, higher-order asymptotic expansions of the resonances and mode shapes perturbations yield such important information.



γ	$noise(\%)$	z_s	z_s^c	$\gamma\epsilon$	$(\gamma\epsilon)^c$
0.01	0	(0.3509, 0.7189)	(0.3509, 0.7189)	0.0004	0.0005
0.01	1	(0.3509, 0.7189)	(0.2695, 0.7532)	0.0004	0.0005
0.01	5	(0.3509, 0.7189)	(-0.0589, 0.7978)	0.0004	0.0005
0.01	10	(0.3509, 0.7189)	(-0.3061, 0.7391)	0.0004	0.0006
2	0	(0.3509, 0.7189)	(0.3509, 0.7189)	0.0785	0.0644
2	1	(0.3509, 0.7189)	(0.3509, 0.7189)	0.0785	0.0656
2	5	(0.3509, 0.7189)	(0.3509, 0.7189)	0.0785	0.0711
2	10	(0.3509, 0.7189)	(0.3684, 0.7101)	0.0785	0.0717
5	0	(0.3509, 0.7189)	(0.3509, 0.7189)	0.1963	0.1043
5	1	(0.3509, 0.7189)	(0.3509, 0.7189)	0.1963	0.1063
5	5	(0.3509, 0.7189)	(0.3509, 0.7189)	0.1963	0.1151
5	10	(0.3509, 0.7189) ⁷³	(0.3684, 0.7101)	0.1963	0.1162

Figure 2.2: $r_i = 0.8, r_e = 1$



γ	noise(%)	z_s	z_s^c	$\gamma\epsilon$	$(\gamma\epsilon)^c$
2	0	(-0.3684, 0.7101)	(-0.3597, 0.7146)	0.2945	0.1200
2	1	(-0.3684, 0.7101)	(-0.3597, 0.7146)	0.2945	0.1199
2	5	(-0.3684, 0.7101)	(-0.3509, 0.7189)	0.2945	0.1235
2	10	(-0.3684, 0.7101)	(-0.3509, 0.7189)	0.2945	0.1271

Figure 2.3: $r_i = 0.8, r_e = 1$

Chapter 3

Ultrasonic Detection of Internal Corrosion

3.1 Introduction

Corrosion detection remains a topic of considerable activity in the inverse problems community. Of special interest are algorithms that make use of a priori information or assumptions concerning the nature of the target's internal structure. Such assumptions can usually be exploited to obtain much faster, simpler and more stable algorithms than would otherwise be possible.

In this chapter we consider the problem of determining the corrosion damage of an inaccessible part of the surface of a specimen from ultrasonic measurements.

The impedance imaging problem for detecting internal corrosion was considered in Chapter 1. In that chapter we propose an algorithm of MUSIC (multiple signal classification) type for detecting corrosion in pipelines from input fluxes. This algorithm is based on an accurate asymptotic representation formula for the steady state voltage perturbations.

In this chapter, we adapt the MUSIC-type algorithm of Chapter 1 to the setting in which multiple ultrasonic boundary measurements are available and also show how one may quantitatively deduce the number of corrosive parts present. We also adapt the propagation-backpropagation algorithm for ultrasound tomography to corrosion detection and present a Fourier-type reconstruction method. All of these different approaches rely on an asymptotic expansion of the ultrasonic reflected wave with respect to the length of the corrosive parts, in much the same spirit as the recent text [4]. We consider only the two-dimensional case, the extension to three dimensions being obvious.

The organization of the chapter is as follows. In Section 3.2 we state the forward and corresponding inverse problem of interest, then review some basic facts on Green's functions. In Section 3.3 we state our main theorem that allows us in Section 3.4 to develop our different algorithms for recovering a collection of corrosive parts. In Section 3.5 we briefly discuss how to resolve the difficulty in solving our inverse problem that is caused by high oscillations in the measurements data. The leading terms of the large-argument large-order asymptotics of the Bessel functions, and their first derivatives are summarized in Section 3.6. Useful calculations on Green's function are recalled in Section 3.7.

3.2 Preliminaries and Formulation of the Inverse Problem

For $\omega > 0$, a fundamental solution $\Phi_\omega(x)$ to the Helmholtz operator $\Delta + \omega^2$ in \mathbb{R}^2 is given by

$$\Phi_\omega(x) = -\frac{i}{4}H_0^{(1)}(\omega|x|),$$

for $x \neq 0$, where $H_0^{(1)}$ is the Hankel function of the first kind of order 0. We recall Graf's addition formula (see for example [1, Theorem 9.1.79])

which expresses as a series a field generated by a source located at some point. Letting $x = (|x|, \theta_x)$ and $y = (|y|, \theta_y)$ in polar coordinates, we have

$$H_0^{(1)}(\omega|x-y|) = \sum_{l \in \mathbb{Z}} H_l^{(1)}(\omega|y|) e^{il\theta_y} J_l(\omega|x|) e^{-il\theta_x}, \quad \text{for } |x| < |y|. \quad (3.2.1)$$

Here, $H_l^{(1)} = J_l + iY_l$, $l \in \mathbb{Z}$, J_l and Y_l are Bessel's functions.

We denote the specimen to be inspected as the annulus $\Omega = \{x : r < |x| < R\}$. Let Γ_e and Γ_i be the circles of radius R and r centered at the origin, respectively. Suppose that the inaccessible surface Γ_i contains some corrosive parts I_s , $s = 1, \dots, m$. The parts I_s are well-separated, and the reciprocal of the surface impedance (the corrosion coefficient) of each I_s , $s = 1, \dots, m$, is $\gamma_s \geq 0$, not identically zero. We assume that each $\gamma_s \in C^1(I_s)$. Let

$$\gamma(x) = \sum_{s=1}^m \gamma_s \chi_s(x), \quad x \in \Gamma_i, \quad (3.2.2)$$

where χ_s denotes the characteristic function on I_s . The annulus Ω in two dimensions may be considered as a cross section of a pipe inside which there are corrosive parts. We assume that the Hausdorff measures of I_s are small:

$$|I_s| = O(\epsilon), \quad s = 1, \dots, m,$$

where ϵ is a small parameter representing the common order of magnitude of I_s . Here and throughout this chapter $|\cdot|$ denotes the Hausdorff measure. Then for each $p \geq 1$, we have

$$\|\gamma\|_{L^p(\Gamma_i)} \leq C\epsilon^{1/p}. \quad (3.2.3)$$

The ultrasonic wave u_γ generated by a source at $y \in \Gamma_e$ satisfies

$$\begin{cases} (\Delta + \omega^2)u_\gamma = 0 & \text{in } \Omega, \\ \frac{\partial u_\gamma}{\partial \nu} + \gamma u_\gamma = 0 & \text{on } \Gamma_i, \\ u_\gamma = \Phi_\omega(\cdot - y) & \text{on } \Gamma_e, \end{cases} \quad (3.2.4)$$

where ν is the outward unit normal to Ω .

Let u_0 denote the solution in absence of the corrosion, *i.e.*, the solution to the problem

$$\begin{cases} (\Delta + \omega^2)u_0 = 0 & \text{in } \Omega, \\ \frac{\partial u_0}{\partial \nu} = 0 & \text{on } \Gamma_i, \\ u_0 = \Phi_\omega(\cdot - y) & \text{on } \Gamma_e. \end{cases} \quad (3.2.5)$$

Throughout this chapter, we suppose that ω is not an eigenvalue of $-\Delta$ in Ω with the Dirichlet boundary condition on Γ_e and the Neumann boundary condition on Γ_i . Using the theory of collectively compact operators [2], we can easily prove that (3.2.4) is uniquely solvable for $\|\gamma\|_{L^p}$ small enough.

Suppose also that ω is not an eigenvalue of $-\Delta$ in the disk of radius R with the Dirichlet boundary condition on Γ_e , *i.e.*, ωR is not a zero of J_l . Using Graf's addition theorem (3.2.1), we compute u_0 to obtain its explicit form in Ω :

$$u_0(x) = \Phi_\omega(x - y) + \frac{i}{4} \sum_{l \in \mathbb{Z}} \left(a_l H_l^{(1)}(\omega|x|) + b_l J_l(\omega|x|) \right) e^{il\theta_y} e^{-il\theta_x},$$

where, for $l \in \mathbb{Z}$,

$$a_l = \frac{H_l^{(1)}(\omega R) J_l'(\omega r)}{(H_l^{(1)})'(\omega r) - \frac{H_l^{(1)}(\omega R)}{J_l(\omega R)} J_l'(\omega r)},$$

and

$$b_l = -\frac{H_l^{(1)}(\omega R)}{J_l(\omega R)} a_l.$$

Using the large-argument large-order (Debye's) asymptotics of the Bessel functions (see Section 3.6), we can prove that

$$\|\nabla u_0\|_{L^\infty(\Gamma_i)} = O(\omega), \quad \text{as } \omega \rightarrow +\infty. \quad (3.2.6)$$

Now we define the Dirichlet function \tilde{G}_ω by

$$\begin{cases} (\Delta_x + \omega^2)\tilde{G}_\omega(x, z) = \delta_z & \text{in } \Omega, \\ \frac{\partial \tilde{G}_\omega}{\partial \nu_x} \Big|_{\Gamma_i} = 0, \\ \tilde{G}_\omega \Big|_{\Gamma_e} = 0. \end{cases}$$

Again from Graf's addition theorem, we compute that

$$\tilde{G}_\omega(x, z) = -\Phi_\omega(x - z) + \frac{i}{4} \sum_{l \in \mathbb{Z}} \left(a_l H_l^{(1)}(\omega|x|) + b_l J_l(\omega|x|) \right) e^{-il\theta_z} e^{il\theta_x}, \quad (3.2.7)$$

where

$$a_l = \frac{J_l'(\omega r)}{(H_l^{(1)})'(\omega r) - \frac{H_l^{(1)}(\omega R)}{J_l(\omega R)} J_l'(\omega r)} \left[\frac{H_l^{(1)}(\omega R) J_l(\omega|z|)}{J_l(\omega R)} - H_l^{(1)}(\omega|z|) \right],$$

and

$$b_l = -\frac{H_l^{(1)}(\omega R)}{J_l(\omega R)} a_l - \frac{H_l^{(1)}(\omega R)}{J_l(\omega R)} J_l(\omega|z|).$$

Let $z \in \Gamma_i$. From Lemma 3.7.1 it follows that

$$\tilde{G}_\omega(x, z) = \frac{i}{2} H_0^{(1)}(\omega|x - z|) + \text{continuous function in } x, \quad \text{for } x \in \Gamma_i.$$

Moreover, combining (3.2.7) and the large-argument large-order asymptotic expansions of the Bessel functions we obtain through elementary but tedious computation that the following estimate

$$\|\tilde{G}_\omega(\cdot, z) - 2\Phi_\omega(\cdot - z)\|_{L^\infty(\Gamma_i)} = O(1) \quad \text{as } \omega \rightarrow +\infty, \quad (3.2.8)$$

holds uniformly in $z \in \Gamma_i$.

To simplify the notation, introduce $\tilde{\mathcal{S}}_{\Gamma_i}^\omega$ be the single layer potential defined by \tilde{G}_ω , that is,

$$\tilde{\mathcal{S}}_{\Gamma_i}^\omega \varphi(x) = \int_{\Gamma_i} \tilde{G}_\omega(x - y) \varphi(y) d\sigma(y), \quad x \in \mathbb{R}^2,$$

for $\varphi \in L^2(\Gamma_i)$.

Estimate (3.2.8) shows that the following lemma holds.

Lemma 3.2.1 For $p > 1$, there exists a positive constant C_p independent of ω such that

$$\|\tilde{\mathcal{S}}_{\Gamma_i}^\omega \varphi\|_{L^\infty(\Gamma_i)} \leq C_p \|\varphi\|_{L^p(\Gamma_i)}, \quad \text{for } \varphi \in L^p(\Gamma_i).$$

3.3 Asymptotic Formula

We derive in this section an asymptotic expansion of the ultrasonic boundary perturbations due to the corrosive parts. This formula is central to our detection techniques. For those purposes using the following theorem it is essential that the quantity $u_0(z_s)$ be non-zero.

Theorem 3.3.1 Suppose that $\lambda = 2\pi/\omega \gg \epsilon$ then the following asymptotic formula holds uniformly on Γ_e for some positive constant α :

$$\frac{\partial(u_\gamma - u_0)}{\partial\nu}(x) = - \sum_{s=1}^m \gamma(z_s) u_0(z_s) |I_s| \frac{\partial \tilde{\mathcal{G}}_\omega}{\partial\nu}(x, z_s) + O(\epsilon^{1+\alpha}), \quad x \in \Gamma_e. \quad (3.3.1)$$

Proof. Let $w := u_\gamma - u_0$. Then w satisfies

$$\begin{cases} \Delta w + \omega^2 w = 0 & \text{in } \Omega, \\ \frac{\partial w}{\partial\nu} + \gamma w = -\gamma u_0 & \text{on } \Gamma_i, \\ w = 0 & \text{on } \Gamma_e. \end{cases}$$

Thus we get

$$w + \tilde{\mathcal{S}}_{\Gamma_i}^\omega(\gamma w) = -\tilde{\mathcal{S}}_{\Gamma_i}^\omega(\gamma u_0) \quad \text{in } \Omega. \quad (3.3.2)$$

Since from Lemma 3.2.1 there exists a positive constant C depending only on p, ω, Γ_i , and Γ_e such that

$$\|\tilde{\mathcal{S}}_{\Gamma_i}^\omega(\gamma w)\|_{L^\infty(\Gamma_i)} \leq C \|\gamma w\|_{L^p(\Gamma_i)} \leq C \epsilon^{\frac{1}{p}} \|w\|_{L^\infty(\Gamma_i)}, \quad p > 1,$$

it follows that

$$w|_{\Gamma_i} = -\tilde{\mathcal{S}}_{\Gamma_i}^\omega(\gamma u_0) + O(\epsilon^{\frac{2}{p}}) \quad \text{in } L^\infty(\Gamma_i).$$

Therefore,

$$\frac{\partial w}{\partial \nu} = - \int_{\Gamma_i} \gamma u_0 \frac{\partial \tilde{G}_\omega}{\partial \nu} d\sigma + O(\epsilon^{\frac{2}{p}}) \quad \text{in } L^\infty(\Gamma_e), p > 1.$$

Using the Taylor expansion of $\frac{\partial \tilde{G}_\omega}{\partial \nu}$ at z_s together with the estimates (3.2.6) and

$$\int_{\Gamma_i} \gamma u_0 d\sigma = |I_s| \gamma(z_s) u_0(z_s) + O(\epsilon^2 \|\nabla u_0\|_{L^\infty(\Gamma_i)}),$$

yields the desired result. \square

Note that from (3.2.7), we have

$$\frac{\partial \tilde{G}_\omega}{\partial \nu}(x, z) = \frac{i\omega}{4} \sum_{l \in \mathbb{Z}} \left[a_l (H_l^{(1)})'(\omega R) + b_l J_l'(\omega R) + (H_l^{(1)})'(\omega R) J_l(\omega r) \right] e^{il\theta_x} e^{-il\theta_z}, \quad (3.3.3)$$

where

$$a_l = \frac{J_l'(\omega r)}{(H_l^{(1)})'(\omega r) - \frac{H_l^{(1)}(\omega R)}{J_l(\omega R)} J_l'(\omega r)} \left[\frac{H_l^{(1)}(\omega R) J_l(\omega r)}{J_l(\omega R)} - H_l^{(1)}(\omega r) \right]$$

and

$$b_l = -\frac{H_l^{(1)}(\omega R)}{J_l(\omega R)} a_l - \frac{H_l^{(1)}(\omega R)}{J_l(\omega R)} J_l(\omega r).$$

Analogously to (3.2.6) and (3.2.8), the large-argument large-order asymptotic expansions of the Bessel functions, we can prove that

$$\left\| \frac{\partial \tilde{G}_\omega}{\partial \nu}(\cdot, z) \right\|_{L^\infty(\Gamma_e)} = O(\omega), \quad (3.3.4)$$

uniformly in $z \in \Gamma_i$.

Note also that for high-frequency $\omega = O(\epsilon^{-1})$, we can derive an asymptotic expansion for the boundary perturbations as follows. From (3.3.2), we have

$$\gamma w = -(I + \gamma \tilde{\mathcal{S}}_{\Gamma_i}^\omega)^{-1}(\gamma \tilde{\mathcal{S}}_{\Gamma_i}^\omega(\gamma u_0)) \quad \text{on } \Gamma_i,$$

and for $x \in \Gamma_e$, we obtain

$$\begin{aligned} \frac{\partial(u_\gamma - u_0)}{\partial\nu}(x) &= - \int_{\Gamma_i} \frac{\partial \tilde{G}_\omega}{\partial\nu}(x, y) \gamma(y) u_0(y) d\sigma(y) \\ &+ \int_{\Gamma_i} \frac{\partial \tilde{G}_\omega}{\partial\nu}(x, y) (I + \gamma \tilde{\mathcal{S}}_{\Gamma_i}^\omega)^{-1}(\gamma \tilde{\mathcal{S}}_{\Gamma_i}^\omega(\gamma u_0))(y) d\sigma(y). \end{aligned}$$

Note that

$$\begin{aligned} \tilde{\mathcal{S}}_{\Gamma_i}^\omega \varphi(x) &= \int_{\{\omega|x-y|>1\} \cap \Gamma_i} \tilde{G}_\omega(x-y) \varphi(y) d\sigma(y) + \int_{\{\omega|x-y|\leq 1\} \cap \Gamma_i} \tilde{G}_\omega(x-y) \varphi(y) d\sigma(y) \\ &:= I + II. \end{aligned}$$

We have $I \leq C\|\varphi\|_\infty$, and from the change of variable we can show that $II \leq C\|\varphi\|_\infty$. Thus

$$\|\gamma \tilde{\mathcal{S}}_{\Gamma_i}^\omega\|_{L^\infty(\Gamma_i) \rightarrow L^\infty(\Gamma_i)} = O(1) \quad \text{when } \omega = O(\epsilon^{-1}),$$

and therefore we have

$$(I + \gamma \tilde{\mathcal{S}}_{\Gamma_i}^\omega)^{-1}(\gamma \tilde{\mathcal{S}}_{\Gamma_i}^\omega(\gamma u_0))(y) = O(\epsilon).$$

Writing the expansion of $\frac{\partial \tilde{G}_\omega}{\partial\nu}(x, y)$ for $x = (R, \theta_x), y = (r, \theta_{z_s} + \epsilon\theta)$ as $\omega = O(\epsilon^{-1})$ goes to $+\infty$ yields a high-frequency asymptotic formula for the boundary perturbations. This formula tends continuously to our low-frequency formula (3.3.1) as the limit of $\omega\epsilon$ goes to zero.

3.4 Reconstruction Methods

In this section, we adapt the MUSIC-type algorithm of Chapter 1 to the setting in which multiple ultrasonic boundary measurements are available and also show how one may quantitatively deduce the number of

corrosive parts present. We also adapt the propagation-backpropagation algorithm for ultrasound tomography to corrosion detection. We finally present a Fourier-type reconstruction method. All of these three different but very closely related approaches rely on our asymptotic expansion (3.3.1) of the ultrasonic reflected wave with respect to the length of the corrosive parts

3.4.1 A MUSIC-Type Algorithm

In this section, we adapt the MUSIC-type algorithm of Chapter 1 to our present setting. We also show how one may easily deduce the number of corrosive parts present from ultrasonic boundary measurements.

Let y_1, \dots, y_n be n point sources uniformly distributed on Γ_e . Rewrite (3.3.1) as follows:

$$\frac{\partial(u_\gamma - u_0)}{\partial\nu}(y) \approx \sum_{s=1}^m \gamma(z_s) |I_s| \left[\int_{\Gamma_e} \frac{\partial \tilde{G}_\omega}{\partial \nu}(y, z_s) \Phi_\omega(y - y_l) d\sigma(y) \right] \frac{\partial \tilde{G}_\omega}{\partial \nu}(y, z_s), \quad (3.4.1)$$

since

$$u_0(z_s) = - \int_{\Gamma_e} \frac{\partial \tilde{G}_\omega}{\partial \nu}(y, z_s) \Phi_\omega(y - y_l) d\sigma(y).$$

In the spirit of the reciprocity gap approach [10, 9], multiplying by $\Phi_\omega(y - y_{l'})$ and integrating over Γ_e we obtain that

$$\begin{aligned} & \int_{\Gamma_e} \frac{\partial(u_\gamma - u_0)}{\partial \nu}(y) \Phi_\omega(y - y_{l'}) d\sigma(y) \\ & \approx \sum_{s=1}^m \gamma(z_s) |I_s| \left[\int_{\Gamma_e} \frac{\partial \tilde{G}_\omega}{\partial \nu}(y, z_s) \Phi_\omega(y - y_l) d\sigma(y) \right] \left[\int_{\Gamma_e} \frac{\partial \tilde{G}_\omega}{\partial \nu}(y, z_s) \Phi_\omega(y - y_{l'}) d\sigma(y) \right]. \end{aligned}$$

Introduce the coefficients

$$a_{ll'} = \sum_{s=1}^m \alpha_s \left[\int_{\Gamma_e} \frac{\partial \tilde{G}_\omega}{\partial \nu}(y, z_s) \Phi_\omega(y - y_l) d\sigma(y) \right] \left[\int_{\Gamma_e} \frac{\partial \tilde{G}_\omega}{\partial \nu}(y, z_s) \Phi_\omega(y - y_{l'}) d\sigma(y) \right],$$

where $\alpha_s = \gamma(z_s)|I_s|$. Then from the asymptotic expansion (3.3.1) the matrix $A = (a_{ll'})_{l,l'=1,\dots,n}$ is approximately known:

$$A \approx \left(\int_{\Gamma_e} \frac{\partial(u_\gamma - u_0)}{\partial\nu}(y) \Phi_\omega(y - y_{l'}) d\sigma(y) \right)_{l,l'=1,\dots,n},$$

where u_γ and u_0 are the solutions corresponding to $\Phi_\omega(\cdot - y_l)$. It is easy to see that the matrix A admits the following decomposition:

$$A = \sum_{s=1}^m \alpha_s v_s v_s^T,$$

where T denotes the transpose and

$$v_s = \left(\int_{\Gamma_e} \frac{\partial \tilde{G}_\omega}{\partial \nu}(y, z_s) \Phi_\omega(y - y_1) d\sigma(y), \dots, \int_{\Gamma_e} \frac{\partial \tilde{G}_\omega}{\partial \nu}(y, z_s) \Phi_\omega(y - y_n) d\sigma(y) \right)^T, \quad s = 1, \dots, m.$$

Following [34], the MUSIC characterization of the locations $z_s, s = 1, \dots, m$ is given by the following theorem.

Theorem 3.4.1 *Let $\{y_n\} \in \Gamma_e$ be a countable set with the property that any analytic function which vanishes in all y_n vanishes identically on Γ_e . Then there exists $N_0 \in \mathbb{N}$ such that if $n \geq N_0$ then a point $z \in \{z_1, \dots, z_m\}$ if and only if the vector w_z defined by*

$$w_z := \left(\int_{\Gamma_e} \frac{\partial \tilde{G}_\omega}{\partial \nu}(y, z) \Phi_\omega(y - y_1) d\sigma(y), \dots, \int_{\Gamma_e} \frac{\partial \tilde{G}_\omega}{\partial \nu}(y, z) \Phi_\omega(y - y_n) d\sigma(y) \right)^T$$

belongs to $\text{Range}(A)$.

Proof. Assume that there is no N_0 which satisfies the necessary and sufficient condition of the theorem, then for each n , there exist z_n, x_n and $a_s^n (s = 1, \dots, m)$ such that

$$h_{z_n}(y_k) = \sum_{s=1}^m a_s^n h_{z_s}(y_k), \quad \text{for } k = 1, \dots, n,$$

and

$$h_{z_n}(x_n) \neq \sum_{s=1}^m a_s^n h_{z_s}(x_n).$$

Letting $\tilde{a}_0^n = \frac{1}{\sum_{s=1}^m a_s^n}$ and $\tilde{a}_s^n = \frac{a_s^n}{\sum_{s=1}^m a_s^n}$, we have

$$-\tilde{a}_0^n h_{z_n}(y_k) + \sum_{s=1}^m \tilde{a}_s^n h_{z_s}(y_k) = 0, \quad \text{for } k = 1, \dots, n,$$

$$-\tilde{a}_0^n h_{z_n}(x_n) + \sum_{s=1}^m \tilde{a}_s^n h_{z_s}(x_n) = 0.$$

We can assume that z_n, x_n and \tilde{a}_s^n ($s = 0, \dots, m$) converge to $z, x \in \Gamma_e$ and $\tilde{a}_s \in [0, 1]$, respectively. So

$$-\tilde{a}_0 h_z(y_k) + \sum_{s=1}^m \tilde{a}_s h_z(y_k) = 0, \quad \text{for all } k \in \mathbb{N}, \quad (3.4.2)$$

and

$$-\tilde{a}_0 h_z(x) + \sum_{s=1}^m \tilde{a}_s h_z(x) \neq 0. \quad (3.4.3)$$

Note that letting $x = Re^{i\theta_x}$, $y = Re^{i\theta_y}$ and $z = re^{i\theta_z}$, we have

$$h_z(x) := \int_{\Gamma_e} \frac{\partial \tilde{G}_\omega}{\partial \nu}(y, z) \Phi_\omega(y - x) d\sigma(y) = \int_{\Gamma_e} \frac{\partial \tilde{G}_\omega}{\partial \nu}(y, ze^{-i\theta_x}) \Phi_\omega(y - R) d\sigma(y).$$

Thus, h_z is analytic for each z , and (3.4.2) leads

$$-\tilde{a}_0 h_z(x) + \sum_{s=1}^m \tilde{a}_s h_z(x) = 0, \quad \text{for all } x \in \Gamma_e,$$

which is a contradiction to (3.4.3). \square

3.4.2 Kaczmarz Procedure

In this section, we adapt the propagation-backpropagation algorithm for ultrasound tomography to corrosion detection. Our iterative algorithm makes use of only one ultrasonic wave generated by a fixed point source.

For $f \in H^{1/2}(\Gamma_e)$, let u_γ is the solution to

$$\begin{cases} (\Delta + \omega^2)u_\gamma = 0 & \text{in } \Omega, \\ \frac{\partial u_\gamma}{\partial \nu} + \gamma u_\gamma = 0 & \text{on } \Gamma_i, \\ u_\gamma = f & \text{on } \Gamma_e, \end{cases} \quad (3.4.4)$$

and u_0 be the solution in the absence of corrosion. According to (3.3.1), we have

$$\frac{\partial(u_\gamma - u_0)}{\partial \nu}(x) = - \sum_{s=1}^m \gamma(z_s)u_0(z_s)|I_s| \frac{\partial G_\omega}{\partial \nu}(x, z_s) + O(\epsilon^{1+\alpha}), \quad x \in \Gamma_e.$$

Let $\alpha_s := \gamma(z_s)|I_s|$ and define for $\alpha = (\alpha_1, \dots, \alpha_m)$ and $q = (z_1, \dots, z_m)$

$$\mathcal{R}(\alpha, q) := \frac{\partial u_0}{\partial \nu} - \sum_{s=1}^m \alpha_s u_0(z_s) \frac{\partial G_\omega}{\partial \nu}(\cdot, z_s). \quad (3.4.5)$$

Note that \mathcal{R} is a nonlinear operator from \mathbb{R}^{2m} into $L^2(\Gamma_e)$.

Let $\frac{\partial u_\gamma^*}{\partial \nu}$ be the measured data on Γ_e . The Kaczmarz procedure of this paper is an iterative scheme updating (α, q) to find (α^*, q^*) so that

$$\mathcal{R}(\alpha^*, q^*) = \frac{\partial u_\gamma^*}{\partial \nu} \quad \text{on } \Gamma_e. \quad (3.4.6)$$

Following Natterer and Wübbeling [39], updating for the Kaczmarz procedure for corrosion detection is done by

$$(\alpha, q) \leftarrow (\alpha, q) - \tau(\mathcal{R}')^* \left(\mathcal{R}(\alpha, q) - \frac{\partial u_\gamma^*}{\partial \nu} \right), \quad (3.4.7)$$

where τ is a relaxation parameter and $(\mathcal{R}')^*$ is the adjoint of the Fréchet derivative of \mathcal{R} . Observe that

$$\frac{\partial \mathcal{R}}{\partial \alpha_s} = -u_0(z_s) \frac{\partial G_\omega}{\partial \nu}(\cdot, z_s),$$

and

$$\frac{\partial \mathcal{R}}{\partial z_s} = -\frac{\partial u_0}{\partial T}(z_s) \frac{\partial G_\omega}{\partial \nu}(\cdot, z_s) - u_0(z_s) \frac{\partial^2 G_\omega}{\partial \nu \partial T}(\cdot, z_s),$$

where $\frac{\partial}{\partial T}$ denotes the tangential derivative on Γ_i and in $\frac{\partial^2 G_\omega}{\partial \nu \partial T}$ the normal derivative is with respect to the first variables and the tangential derivative is with respect to the second variables. Thus we have for $h \in H^{1/2}(\Gamma_e)$

$$(\mathcal{R}')^*(h) = -\left(\overline{u_0(z_1)v(z_1)}, \dots, \overline{u_0(z_m)v(z_m)}, \frac{\partial}{\partial T}(\overline{u_0(z_1)v(z_1)}), \dots, \frac{\partial}{\partial T}(\overline{u_0(z_1)v(z_1)})\right), \quad (3.4.8)$$

where v is the solution to

$$\begin{cases} (\Delta + \omega^2)v = 0 & \text{in } \Omega, \\ \frac{\partial v}{\partial \nu} = 0 & \text{on } \Gamma_i, \\ v = \bar{h} & \text{on } \Gamma_e. \end{cases} \quad (3.4.9)$$

Note that (3.4.9) is nothing but time reversal in the time-harmonic regime.

3.4.3 Fourier Method

The Fourier method is based on a simple relation between the Fourier coefficients of $\partial(u_\gamma - u_0)/\partial \nu$ w.r.t. θ_x and the locations $\theta_{z_s}, s = 1, \dots, m$, of the corrosive parts.

We begin with noticing that using (3.3.3), we immediately get that

$$\frac{\partial \tilde{G}_\omega}{\partial \nu}(x, z) = \sum_{n \in \mathbb{Z}} e^{in\theta_x} e^{-in\theta_z} M(n),$$

where

$$M(n) = \frac{i\omega}{4} \left[a_n (H_n^{(1)})'(\omega R) + b_n J_n'(\omega R) + (H_n^{(1)})'(\omega R) J_n(\omega r) \right].$$

Let c_n denote the Fourier coefficient of $\partial(u_\gamma - u_0)/\partial \nu$ w.r.t. θ_x , i.e.,

$$c_n = \frac{1}{2\pi R} \int_{\Gamma_e} e^{-in\theta_x} \frac{\partial(u_\gamma - u_0)}{\partial \nu}(x) d\sigma(x).$$

It then follows from (3.3.1) that

$$\begin{aligned} c_n &= - \sum_{s=1}^m \gamma(z_s) u_0(z_s) |I_s| \frac{1}{2\pi R} \int_{\Gamma_e} e^{-in\theta_x} \frac{\partial \tilde{G}_\omega}{\partial \nu}(x, z_s) d\sigma(x) + O(\epsilon^{1+\alpha}) \\ &= \sum_{s=1}^m \beta_s \alpha_s^n + O(\epsilon^{1+\alpha}), \quad n = 0, 1, 2, \dots, \end{aligned}$$

where

$$\alpha_s = e^{-i\theta_{z_s}} \quad \text{and} \quad \beta_s = -\gamma(z_s) u_0(z_s) |I_s| M(n).$$

Note that since z_s is on the interior circle Γ_i , we have $z_s = r\alpha_s$.

The Fourier method is based on the following two lemmas from [20, 29].

Lemma 3.4.2 *Suppose that the sequence $\{c_n\}$ takes the form $c_n = \sum_{j=1}^k \beta_j \alpha_j^n$, $n = 0, 1, \dots$. If l_1, \dots, l_k satisfies the generating equation*

$$c_{n+k} + l_1 c_{n+k-1} + \dots + l_k c_n = 0, \quad n = 0, 1, \dots, k-1, \quad (3.4.10)$$

then $\alpha_1, \alpha_2, \dots, \alpha_k$ are solutions of

$$z^k + l_1 z^{k-1} + \dots + l_k = 0. \quad (3.4.11)$$

The converse is also true. Furthermore, if (3.4.10) holds, then it holds for all n .

Lemma 3.4.3 *Let c_n be as in the Lemma 3.4.2 and let*

$$D_n = \det \begin{pmatrix} c_0 & c_1 & \dots & c_{n-1} \\ c_1 & c_2 & \dots & c_n \\ \vdots & \vdots & & \vdots \\ c_{n-1} & c_n & \dots & c_{2n-2} \end{pmatrix}.$$

Then

$$D_n = \begin{cases} \beta_1 \beta_2 \dots \beta_m \prod_{i < j} (\alpha_i - \alpha_j)^2 & \text{if } n = m, \\ 0 & \text{if } n > m. \end{cases} \quad (3.4.12)$$

We have the following Fourier reconstruction procedure.

- (Numbering) Start with a bound N and compute the determinants in (3.4.12) for $n = N, N - 1, \dots$, until it becomes nonzero. The first number for which the determinant is nonzero is m .
- Solve for l_1, l_2, \dots, l_N the system of linear equations

$$\begin{pmatrix} c_0 & c_1 & \cdots & c_{N-1} \\ c_1 & c_2 & \cdots & c_N \\ \vdots & \vdots & & \vdots \\ c_{N-1} & c_N & \cdots & c_{2N-2} \end{pmatrix} \begin{pmatrix} l_N \\ l_{N-1} \\ \vdots \\ l_1 \end{pmatrix} = \begin{pmatrix} -c_N \\ -c_{N+1} \\ \vdots \\ -c_{2N-1} \end{pmatrix}. \quad (3.4.13)$$

- (Localizing) Find zeros $\alpha_1, \dots, \alpha_N$ of the polynomial equation $z^N + l_1 z^{N-1} + \dots + l_N = 0$.
- (Size estimation) Solve the equation

$$\begin{pmatrix} 1 & 1 & \cdots & 1 \\ \alpha_1 & \alpha_2 & \cdots & \alpha_N \\ \vdots & \vdots & & \vdots \\ \alpha_1^{N-1} & \alpha_2^{N-1} & \cdots & \alpha_N^{N-1} \end{pmatrix} \begin{pmatrix} \beta_1 \\ \beta_2 \\ \vdots \\ \beta_N \end{pmatrix} = \begin{pmatrix} c_0 \\ c_1 \\ \vdots \\ c_{N-1} \end{pmatrix}$$

to find β_1, \dots, β_N .

3.5 High Frequency Instabilities

In many practical situations, $R - r = O(r) \gg \lambda \gg \epsilon$. In this case, formula (3.3.1) remains valid but does not yield a stable detection procedure because of high oscillations in the measurements data. To resolve this difficulty, we first introduce the truncation operator P defined by $P(f) := \sum_{|l| \leq \omega r} f_l e^{il\theta}$ for $f = \sum_{l \in \mathbb{Z}} f_l e^{il\theta}$, i.e., P is a low pass filter operator.

To justify the validity of filtering, consider the Helmholtz equation $(\Delta + \omega^2)w = 0$ in $|x| > r$ with the boundary condition $w = f$ on $|x| = r$. Then we have

$$w(R, \theta) = \sum_{l \in \mathbb{Z}} f_l \frac{H_l^{(1)}(\omega R)}{H_l^{(1)}(\omega r)} e^{il\theta}, \quad R > r.$$

By making use of Debey's asymptotic expansion [1, page 366],

$$\frac{H_l^{(1)}(\omega R)}{H_l^{(1)}(\omega r)} \approx \frac{e^{l(\alpha - \tanh \alpha)}}{e^{l(\alpha' - \tanh \alpha')}}, \quad \text{for } l > \omega R, \quad (3.5.1)$$

where $\omega R = l \operatorname{sech} \alpha$ and $\omega r = l \operatorname{sech} \alpha'$. Note that $\alpha' > \alpha$. Moreover, from the asymptotic behavior of Hankel functions [1, 9.3.3], i.e.

$$H_l^{(1)}(l \sec \beta) = \sqrt{2/(\pi l \tan \beta)} \{e^{i(l \tan \beta - l\beta - \frac{1}{4}\pi)} + O(l^{-1})\}, \quad 0 < \beta < \frac{1}{2}\pi,$$

we have

$$\frac{H_l^{(1)}(\omega R)}{H_l^{(1)}(\omega r)} \approx \sqrt{\frac{\tan \beta'}{\tan \beta}} e^{i(l \tan \beta - l\beta - l \tan \beta' + l\beta')}, \quad \text{for } l < \omega r, \quad (3.5.2)$$

where $\omega R = l \sec \beta$ and $\omega r = l \sec \beta'$.

From (3.5.1) we arrive that the Helmholtz operator acts as a low pass filter, and moreover (3.5.2) would suggest that the angular resolution is of order $2\pi/\omega r = \lambda/r$, which is beyond the Rayleigh resolution limit.

Now it follows from (3.3.1) that

$$\frac{\partial(u_\gamma - u_0)}{\partial \nu} \approx - \sum_{s=1}^m \gamma(z_s) u_0(z_s) |I_s| P\left(\frac{\partial \tilde{G}_\omega}{\partial \nu}\right)(\cdot, z_s) \quad \text{on } \Gamma_e,$$

since P is linear. The necessary modifications of our MUSIC and Fourier procedures are obvious.

We now indicate how to modify the Kaczmarz procedure in order to detect in a stable way the corrosive parts. The only remaining problem is to stably determine $u_\gamma(z_s)$. In very much the same spirit as the

marching scheme of Natterer and Wübbeling [40], we define u_l to be the solution of the initial boundary ODE problem:

$$\frac{d^2 u_l}{dt^2} + \frac{1}{t} \frac{du_l}{dt} + \left(\omega^2 - \frac{1}{t^2}\right) u_l = 0, \quad r < t < R,$$

with the initial boundary conditions:

$$u_l(R) = \frac{1}{2\pi} \int_0^{2\pi} P(\Phi_\omega) e^{-i\theta} d\theta, \quad \frac{du_l}{dt}(R) = \frac{1}{2\pi} \int_0^{2\pi} P\left(\frac{\partial u_\gamma}{\partial \nu}\right) e^{-i\theta} d\theta.$$

Recall that $\frac{\partial u_\gamma}{\partial \nu}$ is the measured data and so is known. The value $u_\gamma(z_s)$ is then given by

$$u_\gamma(z_s) = \sum_{|l| \leq \omega r} u_l(r) e^{i\theta z_s}.$$

3.6 Large-Argument Large-Order Asymptotics of the Bessel Functions

The leading terms of the large-argument large-order asymptotics of the Bessel functions, and their first derivatives are summarized below.

- Regime I: $\nu < x$

$$J_\nu(x) \sim \sqrt{\frac{2}{\pi}} (x^2 - \nu^2)^{-1/4} \cos \alpha, \quad Y_\nu(x) \sim \sqrt{\frac{2}{\pi}} (x^2 - \nu^2)^{-1/4} \sin \alpha,$$

$$J'_\nu(x) \sim -\sqrt{\frac{2}{\pi}} \frac{(x^2 - \nu^2)^{1/4}}{x} \sin \alpha, \quad Y'_\nu(x) \sim \sqrt{\frac{2}{\pi}} \frac{(x^2 - \nu^2)^{1/4}}{x} \cos \alpha,$$

with the notation, $\alpha = (x^2 - \nu^2)^{1/2} - \nu \cos^{-1}(\nu/x) - \pi/4$.

- Regime II: $\nu \sim x$

$$J_\nu(x) \sim \left(\frac{2}{x}\right)^{1/3} Ai\left(\left(\frac{2}{x}\right)^{1/3}(\nu - x)\right), \quad Y_\nu(x) \sim -\left(\frac{2}{x}\right)^{1/3} Bi\left(\left(\frac{2}{x}\right)^{1/3}(\nu - x)\right),$$

$$J'_\nu(x) \sim -\left(\frac{2}{x}\right)^{2/3} Ai'\left(\left(\frac{2}{x}\right)^{1/3}(\nu - x)\right), \quad Y'_\nu(x) \sim \left(\frac{2}{x}\right)^{2/3} Bi'\left(\left(\frac{2}{x}\right)^{1/3}(\nu - x)\right),$$

where Ai and Bi are the Airy functions.

- Regime III: $\nu > x$

$$J_\nu(x) \sim \frac{1}{\sqrt{2\pi}} (\nu^2 - x^2)^{-1/4} e^\beta, \quad Y_\nu(x) \sim -\sqrt{\frac{2}{\pi}} (\nu^2 - x^2)^{-1/4} e^{-\beta},$$

$$J'_\nu(x) \sim \frac{1}{\sqrt{2\pi}} \frac{(\nu^2 - x^2)^{1/4}}{x} e^\beta, \quad Y'_\nu(x) \sim \sqrt{\frac{2}{\pi}} \frac{(\nu^2 - x^2)^{1/4}}{x} e^{-\beta},$$

where we use notation, $\beta = (\nu^2 - x^2)^{1/2} - \nu \cosh^{-1}(\nu/x)$.

3.7 Green's Function

We first recall that

$$J_l(x) = \frac{x^l}{2^l l!} \left(1 + O\left(\frac{1}{l}\right)\right), \quad l \rightarrow \infty, \quad (3.7.1)$$

uniformly on compact subsets of \mathbb{R} and

$$H_l^{(1)}(x) = -i \frac{2^l (l-1)!}{\pi x^l} \left(1 + O\left(\frac{1}{l}\right)\right), \quad l \rightarrow \infty, \quad (3.7.2)$$

uniformly on compact subsets of $(0, \infty)$. See for example [19, Section 3.4]. From these expansions we can derive that

$$H_l^{(1)}(x) J_l(x) = -\frac{i}{l\pi} \left(1 + O\left(\frac{1}{l}\right)\right), \quad \text{as } l \rightarrow \infty,$$

$$\frac{H_l^{(1)}(x)}{J_l(x)} = -\frac{i 4^l l! (l-1)!}{\pi x^{2l}} \left(1 + O\left(\frac{1}{l}\right)\right), \quad \text{as } l \rightarrow \infty.$$

Suppose now that ωR is not a zero of Bessel's function J_l and that $|\omega| < M$, for some positive bound M . For $z \in \Omega$, we have

$$\tilde{G}_\omega(x, z) = \frac{i}{4} H_0^{(1)}(\omega|x-z|) + \frac{i}{4} \sum_{l \in \mathbb{Z}} \left(a_l H_l^{(1)}(\omega|x|) + b_l J_l(\omega|x|) \right) e^{-il\theta_z} e^{il\theta_x},$$

where

$$a_l = \frac{J'_l(\omega r)}{(H_l^{(1)})'(\omega r) - \frac{H_l^{(1)}(\omega R)}{J_l(\omega R)} J'_l(\omega r)} \left[\frac{H_l^{(1)}(\omega R) J_l(\omega|z|)}{J_l(\omega R)} - H_l^{(1)}(\omega|z|) \right],$$

and

$$b_l = -\frac{H_l^{(1)}(\omega R)}{J_l(\omega R)}a_l - \frac{H_l^{(1)}(\omega R)J_l(\omega|z|)}{J_l(\omega R)}.$$

Lemma 3.7.1 For $x, z \in \Omega$, we have that

$$\tilde{G}_\omega(x, z) = \frac{i}{4}H_0^{(1)}(\omega|x-z|) + \frac{i}{4}\sum_{l \in \mathbb{Z}} \left(\frac{r}{|z|}\right)^l J_l(\omega r)H_l^{(1)}(\omega|x|)e^{-il\theta_z}e^{il\theta_x} + K^\omega(x, z),$$

where K^ω is a continuous function in $\bar{\Omega}$. In particular,

$$\tilde{G}_\omega(x, z) = \frac{i}{2}H_0^{(1)}(\omega|x-z|) + K^\omega(x, z), \quad \text{for } x \in \Gamma_i.$$

Proof. Note that we have the recurrence relation

$$\frac{d}{dx}C_l(x) = \frac{lC_l(x)}{x} - C_{l+1}(x),$$

where C_l denotes either J_l or $H_l^{(1)}$. From (3.7.1) and (3.7.2), we obtain that

$$\frac{J_l'(\omega r)}{(H_l^{(1)})'(\omega r) - \frac{H_l^{(1)}(\omega R)}{J_l(\omega R)}J_l'(\omega r)} = -\frac{J_l(\omega r)}{H_l^{(1)}(\omega r)}\left(1 + O\left(\frac{1}{l}\right)\right).$$

We compute

$$\begin{aligned} a_l H_l^{(1)}(\omega|x|) &= -\frac{J_l(\omega r)}{H_l^{(1)}(\omega r)} \left[\frac{H_l^{(1)}(\omega R)}{J_l(\omega R)} J_l(\omega|z|)J_l(\omega|x|) - H_l^{(1)}(\omega|z|)J_l(\omega|x|) \right] \left(1 + O\left(\frac{1}{l}\right)\right) \\ &= \left[\frac{i}{l\pi} \left(\frac{r}{R}\right)^{2l} \left(\frac{|z|}{|x|}\right)^l + \left(\frac{r}{|z|}\right)^l J_l(\omega r)H_l^{(1)}(\omega|x|) \right] \left(1 + O\left(\frac{1}{l}\right)\right) \\ &= \left(\frac{r}{|z|}\right)^l J_l(\omega r)H_l^{(1)}(\omega|x|) + O\left(\frac{1}{l^2}\right). \end{aligned} \quad (3.7.3)$$

In the same way, we can get

$$b_l J_l(\omega|x|) = O\left(\frac{|x||z|}{R^2}\right)^l. \quad (3.7.4)$$

Combining these expansions yields the desired result. \square

Chapter 4

An Asymptotic Formalism for Reconstructing Small Perturbations of Scatterers from Electric or Acoustic Far-Field Measurements

4.1 Introduction

The field of inverse shape problems has been an active area of research for several decades. Several related scalar problems belong to this field: electric and acoustic scattering form two large classes. In direct problems one wants to calculate the field outside a given object. In two common situations, one knows either the values of the field on the object (the Dirichlet problem), or the values of the normal derivative of the field on the boundary (the Neumann problem). Direct problems are usually well posed. Inverse shape problems involve reconstructing the shape of an object from measurements of the electric or acoustic field.

These problems are ill posed: the solution has an unstable dependence on the input data.

The formulation of the electric scattering problem is based on the quasi-static approximation and the related Laplace equation for the electric scalar potential. When a perfect conductor is exposed to extremely low-frequency electric fields the problem is equivalent to the Dirichlet boundary value problem for the Laplace operator.

The sound-soft acoustic scattering problem is characterized by the condition that the total field vanishes on the boundary of the scatterer. Thus, acoustic scattering is equivalent to the Dirichlet boundary value problem for the Helmholtz operator, with the scattered field equal to the negative of the known incident field.

These two problems are frequently solved by methods of potential theory. The single- and double-layer potentials relate a charge density on the boundary of the object to the limiting values of the field and its normal derivative. The resulting integral equations are then solved in an appropriate function space, a common choice being the Lebesgue space L^2 .

In this chapter, assuming that the unknown object boundary is a small perturbation of a unit circle, we develop for both electric and acoustic problems a linearized relation between the far-field data that result from fixed Dirichlet boundary conditions, entering as parameters, and the shape of the object, entering as variables. This relation is used to find the Fourier coefficients of the perturbation. Suppose that the angular oscillations in the perturbation are less than $1/n$. In order to detect that perturbation, it turns out that one needs to use the first n eigenvectors of the Dirichlet-to-Neumann operator corresponding to the unperturbed shape as Dirichlet boundary data. We may think that this result is quite general. Our asymptotic formulae for the Dirichlet-to-Neumann operator in terms of the small perturbations of the shape

of the scatterer follow the expansions of Dirichlet-to-Neumann operators for rough non-periodic surfaces [37, 17] and for periodic interfaces [41].

Our approach relies on asymptotic expansions of the far-field data with respect to the perturbations in the boundary, in much the same spirit as the recent work [8] and the text [4]. It makes use of an expansion of the Dirichlet-to-Neumann operator. We consider only the two-dimensional case, the extension to three dimensions being obvious. In connection with our work, we should also mention the paper by Kaup and Santosa [31] on detecting corrosion from steady-state voltage boundary perturbations and the work by Tolmasky and Wiegmann [44] on the reconstruction of small perturbations of an interface for the inverse conductivity problem.

4.2 Formulation of the Electric Problem

Let D be a unit disk in \mathbb{R}^2 . When the boundary value is given by $\Psi \in \mathcal{C}^\infty(\partial D)$ satisfying $\int \Psi ds = 0$, the voltage potential outside the disk is given by the harmonic function u_0 which satisfies the following:

$$\begin{cases} \Delta u_0 = 0, & \text{in } \mathbb{R}^2 \setminus \overline{D}, \\ u_0 = \Psi, & \text{on } \partial D, \\ u_0(x) \longrightarrow 0, & \text{as } |x| \longrightarrow +\infty. \end{cases} \quad (4.2.1)$$

We consider the boundary perturbation of D given by a Lipschitz function f and a small number ϵ . Define \tilde{D} by

$$\partial \tilde{D} (= \partial D + \epsilon f \nu) := \left\{ (1 + \epsilon f(\theta)) e_\theta, \theta \in [0, 2\pi] \right\},$$

where ν is the outward unit normal vector to ∂D and $e_\theta = (\cos \theta, \sin \theta)$.

Let u be the voltage potential outside the perturbed domain \tilde{D} with the fixed Dirichlet data Ψ on the boundary, i.e.,

$$\begin{cases} \Delta u = 0, & \text{in } \mathbb{R}^2 \setminus \overline{\tilde{D}}, \\ u(x_\theta) = \Psi, & \text{on } \partial\tilde{D}, \\ u(x) \longrightarrow 0, & \text{as } |x| \longrightarrow +\infty, \end{cases} \quad (4.2.2)$$

where $x_\theta = (1 + \epsilon f(\theta))e_\theta$.

4.2.1 Representation Formula

It is known that a fundamental solution to the Laplacian in \mathbb{R}^2 is given by

$$\Gamma(x) = \frac{1}{2\pi} \ln |x|.$$

Using Green's theorem, the solution u to (4.2.2) can be expressed as

$$u(x) = \int_{\partial\tilde{D}} \Gamma(x-y) \frac{\partial u}{\partial \nu_y}(y) d\sigma_y - \int_{\partial\tilde{D}} \frac{\partial \Gamma}{\partial \nu_y}(x-y) u(y) d\sigma_y, \quad \text{for } x \in \mathbb{R}^2 \setminus \overline{\tilde{D}}. \quad (4.2.3)$$

We change the variable from y to $y = (1 + \epsilon f(\theta))e_\theta$. The outward normal vector ν_y is

$$\nu_y = \frac{N_\theta}{|N_\theta|}, \quad (4.2.4)$$

where

$$N_\theta = (1 + \epsilon f(\theta))e_\theta - \epsilon \dot{f} \tau_\theta, \quad \tau_\theta = (-\sin \theta, \cos \theta). \quad (4.2.5)$$

Here \dot{f} is the derivative of f with respect to θ . Note that since f is Lipschitz continuous, it is differentiable almost everywhere. Moreover,

$$|\dot{f}| \leq M,$$

where M is the Lipschitz constant of f . We also have

$$d\sigma_y = |N_\theta| d\theta.$$

Now we define the operator $\mathcal{N}_{\epsilon f}$ using polar coordinates by

$$\mathcal{N}_{\epsilon f}(\Psi)(\theta) := \frac{\partial u}{\partial N_\theta}(1 + \epsilon f(\theta), \theta). \quad (4.2.6)$$

Then (4.2.3) becomes

$$u(x) = \frac{1}{2\pi} \int_0^{2\pi} \left[\ln |x - (1 + \epsilon f(\theta))e_\theta| \mathcal{N}_{\epsilon f}(\Psi) - \frac{\langle (1 + \epsilon f(\theta))e_\theta - x, N_\theta \rangle}{|(1 + \epsilon f(\theta))e_\theta - x|^2} \Psi \right] d\theta. \quad (4.2.7)$$

Letting $f = 0$, we have

$$u_0(x) = \frac{1}{2\pi} \int_0^{2\pi} \left[\ln |x - e_\theta| \mathcal{N}_0(\Psi) - \frac{\langle e_\theta - x, e_\theta \rangle}{|x - e_\theta|^2} \Psi \right] d\theta, \quad (4.2.8)$$

where

$$\mathcal{N}_0(\Psi)(\theta) = \partial_r u_0(1, \theta).$$

Note that \mathcal{N}_0 is the *Dirichlet-to-Neumann operator* of the unit disk in \mathbb{R}^2 .

In the next section, we expand $\mathcal{N}_{\epsilon f}$ in terms of ϵ , f and Ψ .

4.2.2 Expansion of $\mathcal{N}_{\epsilon f}$ using the field expansions method

In this section, we use the polar coordinates. We start by the simple computation:

$$\begin{aligned} \mathcal{N}_{\epsilon f}(\Psi)(\theta) &= \left(\begin{array}{c} \frac{\partial u}{\partial r} \\ \frac{1}{r} \frac{\partial u}{\partial \theta} \end{array} \right) \Big|_{r=1+\epsilon f(\theta)} \cdot \left(\begin{array}{c} (1 + \epsilon f(\theta)) \\ -\epsilon \dot{f}(\theta) \end{array} \right) \\ &= (1 + \epsilon f(\theta)) \frac{\partial u}{\partial r} \Big|_{r=1+\epsilon f(\theta)} - \frac{\epsilon \dot{f}(\theta)}{1 + \epsilon f(\theta)} \frac{\partial u}{\partial \theta} \Big|_{r=1+\epsilon f(\theta)} \\ &= (1 + \epsilon f(\theta)) \frac{\partial u}{\partial r} \Big|_{r=1+\epsilon f(\theta)} - \epsilon \dot{f} \frac{\partial u}{\partial \theta} \Big|_{r=1+\epsilon f(\theta)} + O(\epsilon^2) \\ &=: A(\epsilon, f) + O(\epsilon^2). \end{aligned}$$

Here $O(\epsilon^2)$ depends on $\|f\|_\infty$ and the Lipschitz constant of f .

To derive an asymptotic expansion of $A(\epsilon, f)$, we apply the method of field expansion (F.E) (see [41]). Firstly, we expand u only in powers of ϵ , i.e.,

$$u(r, \theta) = \sum_{n=0}^{\infty} u_n(r, \theta) \epsilon^n, \quad \mathcal{N}_{\epsilon f}(\Psi) = \sum_{n=0}^{\infty} \mathcal{N}_f^n(\Psi)(r, \theta) \epsilon^n.$$

Now expanding in terms of r and evaluating the derivatives of u at $r = 1 + \epsilon f$, we obtain that

$$\left. \frac{\partial u}{\partial r} \right|_{r=1+\epsilon f(\theta)} = \sum_{n=0}^{\infty} \sum_{l=0}^n \partial_r^{l+1} u_{n-l}(1, \theta) \frac{f^l}{l!} \epsilon^n,$$

and

$$\left. \frac{\partial u}{\partial \theta} \right|_{r=1+\epsilon f(\theta)} = \sum_{n=0}^{\infty} \sum_{l=0}^n \partial_r^l \partial_{\theta} u_{n-l}(1, \theta) \frac{f^l}{l!} \epsilon^n.$$

Putting together these expansions, we arrive at

$$\begin{aligned} A(\epsilon, f) &= \sum_{n=0}^{\infty} \sum_{l=0}^n \partial_r^{l+1} u_{n-l}(1, \theta) \frac{f^l(\theta)}{l!} \epsilon^n + f(\theta) \sum_{n=0}^{\infty} \sum_{l=0}^n \partial_r^{l+1} u_{n-l}(1, \theta) \frac{f^l(\theta)}{l!} \epsilon^{n+1} \\ &\quad - \dot{f}(\theta) \sum_{n=0}^{\infty} \sum_{l=0}^n \partial_r^l \partial_{\theta} u_{n-l}(1, \theta) \frac{f^l(\theta)}{l!} \epsilon^{n+1}, \end{aligned}$$

and therefore

$$\begin{aligned} \mathcal{N}_{\epsilon f}(\Psi)(\theta) &= \partial_r u_0(1, \theta) + \epsilon \left(\partial_r u_1(1, \theta) \right. \\ &\quad \left. + \partial_r^2 u_0(1, \theta) f(\theta) + \partial_r u_0(1, \theta) \dot{f}(\theta) - \partial_{\theta} u_0(1, \theta) \dot{f}(\theta) \right) + O(\epsilon^2). \end{aligned} \quad (4.2.9)$$

Here $O(\epsilon^2)$ depends on $\|f\|_{\infty}$ and the Lipschitz constant of f .

We express the equation (4.2.9) in terms of Ψ and f . At first, we have

$$\partial_{\theta} u_0(1, \theta) = \dot{\Psi}. \quad (4.2.10)$$

To change $\partial_r u_1(1, \theta)$, $\partial_r^2 u_0(1, \theta)$ and $\partial_r u_0(1, \theta)$, we start from the Fourier series of Ψ :

$$\Psi(\theta) = \sum_{n=1}^{+\infty} [\hat{a}_n(\Psi) \cos(n\theta) + \hat{b}_n(\Psi) \sin(n\theta)],$$

where

$$\hat{a}_n(\Psi) = \frac{1}{\pi} \int_0^{2\pi} \Psi(\theta) \cos(n\theta) d\theta, \quad \hat{b}_n(\Psi) = \frac{1}{\pi} \int_0^{2\pi} \Psi(\theta) \sin(n\theta) d\theta. \quad (4.2.11)$$

By the uniqueness of a solution to (4.2.1), u_0 satisfies

$$u_0(r, \theta) = \sum_{n=1}^{\infty} \left[\hat{a}_n(\Psi) \frac{\cos(n\theta)}{r^n} + \hat{b}_n(\Psi) \frac{\sin(n\theta)}{r^n} \right].$$

Hence the *Dirichlet-to-Neumann operator* \mathcal{N}_0 of D is given by

$$\mathcal{N}_0(\Psi)(\theta) (= \partial_r u_0(1, \theta)) = - \sum_{n=1}^{+\infty} \left[n \hat{a}_n(\Psi) \cos(n\theta) + n \hat{b}_n(\Psi) \sin(n\theta) \right]. \quad (4.2.12)$$

We also define the operator \mathcal{D}_0 by

$$\mathcal{D}_0(\Psi)(\theta) := - \sum_{n=1}^{+\infty} \left[(n+1) \hat{a}_n(\Psi) \cos(n\theta) + (n+1) \hat{b}_n(\Psi) \sin(n\theta) \right], \quad (4.2.13)$$

to write

$$\partial_r^2 u_0(1, \theta) = \mathcal{D}_0 \mathcal{N}_0(\Psi)(\theta). \quad (4.2.14)$$

Lemma 4.2.1 *For a given Lipschitz function f and $\Psi \in \mathcal{C}^\infty[0, 2\pi]$, we have*

$$\mathcal{N}_{\epsilon f}(\Psi) = \mathcal{N}_f^0(\Psi) + \epsilon \mathcal{N}_f^1(\Psi) + O(\epsilon^2),$$

where

$$\mathcal{N}_f^0(\Psi) = \mathcal{N}_0(\Psi),$$

and

$$\mathcal{N}_f^1(\Psi) = \mathcal{D}_0 \mathcal{N}_0(\Psi) f - \mathcal{N}_0(\mathcal{N}_0(\Psi) f) + \mathcal{N}_0(\Psi) f - f \dot{\Psi}. \quad (4.2.15)$$

Here the remainder $O(\epsilon^2)$ depends on $\|f\|_\infty$ and the Lipschitz constant of f .

Proof. From (4.2.10), (4.2.12) and (4.2.13), we are left to calculate $\partial_r u_1(1, \theta)$. From the field expansion method, we have

$$u(r, \theta) \Big|_{r=1+\epsilon f(\theta)} = \sum_{n=0}^{\infty} \sum_{l=0}^n \partial_r^l u_{n-l}(1, \theta) \frac{f^l}{l!} \epsilon^n.$$

Therefore

$$u(1 + \epsilon f(\theta), \theta) = u_0(1, \theta) + (u_1(1, \theta) + \partial_r u_0(1, \theta) f) \epsilon + O(\epsilon^2).$$

Since $u(1 + \epsilon f(\theta), \theta) = u_0(1, \theta) = \Psi(\theta)$, we deduce that $u_1(r, \theta)$ satisfies

$$\begin{cases} \Delta u_1 = 0, & \text{in } \mathbb{R}^2 \setminus \widetilde{D}, \\ u_1(1, \theta) = -\mathcal{N}_0(\Psi)(\theta) f(\theta), & \text{on } \partial \widetilde{D}, \\ u_1(r, \theta) \longrightarrow 0, & \text{as } r \longrightarrow +\infty. \end{cases}$$

Therefore we have

$$\partial_r u_1(1, \theta) = -\mathcal{N}_0(\mathcal{N}_0(\Psi) f), \quad (4.2.16)$$

which completes the proof. \square

It is worth mentioning, in connection with our asymptotic expansion in Lemma 4.2.1, the expansions of Dirichlet-to-Neumann operators for rough non-periodic surfaces [37, 17] and for periodic interfaces [41].

4.2.3 Far Field Expansion

Define $\widetilde{\Omega} := \{x \in \mathbb{R}^2, \text{dist}(x, D) > d_0\}$ and suppose that $\|f\|_{\infty} < c_0$. For $x \in \widetilde{\Omega}$, we have

$$|x - e_{\theta} - \epsilon f(\theta) e_{\theta}|^2 = |x - e_{\theta}|^2 \left(1 - 2\epsilon f(\theta) \frac{\langle x - e_{\theta}, e_{\theta} \rangle}{|x - e_{\theta}|^2} \right) + O(\epsilon^2).$$

Using this, we obtain

$$\ln |x - e_{\theta} - \epsilon f(\theta) e_{\theta}| = \ln |x - e_{\theta}| - \epsilon f(\theta) \frac{\langle x - e_{\theta}, e_{\theta} \rangle}{|x - e_{\theta}|^2} + O(\epsilon^2), \quad (4.2.17)$$

and

$$\begin{aligned}
\frac{\langle e_\theta - x + \epsilon f(\theta)e_\theta, N_\theta \rangle}{|x - e_\theta - \epsilon f(\theta)e_\theta|^2} &= \frac{\langle e_\theta - x, e_\theta \rangle}{|x - e_\theta|^2} \\
&+ \epsilon f(\theta) \frac{\langle e_\theta - x, e_\theta \rangle}{|x - e_\theta|^2} + \epsilon \frac{f(\theta)}{|x - e_\theta|^2} \\
&- \epsilon \dot{f}(\theta) \frac{\langle e_\theta - x, \tau_\theta \rangle}{|x - e_\theta|^2} - 2\epsilon f(\theta) \frac{(\langle e_\theta - x, e_\theta \rangle)^2}{|x - e_\theta|^4} + O(\epsilon^2).
\end{aligned} \tag{4.2.18}$$

Here $O(\epsilon^2)$ is bounded by $c\epsilon^2$ where c depends only on d_0 , c_0 and the Lipschitz constant of f .

From Lemma 4.2.1, (4.2.7) and (4.2.8), we have

$$\begin{aligned}
u(x) - u_0(x) &= \frac{\epsilon}{2\pi} \int_0^{2\pi} \left[\ln|x - e_\theta| \mathcal{N}_f^1(\Psi) + \frac{\langle e_\theta - x, e_\theta \rangle}{|x - e_\theta|^2} \mathcal{N}_0(\Psi) f \right. \\
&\quad \left. - \frac{x \cdot \tau_\theta}{|x - e_\theta|^2} \Psi \dot{f} + \left(\frac{x \cdot e_\theta - 2}{|x - e_\theta|^2} + \frac{2(\langle e_\theta - x, e_\theta \rangle)^2}{|x - e_\theta|^4} \right) \Psi f \right] d\theta + O(\epsilon^2).
\end{aligned}$$

Integration by parts yields the following lemma.

Lemma 4.2.2 For $x \in \tilde{\Omega} (= \{x \in \mathbb{R}^2, \text{dist}(x, D) > d_0\})$, we have

$$\begin{aligned}
u(x) - u_0(x) &= \frac{\epsilon}{2\pi} \int_0^{2\pi} \ln|x - e_\theta| \left(\mathcal{D}_0 \mathcal{N}_0(\Psi) f - \mathcal{N}_0(\mathcal{N}_0(\Psi) f) + \mathcal{N}_0(\Psi) f \right) d\theta \\
&+ \frac{\epsilon}{2\pi} \int_0^{2\pi} \frac{\langle e_\theta - x, e_\theta \rangle}{|x - e_\theta|^2} \mathcal{N}_0(\Psi) f d\theta + \frac{\epsilon}{2\pi} \int_0^{2\pi} \ln|x - e_\theta| \ddot{\Psi} f d\theta \\
&+ \frac{\epsilon}{2\pi} \int_0^{2\pi} \left(-\frac{2}{|x - e_\theta|^2} + \frac{2(x \cdot \tau_\theta)^2 + 2(\langle e_\theta - x, e_\theta \rangle)^2}{|x - e_\theta|^4} \right) \Psi f d\theta + O(\epsilon^2),
\end{aligned} \tag{4.2.19}$$

where $O(\epsilon^2)$ is bounded by $c\epsilon^2$ with c depending on d_0 and $\|f\|_\infty$.

Rewrite (4.2.19) as

$$u(x) - u_0(x) = \epsilon \mathcal{H}(x) + O(\epsilon^2).$$

By a change of coordinates from Cartesian to polar in (4.2.19), we get the following asymptotic formula for \mathcal{H} when $|x| \gg 1$.

Lemma 4.2.3 For $x = re_\varphi$, $r \gg 1$, we have

$$\begin{aligned} \mathcal{H}(x) &= -\frac{1}{2r}\hat{a}_1 \left[\mathcal{D}_0 \mathcal{N}_0(\Psi)f - \mathcal{N}_0(\mathcal{N}_0(\Psi)f) + 2\mathcal{N}_0(\Psi)f + \ddot{\Psi}f \right] \cos(\varphi) \\ &\quad - \frac{1}{2r}\hat{b}_1 \left[\mathcal{D}_0 \mathcal{N}_0(\Psi)f - \mathcal{N}_0(\mathcal{N}_0(\Psi)f) + 2\mathcal{N}_0(\Psi)f + \ddot{\Psi}f \right] \sin(\varphi) + O\left(\frac{1}{r^2}\right), \end{aligned} \quad (4.2.20)$$

where \hat{a}_1 and \hat{b}_1 are defined by (4.2.11).

Proof. Since

$$|re_\varphi - e_\theta| = r\left(1 - \frac{1}{r}\langle e_\varphi, e_\theta \rangle + O\left(\frac{1}{r^2}\right)\right),$$

we have

$$\ln |re_\varphi - e_\theta| = \ln(r) - \frac{1}{r}\langle e_\varphi, e_\theta \rangle + O\left(\frac{1}{r^2}\right), \quad (4.2.21)$$

and

$$\frac{1}{|re_\varphi - e_\theta|} = \frac{1}{r} + O\left(\frac{1}{r^2}\right). \quad (4.2.22)$$

Substituting these equations into (4.2.19), we obtain

$$\mathcal{H}(r, \varphi) = -\frac{1}{2\pi r} \int_0^{2\pi} \langle e_\varphi, e_\theta \rangle \left(\mathcal{D}_0 \mathcal{N}_0(\Psi)f - \mathcal{N}_0(\mathcal{N}_0(\Psi)f) + 2\mathcal{N}_0(\Psi)f + \ddot{\Psi}f \right) d\theta + O\left(\frac{1}{r^2}\right),$$

as desired. \square

Now we rewrite (4.2.20) in terms of the Fourier coefficients of Ψ and f .

Lemma 4.2.4 We have

$$\sum_{k=0}^{\infty} \begin{pmatrix} -\hat{b}_{k+1}(\dot{\Psi}) - \hat{b}_{k-1}(\dot{\Psi}) & \hat{a}_{k+1}(\dot{\Psi}) + \hat{a}_{k-1}(\dot{\Psi}) \\ \hat{a}_{k+1}(\dot{\Psi}) - \hat{a}_{k-1}(\dot{\Psi}) & \hat{b}_{k+1}(\dot{\Psi}) - \hat{b}_{k-1}(\dot{\Psi}) \end{pmatrix} \begin{pmatrix} \hat{a}_k(f) \\ \hat{b}_k(f) \end{pmatrix} = \begin{pmatrix} c_1 \\ d_1 \end{pmatrix},$$

where

$$c_1(\Psi) := 2 \lim_{r \rightarrow +\infty} \hat{a}_1(r\mathcal{H}(r, \theta)),$$

$$d_1(\Psi) := 2 \lim_{r \rightarrow +\infty} \hat{b}_1(r\mathcal{H}(r, \theta)).$$

Proof. Note that $\hat{a}_1(\mathcal{N}_0(\mathcal{N}_0(\Psi)f)) = -\hat{a}_1(\mathcal{N}_0(\Psi)f)$. From (4.2.12) and (4.2.13), we get

$$\begin{aligned}\hat{a}_k\left(\mathcal{D}_0\mathcal{N}_0(\Psi) + 3\mathcal{N}_0(\Psi) + \ddot{\Psi}\right) &= (k(k+1) - 3k - k^2)\hat{a}_k(\Psi) \\ &= -2k\hat{a}_k(\Psi),\end{aligned}$$

$$\hat{b}_k\left(\mathcal{D}_0\mathcal{N}_0(\Psi) + 3\mathcal{N}_0(\Psi) + \ddot{\Psi}\right) = -2k\hat{b}_k(\Psi).$$

Moreover, we have

$$k\hat{a}_k(\Psi) = -\hat{b}_k(\dot{\Psi}) \text{ and } k\hat{b}_k(\Psi) = \hat{a}_k(\dot{\Psi}).$$

Letting $\hat{a}_{-n} = 0$ for $n \geq 1$ and $\hat{b}_{-n} = 0$ for $n \geq 0$, we observe that

$$\hat{a}_1(FG) = \sum_{k=0}^{\infty} \frac{\hat{a}_k(F)}{2} [\hat{a}_{k+1}(G) + \hat{a}_{k-1}(G)] + \sum_{k=0}^{\infty} \frac{\hat{b}_k(F)}{2} [\hat{b}_{k+1}(G) + \hat{b}_{k-1}(G)],$$

$$\hat{b}_1(FG) = \sum_{k=0}^{\infty} \frac{\hat{a}_k(F)}{2} [\hat{b}_{k+1}(G) - \hat{b}_{k-1}(G)] + \sum_{k=0}^{\infty} \frac{\hat{b}_k(F)}{2} [\hat{a}_{k-1}(G) - \hat{a}_{k+1}(G)].$$

This completes the proof. \square

4.2.4 Algorithm for the Inverse Shape Problem

Define Ψ_n and Φ_n , for $n \in \mathbb{N}$, by

$$\Psi_n(\theta) = \frac{1}{n} \sin(n\theta), \Phi_n(\theta) = -\frac{1}{n} \cos(n\theta).$$

From Lemma 4.2.4, it follows that

$$\begin{pmatrix} 0 & 1 \\ 1 & 0 \end{pmatrix} \begin{pmatrix} \hat{a}_{n-1}(f) \\ \hat{b}_{n-1}(f) \end{pmatrix} + \begin{pmatrix} 0 & 1 \\ -1 & 0 \end{pmatrix} \begin{pmatrix} \hat{a}_{n+1}(f) \\ \hat{b}_{n+1}(f) \end{pmatrix} = \begin{pmatrix} c_1(\Psi_n) \\ d_1(\Psi_n) \end{pmatrix} \quad (4.2.23)$$

$$\begin{pmatrix} -1 & 0 \\ 0 & 1 \end{pmatrix} \begin{pmatrix} \hat{a}_{n-1}(f) \\ \hat{b}_{n-1}(f) \end{pmatrix} + \begin{pmatrix} -1 & 0 \\ 0 & -1 \end{pmatrix} \begin{pmatrix} \hat{a}_{n+1}(f) \\ \hat{b}_{n+1}(f) \end{pmatrix} = \begin{pmatrix} c_1(\Phi_n) \\ d_1(\Phi_n) \end{pmatrix} \quad (4.2.24)$$

Thus we obtain that

$$\hat{b}_{n-1}(f) + \hat{b}_{n+1}(f) = c_1(\Psi_n), \quad \hat{a}_{n-1}(f) - \hat{a}_{n+1}(f) = d_1(\Psi_n),$$

and

$$\hat{b}_{n-1}(f) - \hat{b}_{n+1}(f) = d_1(\Phi_n), \quad -\hat{a}_{n-1}(f) - \hat{a}_{n+1}(f) = c_1(\Phi_n).$$

Therefore, we arrive at

$$\hat{b}_{n-1}(f) = \frac{c_1(\Psi_n) + d_1(\Phi_n)}{2},$$

and

$$\hat{a}_{n-1}(f) = \frac{d_1(\Psi_n) - c_1(\Phi_n)}{2}, \quad n \geq 1.$$

This simple calculation shows that in order to detect a perturbation that has oscillations of order $1/n$, one needs to use the first n eigenvectors $(e^{il\theta}, l = 1, \dots, n)$ of the Dirichlet-to-Neumann operator \mathcal{N}_0 as Dirichlet boundary data. This is a relatively simple but quite deep observation. We conjecture that this result holds for general domains. Another observation is that our asymptotic formula is in fact a low-frequency expansion which holds for fixed n as ϵ goes to zero. It would be interesting to derive an expansion which is valid for high-frequencies, not just for finite n .

4.3 Formulation of the Acoustic Problem

We study the Helmholtz problem analogously to the Laplacian one. Let D be a unit disk in \mathbb{R}^2 centered at 0, and u_0 be the solution to the Helmholtz problem with prescribed boundary Dirichlet data $\Psi \in \mathcal{C}^\infty([0, 2\pi])$, i.e.,

$$\begin{cases} \Delta u_0 + k^2 u_0 = 0, & \text{in } \mathbb{R}^2 \setminus \overline{D}, \\ u_0(1, \theta) = \Psi(\theta), & \text{on } \partial D, \\ \frac{\partial}{\partial r} u_0(r, \theta) - ik u_0(r, \theta) = o(r^{-\frac{1}{2}}), & r \longrightarrow +\infty. \end{cases} \quad (4.3.1)$$

Here we used the polar coordinates $x = r(\cos \theta, \sin \theta)$. As before we consider the solution u corresponding to the perturbed domain \tilde{D} :

$$\begin{cases} \Delta u + k^2 u = 0, & \text{in } \mathbb{R}^2 \setminus \tilde{D}, \\ u(1 + \epsilon f(\theta), \theta) = \Psi(\theta), & \text{on } \partial \tilde{D}, \\ \frac{\partial}{\partial r} u(r, \theta) - ik u(r, \theta) = o(r^{-\frac{1}{2}}), & r \longrightarrow +\infty, \end{cases} \quad (4.3.2)$$

where

$$\partial \tilde{D} (= \partial D + \epsilon f\nu) := \{(1 + \epsilon f(\theta))e_\theta, \theta \in [0, 2\pi]\}.$$

4.3.1 Representation Formula

The outgoing fundamental solution to the Helmholtz operator $(\Delta + k^2)$ in \mathbb{R}^2 is given by

$$\Phi_k(x, y) = -\frac{i}{4} H_0^{(1)}(k|x - y|),$$

for $x \neq 0$, where $H_0^{(1)}$ is the Hankel function of the first kind of order 0. In other words, Φ_k satisfies

$$(\Delta + k^2)\Phi_k(\cdot, y) = \delta_y \quad \text{in } \mathbb{R}^2,$$

and

$$\frac{\partial}{\partial r} \Phi_k(\cdot, y) - ik \Phi_k(\cdot, y) = o(r^{-\frac{1}{2}}) \quad \text{as } r \rightarrow \infty.$$

Using Green's formula, we have

$$u(x) = \int_{\partial \tilde{D}} \Phi_k(y, x) \frac{\partial u}{\partial \nu_y}(y) d\sigma_y - \int_{\partial \tilde{D}} \frac{\partial \Phi_k}{\partial \nu_y}(y, x) u(y) d\sigma_y, \quad \text{for } x \in \mathbb{R}^2 \setminus \overline{\tilde{D}}. \quad (4.3.3)$$

Note that

$$\frac{d}{dz} H_0^{(1)}(z) = -H_1^{(1)}(z). \quad (4.3.4)$$

From (4.2.4) and (4.2.5), we get

$$u(x) = -\frac{i}{4} \int_0^{2\pi} \left[k \frac{\langle (1 + \epsilon f(\theta))e_\theta - x, N_\theta \rangle}{|(1 + \epsilon f(\theta))e_\theta - x|} H_1^{(1)}(k|(1 + \epsilon f(\theta))e_\theta - x|) \Psi(\theta) \right. \\ \left. + H_0^{(1)}(k|(1 + \epsilon f(\theta))e_\theta - x|) \mathcal{N}_{\epsilon f}(\Psi)(\theta) \right] d\theta, \quad (4.3.5)$$

and

$$u_0(x) = -\frac{i}{4} \int_0^{2\pi} \left[k \frac{\langle e_\theta - x, e_\theta \rangle}{|e_\theta - x|} H_1^{(1)}(k|e_\theta - x|) + H_0^{(1)}(k|e_\theta - x|) \mathcal{N}_0(\Psi)(\theta) \right] d\theta, \quad (4.3.6)$$

where

$$\mathcal{N}_{\epsilon f}(\Psi)(\theta) := \frac{\partial u}{\partial N_\theta}(1 + \epsilon f(\theta), \theta),$$

and

$$\mathcal{N}_0(\Psi)(\theta) := \partial_r u_0(1, \theta).$$

4.3.2 Expansion of $\mathcal{N}_{\epsilon f}$

We parametrize the unit circle S , which is the boundary of D , by $\theta \in [0, 2\pi]$ and expand the 2π -periodic function $\Psi(= u|_S)$ as

$$\Psi(\theta) = \sum_{n \in \mathbb{Z}} \hat{c}_n e^{in\theta}.$$

Now we consider the *Dirichlet-to-Neumann operator* \mathcal{N}_0 with respect to D :

$$\mathcal{N}_0 : u_0|_S \rightarrow \partial_r u_0|_S.$$

By the uniqueness of a solution to (4.3.1), we find that

$$u_0(r, \theta) = \sum_{n \in \mathbb{Z}} \frac{H_{|n|}^{(1)}(kr)}{H_{|n|}^{(1)}(k)} \hat{c}_n(\Psi) e^{in\theta}.$$

Therefore, in a pseudodifferential fashion, \mathcal{N}_0 can be written as follows (see [33]):

$$\mathcal{N}_0(\Psi)(\theta) = \sum_{n \in \mathbb{Z}} \sigma_1(n, k) \hat{c}_n e^{in\theta}, \quad (4.3.7)$$

where the so-called *discrete symbol* σ_1 of \mathcal{N}_0 is given by

$$\sigma_1 = k \frac{H_{|n|}^{(1)'}(k)}{H_{|n|}^{(1)}(k)} = -k \frac{H_{|n+1|}^{(1)}(k)}{H_{|n|}^{(1)}(k)} + |n|.$$

We also define

$$\mathcal{D}_0(\Psi)(\theta) := \sum_{n \in \mathbb{Z}} \sigma_2(n, k) \hat{c}_n(\Psi) e^{in\theta}, \quad (4.3.8)$$

with

$$\sigma_2(n, k) = k \frac{H_{|n|}^{(1)''}(k)}{H_{|n|}^{(1)'}(k)}.$$

With this notation, we have the following asymptotic expansion for $\mathcal{N}_{\epsilon f}$.

Lemma 4.3.1 *For any 2π -periodic function $\Psi \in C^2([0, 2\pi])$, we have that*

$$\mathcal{N}_{\epsilon f}(\Psi) = \mathcal{N}_f^0(\Psi) + \epsilon \mathcal{N}_f^1(\Psi) + O(\epsilon^2),$$

where

$$\mathcal{N}_f^0(\Psi) = \mathcal{N}_0(\Psi),$$

and

$$\mathcal{N}_f^1(\Psi) = \mathcal{D}_0 \mathcal{N}_0(\Psi) f - \mathcal{N}_0(\mathcal{N}_0(\Psi) f) + \mathcal{N}_0(\Psi) f - f \dot{\Psi}.$$

Proof. Note that (4.2.9), (4.2.10) and (4.2.16) are also valid in the case of the Helmholtz problem. We finish the proof by computing $\partial_r^2 u_0(1, \theta)$:

$$\begin{aligned} \partial_r^2 u_0(1, \theta) &= \sum_{n \in \mathbb{Z}} k^2 \frac{H_{|n|}^{(1)''}(k)}{H_{|n|}^{(1)'}(k)} \hat{c}_n(\Psi) e^{in\theta} \\ &= \sum_{n \in \mathbb{Z}} \sigma_2(n, k) \sigma_1(n, k) \hat{c}_n(\Psi) e^{in\theta} = \mathcal{D}_0 \mathcal{N}_0(\Psi)(\theta). \end{aligned}$$

□

4.3.3 Far-Field Asymptotic Formula

We define $\tilde{\Omega} := \{x \in \mathbb{R}^2, \text{dist}(x, D) > d_0\}$ and assume that $\|f\|_\infty < c_0$.

Lemma 4.3.2 *As ϵ tends to 0 and $x \in \tilde{\Omega}$, we have*

$$u(x) - u_0(x) = \frac{i\epsilon}{4} \mathcal{H}(x) + O(\epsilon^2),$$

where

$$\begin{aligned} \mathcal{H}(x) &= \int_0^{2\pi} H_0^{(1)}(k|x - e_\theta|) \left[-(\mathcal{D}_0 \mathcal{N}_0(\Psi) + \mathcal{N}_0(\Psi) + \ddot{\Psi})f + \mathcal{N}_0(\mathcal{N}_0(\Psi)f) \right](\theta) d\theta \\ &\quad - k^2 \int_0^{2\pi} H_0^{(1)}(k|x - e_\theta|) \frac{(x \cdot \tau_\theta)^2 + (1 - x \cdot e_\theta)^2}{|x - e_\theta|^2} \Psi(\theta) f(\theta) d\theta \\ &\quad + k \int_0^{2\pi} H_1^{(1)}(k|x - e_\theta|) \frac{1 - x \cdot e_\theta}{|x - e_\theta|} \mathcal{N}_0(\Psi)(\theta) f(\theta) d\theta \\ &\quad - k \int_0^{2\pi} H_1^{(1)}(k|x - e_\theta|) \left(\frac{2}{|x - e_\theta|} - 2 \frac{(x \cdot \tau_\theta)^2 + (1 - x \cdot e_\theta)^2}{|x - e_\theta|^3} \right) \Psi(\theta) f(\theta) d\theta. \end{aligned}$$

Here $O(\epsilon^2)$ is bounded by $c\epsilon^2$ with c depending only on c_0 and d_0 .

Proof. For any $x \in \tilde{\Omega}$, we have that

$$\begin{aligned} H_0^{(1)}(k|x - e_\theta - \epsilon f(\theta)e_\theta|) &= H_0^{(1)}(k|x - e_\theta|) \\ &\quad + \epsilon k f(\theta) \frac{\langle x - e_\theta, e_\theta \rangle}{|x - e_\theta|} H_1^{(1)}(k|x - e_\theta|) + O(\epsilon^2), \end{aligned}$$

and

$$\begin{aligned} H_1^{(1)}(k|x - e_\theta - \epsilon f(\theta)e_\theta|) &= H_1^{(1)}(k|x - e_\theta|) \\ &\quad - \epsilon f(\theta) \frac{\langle x - e_\theta, e_\theta \rangle}{|x - e_\theta|} \left[k H_0^{(1)}(k|x - e_\theta|) - \frac{H_1^{(1)}(k|x - e_\theta|)}{|x - e_\theta|} \right] + O(\epsilon^2). \end{aligned}$$

From (4.3.5), (4.3.6), and Lemma 4.3.1, we obtain that

$$\begin{aligned}
\mathcal{H}(x) &= - \int_0^{2\pi} H_0^{(1)}(k|x - e_\theta|) \mathcal{N}_f^1(\Psi)(\theta) d\theta \\
&+ k \int_0^{2\pi} \frac{\langle e_\theta - x, e_\theta \rangle}{|x - e_\theta|} H_1^{(1)}(k|x - e_\theta|) (\mathcal{N}_0 - I) \Psi(\theta) f(\theta) d\theta \\
&- k \int_0^{2\pi} \frac{1}{|x - e_\theta|} H_1^{(1)}(k|x - e_\theta|) \Psi(\theta) f(\theta) d\theta + k \int_0^{2\pi} \frac{\langle e_\theta - x, \tau_\theta \rangle}{|x - e_\theta|} H_1^{(1)}(k|x - e_\theta|) \Psi(\theta) \dot{f}(\theta) d\theta \\
&- k \int_0^{2\pi} \frac{(\langle e_\theta - x, e_\theta \rangle)^2}{|x - e_\theta|^2} \left(k H_0^{(1)}(k|x - e_\theta|) - \frac{1}{|x - e_\theta|} H_1^{(1)}(k|x - e_\theta|) \right) \Psi(\theta) f(\theta) d\theta \\
&+ k \int_0^{2\pi} \frac{(\langle e_\theta - x, e_\theta \rangle)^2}{|x - e_\theta|^3} H_1^{(1)}(k|x - e_\theta|) \Psi(\theta) f(\theta) d\theta.
\end{aligned}$$

Integrating by parts, we get

$$\begin{aligned}
&\int_0^{2\pi} H_0^{(1)}(k|x - e_\theta|) \dot{\Psi}(\theta) \dot{f}(\theta) d\theta \\
&= \int_0^{2\pi} \left[H_1^{(1)}(k|x - e_\theta|) \frac{-kx \cdot \tau_\theta}{|x - e_\theta|} \dot{\Psi} - H_0^{(1)}(k|x - e_\theta|) \ddot{\Psi} \right] f d\theta,
\end{aligned}$$

and

$$\begin{aligned}
&k \int_0^{2\pi} \frac{\langle e_\theta - x, \tau_\theta \rangle}{|x - e_\theta|} H_1^{(1)}(k|x - e_\theta|) \Psi(\theta) \dot{f}(\theta) d\theta \\
&= - \int_0^{2\pi} H_0^{(1)}(k|x - e_\theta|) \frac{k^2(x \cdot \tau_\theta)^2}{|x - e_\theta|^2} \Psi f d\theta + \int_0^{2\pi} H_1^{(1)}(k|x - e_\theta|) \frac{kx \cdot \tau_\theta}{|x - e_\theta|} \dot{\Psi} f d\theta \\
&- \int_0^{2\pi} H_1^{(1)}(k|x - e_\theta|) \left[\frac{kx \cdot e_\theta}{|x - e_\theta|} - \frac{2k(x \cdot \tau_\theta)^2}{|x - e_\theta|^3} \right] \Psi f d\theta.
\end{aligned}$$

Here we have used (4.3.4) together with the identity

$$\frac{d}{dz} H_1^{(1)}(z) = H_0^{(1)}(z) - \frac{1}{z} H_1^{(1)}(z).$$

□

Lemma 4.3.3 For any $x = r e_\varphi$ with $r \gg 1$, we have

$$\frac{i}{4} \mathcal{H}(r, \varphi) = \frac{e^{i\frac{\pi}{4}} e^{ikr}}{\sqrt{8\pi kr}} \tilde{\mathcal{H}}(\varphi) + O\left(\frac{1}{r}\right),$$

where

$$\begin{aligned} \tilde{\mathcal{H}}(\varphi) = \int_0^{2\pi} e^{-ik\langle e_\theta, e_\varphi \rangle} \left[-(\mathcal{D}_0 \mathcal{N}_0(\Psi) + \mathcal{N}_0(\Psi) + \ddot{\Psi})(\theta) f(\theta) + \mathcal{N}_0(\mathcal{N}_0(\Psi) f)(\theta) \right. \\ \left. + ik\langle e_\varphi, e_\theta \rangle \mathcal{N}_0(\Psi)(\theta) f(\theta) - k^2 \Psi(\theta) f(\theta) \right] d\theta. \end{aligned} \quad (4.3.9)$$

Proof. It is known that, for a fixed n , the Hankel function of the first kind satisfies

$$H_n^{(1)}(x) = \sqrt{\frac{2}{\pi x}} e^{i(x - \frac{\pi}{4} - n\frac{\pi}{2})} + O(|x|^{-1}), \quad x \gg n.$$

We refer to [1] for more properties of the Hankel function.

Putting re_φ instead of x , we have

$$H_0^{(1)}(k|re_\varphi - e_\theta|) = \sqrt{\frac{2}{\pi k|re_\varphi - e_\theta|}} e^{i(k|re_\varphi - e_\theta| - \frac{\pi}{4})} + O\left(\frac{1}{r}\right).$$

From the fact that

$$|re_\varphi - e_\theta| = r - \langle e_\varphi, e_\theta \rangle + O\left(\frac{1}{r}\right)$$

and

$$\frac{1}{|re_\varphi - e_\theta|} = \frac{1}{r} + O\left(\frac{1}{r^2}\right),$$

we can obtain

$$\frac{i}{4} H_0^{(1)}(k|re_\varphi - e_\theta|) = \frac{e^{i\frac{\pi}{4}} e^{ikr}}{\sqrt{8\pi kr}} e^{-ik\langle e_\varphi, e_\theta \rangle} + O\left(\frac{1}{r}\right).$$

Similarly, we have

$$\frac{i}{4} H_1^{(1)}(k|re_\varphi - e_\theta|) = (-i) \frac{e^{i\frac{\pi}{4}} e^{ikr}}{\sqrt{8\pi kr}} e^{-ik\langle e_\varphi, e_\theta \rangle} + O\left(\frac{1}{r}\right).$$

Substituting these approximations into the integral expression of \mathcal{H} in Lemma 4.3.2, we arrive at the desired result. \square

4.3.4 Algorithm for the Inverse Shape Problem

In this subsection we use the field $\tilde{\mathcal{H}}(\theta)$ to find the shape of $\partial\tilde{D}$.

From the Jacobi-Anger Expansion (see for example [19], Section 3.4):

$$e^{ik \cos \theta} = \sum_{n=-\infty}^{\infty} i^n J_n(k) e^{in\theta},$$

where J_n is the Bessel function of the first kind, we have

$$e^{-ik \langle e_\theta, e_\varphi \rangle} = \sum_{n=-\infty}^{\infty} (-1)^n J_n(k) e^{in\varphi} e^{-in\theta}. \quad (4.3.10)$$

From (4.3.9) and (4.3.10), we have

$$\tilde{\mathcal{H}}(\varphi) = \sum_{n \in \mathbb{Z}} (-1)^n J_n(k) A_n(\varphi) e^{in\varphi}, \quad (4.3.11)$$

where

$$A_n(\varphi) = \int_0^{2\pi} e^{-in\theta} \left[-(\mathcal{D}_0 \mathcal{N}_0(\Psi) + \mathcal{N}_0(\Psi) + \ddot{\Psi})(\theta) f(\theta) + \mathcal{N}_0(\mathcal{N}_0(\Psi) f)(\theta) + ik \langle e_\varphi, e_\theta \rangle \mathcal{N}_0(\Psi)(\theta) f(\theta) - k^2 \Psi(\theta) f(\theta) \right] d\theta.$$

Lemma 4.3.4 *We have*

$$\tilde{\mathcal{H}}(\varphi) = \sum_{n \in \mathbb{Z}} (-1)^n J_n(k) \hat{c}_n(\tilde{\mathcal{H}}) e^{in\varphi},$$

where

$$\hat{c}_n(\tilde{\mathcal{H}}) = 2\pi \sum_{p \in \mathbb{Z}} \mathcal{M}_{n,p} \hat{c}_p(\Psi) \hat{c}_{n-p}(f),$$

and

$$\mathcal{M}_{n,p} = \left[-\sigma_1(p, k) \sigma_2(p, k) + \sigma_1(n, k) \sigma_1(p, k) - \sigma_1(p, k) + p^2 - k^2 \right] - in \sigma_1(p, k).$$

Proof. Let

$$\begin{aligned}
A_n(\varphi) &= \int_0^{2\pi} e^{-in\theta} \left[-\mathcal{D}_0 \mathcal{N}_0(\Psi) f + \mathcal{N}_0(\mathcal{N}_0(\Psi) f) - \mathcal{N}_0(\Psi) f - \ddot{\Psi} f - k^2 \Psi f \right] d\theta \\
&\quad + \int_0^{2\pi} e^{-in\theta} ik \langle e_\varphi, e_\theta \rangle \mathcal{N}_0(\Psi) f d\theta \\
&=: I(n) + II(n).
\end{aligned}$$

From (4.3.7) and (4.3.8), we have

$$\begin{aligned}
&\hat{c}_p \left(-\mathcal{D}_0 \mathcal{N}_0(\Psi) - \mathcal{N}_0(\Psi) - \ddot{\Psi} - k^2 \Psi \right) \\
&= [-\sigma_1(p, k) \sigma_2(p, k) - \sigma_1(p, k) + p^2 - k^2] \hat{c}_p(\Psi).
\end{aligned}$$

Using the fact that

$$\hat{c}_n(fg) = \sum_{p \in \mathbb{Z}} \hat{c}_p(f) \hat{c}_{n-p}(g),$$

we can obtain

$$\begin{aligned}
\hat{c}_n \left[\mathcal{N}_0(\mathcal{N}_0(\Psi) f) \right] &= \sigma_1(n, k) \hat{c}_n \left[\mathcal{N}_0(\Psi) f \right] \\
&= \sum_{p \in \mathbb{Z}} \sigma_1(n, k) \sigma_1(p, k) \hat{c}_p(\Psi) \hat{c}_{n-p}(f)
\end{aligned}$$

and

$$I(n) = 2\pi \sum_{p \in \mathbb{Z}} [-\sigma_1(p, k) \sigma_2(p, k) + \sigma_1(n, k) \sigma_1(p, k) - \sigma_1(p, k) + p^2 - k^2] \hat{c}_p(\Psi) \hat{c}_{n-p}(f). \tag{4.3.12}$$

Note that

$$\langle e_\varphi, e_\theta \rangle = \frac{e^{i\varphi} e^{-i\theta}}{2} + \frac{e^{-i\varphi} e^{i\theta}}{2}.$$

We have

$$\begin{aligned}
II(n) &= ik\pi e^{i\varphi} \hat{c}_{n+1}[\mathcal{N}_0(\Psi) f] + ik\pi e^{-i\varphi} \hat{c}_{n-1}[\mathcal{N}_0(\Psi) f] \\
&= ik\pi e^{i\varphi} \sum_{p \in \mathbb{Z}} \sigma_1(p, k) \hat{c}_p(\Psi) \hat{c}_{n+1-p}(f) + ik\pi e^{-i\varphi} \sum_{p \in \mathbb{Z}} \sigma_1(p, k) \hat{c}_p(\Psi) \hat{c}_{n-1-p}(f).
\end{aligned}$$

Therefore

$$\begin{aligned}
& \sum_{n \in \mathbb{Z}} (-1)^n J_n(k) II(n) e^{in\varphi} \\
&= ik\pi \sum_{n \in \mathbb{Z}} (-1)^n J_n(k) e^{i(n+1)\varphi} \sum_{p \in \mathbb{Z}} \sigma_1(p, k) \hat{c}_p(\Psi) \hat{c}_{n+1-p}(f) \\
&\quad + ik\pi \sum_{n \in \mathbb{Z}} (-1)^n J_n(k) e^{i(n-1)\varphi} \sum_{p \in \mathbb{Z}} \sigma_1(p, k) \hat{c}_p(\Psi) \hat{c}_{n+1-p}(f) \\
&= -ik\pi \sum_{n \in \mathbb{Z}} (-1)^n \left[J_{n-1}(k) + J_{n+1}(k) \right] e^{in\varphi} \sum_{p \in \mathbb{Z}} \sigma_1(p, k) \hat{c}_p(\Psi) \hat{c}_{n-p}(f) \\
&= -ik\pi \sum_{n \in \mathbb{Z}} (-1)^n \frac{2n}{k} J_n(k) e^{in\varphi} \sum_{p \in \mathbb{Z}} \sigma_1(p, k) \hat{c}_p(\Psi) \hat{c}_{n-p}(f). \tag{4.3.13}
\end{aligned}$$

Here we used recurrence relations of Bessel function, i.e.,

$$J_{n-1}(k) + J_{n+1}(k) = \frac{2n}{k} J_n(k).$$

From (4.3.12) and (4.3.13), we proves the lemma. □

Suppose now that

$$\Psi = e^{ip\theta}.$$

Then from Lemma 4.3.4, for each n , we obtain the coefficient $\mathcal{M}_{n,p} \hat{c}_{n-p}(f)$ from the far-field measurements. This yields to stable reconstruction of the Fourier coefficients $\hat{c}_{n-p}(f)$ for all $n, p, p \leq n$, such that $\mathcal{M}_{n,p}$ is not too small.

Bibliography

- [1] M. Abrohmitz and I. A. Stegun, *Handbook of Mathematical Functions*, New York: Dover, 1974.
- [2] P.M. Anselone, *Collectively Compact Operator Approximation Theory and Applications to Integral Equations*, Prentice-Hall, Englewood Cliffs, 1971.
- [3] H. Ammari and H. Kang, High-order terms in the asymptotic expansions of the steady-state voltage potentials in the presence of conductivity inhomogeneities of small diameter, *SIAM J. Math. Anal.*, 34 (2003), 1152-1166.
- [4] H. Ammari and H. Kang, *Reconstruction of Small Inhomogeneities from Boundary Measurements*, Lecture Notes in Mathematics, Volume 1846, Springer-Verlag, Berlin, 2004.
- [5] H. Ammari, H. Kang, E. Kim, K. Louati, and M. Vogelius, A MUSIC-type method for detecting internal corrosion from steady state voltage boundary perturbations, preprint.
- [6] H. Ammari, H. Kang, E. Kim, H. Lee, and K. Louati, Vibration testing for detecting internal corrosion, preprint.
- [7] H. Ammari, H. Kang, E. Kim, M. Lim, and K. Louati, Ultrasonic detection of internal corrosion, preprint.

- [8] H. Ammari, H. Kang, M. Lim, and H. Zribi, Layer potential techniques in spectral analysis. Part I: Complete asymptotic expansions for eigenvalues of the Laplacian in domains with small inclusions, preprint.
- [9] H. Ammari, S. Moskow, and M. Vogelius, Boundary integral formulae for the reconstruction of electric and electromagnetic inhomogeneities of small volume, *ESAIM: Cont. Opt. Calc. Var.* 9 (2003), 49-66.
- [10] S. Andrieux and A. Ben Abda, Identification de fissures planes par une donnée de bord unique; un procédé direct de localisation et d'identification, *C. R. Acad. Sci., Paris I* 315 (1992), 1323-1328.
- [11] H.T. Banks, M.L. Joyner, B. Wincheski, and W.P. Winfree, Real time computational algorithms for eddy-current-based damage detection, *Inverse Problems* 18 (2002), 795-823.
- [12] M. Brühl, M. Hanke, and M.S. Vogelius, A direct impedance tomography algorithm for locating small inhomogeneities, *Numer. Math.*, 93 (2003), 635-654.
- [13] G. Buttazzo and R.V. Kohn, Reinforcement by a thin layer with oscillating thickness, *Appl. math. Opt.*, 16 (1988), 247-261.
- [14] A.P. Calderón, On an inverse boundary value problem, *Seminar on Numerical Analysis and its Applications to Continuum Physics*, Soc. Brasileira de Matemática, Rio de Janeiro, 1980, 65-73.
- [15] D.J. Cedio-Fengya, S. Moskow, and M.S. Vogelius, Identification of conductivity imperfections of small diameter by boundary measurements. Continuous dependence and computational reconstruction, *Inverse Problems*, 14 (1998), 553-595.

- [16] M. Cheney, The linear sampling method and the MUSIC algorithm, *Inverse Problems*, 17 (2001), 591-595.
- [17] R. Coifman, M. Goldberg, T. Hrycak, M. Israeli, and V. Rokhlin, An improved operator expansion algorithm for direct and inverse scattering computations, *Waves Random Media* 9 (1999), 441-457.
- [18] R.R. Coifman, A. McIntosh, and Y. Meyer, L'intégrale de Cauchy définit un opérateur borné sur L^2 pour les courbes lipschitziennes, *Ann. of Math. (2)*, 116 (1982), 361-387.
- [19] D. Colton and A. Kirsch, A simple method for solving inverse scattering problems in the resonance region, *Inverse Problems*, 12 (1996), 383-393.
- [20] A. El Badia and T. Ha-Duong, An inverse source problem in potential analysis, *Inverse Problems*, 16 (2000), 651-663.
- [21] G.B. Folland, *Introduction to Partial Differential Equations*, Princeton University Press, Princeton, NJ, 1976.
- [22] A. Friedman and M.S. Vogelius, Identification of small inhomogeneities of extreme conductivity by boundary measurements: a theorem on continuous dependence, *Arch. Rat. Mech. Anal.*, 105 (1989), 299-326.
- [23] I.T.S. Gohberg and E.I. Sigal, Operator extension of the logarithmic residue theorem and Rouché's theorem, *Mat. Sb. (N.S.)* 84 (1971), 607-642.
- [24] M. Ikehata, Enclosing a polygonal cavity in a two-dimensional bounded domain from Cauchy data, *Inverse Problems* 15 (1999), 1231-1241.

- [25] G. Inglese, An inverse problem in corrosion detection, *Inverse Problems* 13 (1997), 977-994.
- [26] B. Luong and F. Santosa, Quantitative imaging of corrosion in-plates by eddy current methods, *SIAM J. Appl. Math.* 58 (1998), 1509-1531.
- [27] H. Kang and J.K. Seo, Layer potential technique for the inverse conductivity problem, *Inverse Problems*, 12 (1996), 267-278.
- [28] —————, Recent progress in the inverse conductivity problem with single measurement, in *Inverse Problems and Related Fields*, CRC Press, Boca Raton, FL, 2000, 69-80.
- [29] H. Kang and H. Lee, Identification of simple poles via boundary measurements and an application to EIT, *Inverse Problems*, 20 (2004), 1853-1863.
- [30] T. Kato, *Perturbation Theory for Linear Operators*, Springer-Verlag, New York, 1976.
- [31] P. Kaup and F. Santosa, Nondestructive evaluation of corrosion damage using electrostatic measurements, *J. Nondestructive Eval.* 14 (1995), 127-136.
- [32] P. Kaup, F. Santosa, and M. Vogelius, A method for imaging corrosion damage in thin plates from electrostatic data, *Inverse Problems* 12 (1996), 279-293.
- [33] M. F. Kondratieva and S. Yu. Sadov, Symbol of the Dirichlet-to-Neumann operator in 2D diffraction problems with large wavenumber, *Day on Diffraction, 2003 Proceedings. International Seminar*, 88 - 98.

- [34] A. Kirsch, The MUSIC algorithm and the factorisation method in inverse scattering theory for inhomogeneous media, *Inverse Problems*, 18 (2002), 1025-1040.
- [35] O. Kwon, J.K. Seo, and J.R. Yoon, A real-time algorithm for the location search of discontinuous conductivities with one measurement, *Comm. Pure Appl. Math.*, 55 (2002), 1-29.
- [36] M. Lim, K. Louati, and H. Zribi, An asymptotic formalism for reconstructing small perturbations of scatterers from electric or acoustic far-field measurements, preprint.
- [37] D.M. Milder, An improved formalism for wave scattering from rough surfaces, *J. Acoust. Soc. Am.*, 89 (1991), 529-541.
- [38] P.E. Mix, *Introduction to Nondestructive Testing (Second Edition)*, Wiley, 2005.
- [39] F. Natterer and F. Wübbeling, *Mathematical Methods in Image Reconstruction*, SIAM Monographs on Mathematical Modeling and Computation, SIAM, Philadelphia, 2001.
- [40] F. Natterer and F. Wübbeling, Marching schemes for inverse acoustic scattering problems, *Numer. Math.*, 100 (2005), 697-710.
- [41] D.P. Nicholls and F. Reitich, Analytic continuation of Dirichlet-Neumann operators, *Numer. Math.* 94 (2003), 107-146.
- [42] E.M. Stein, *Singular Integrals and Differentiability Properties of Functions*, Princeton University Press, Princeton, NJ, 1970.
- [43] C.W. Therrien, *Discrete Random Signals and Statistical Signal Processing*, Prentice-Hall, Englewood Cliffs, NJ, 1992.

- [44] C.F. Tolmasky and A. Wiegmann, Recovery of small perturbations of an interface for an elliptic inverse problem via linearization, *Inverse Problems* 15 (1999), 465-487.
- [45] G.C. Verchota, Layer potentials and boundary value problems for Laplace's equation in Lipschitz domains, *J. Funct. Anal.*, 59 (1984), 572-611.
- [46] M. Vogelius and J. Xu, A nonlinear elliptic boundary value problem related to corrosion modelling, *Quart. Appl. Math.* 56 (1998), 479-505.
- [47] X. Yang, M. Choulli, and J. Cheng, An iterative BEM for the inverse problem of detecting corrosion in a pipe, *Numer. Math. J. Chinese Univ.*, 14 (2005), 252-266.